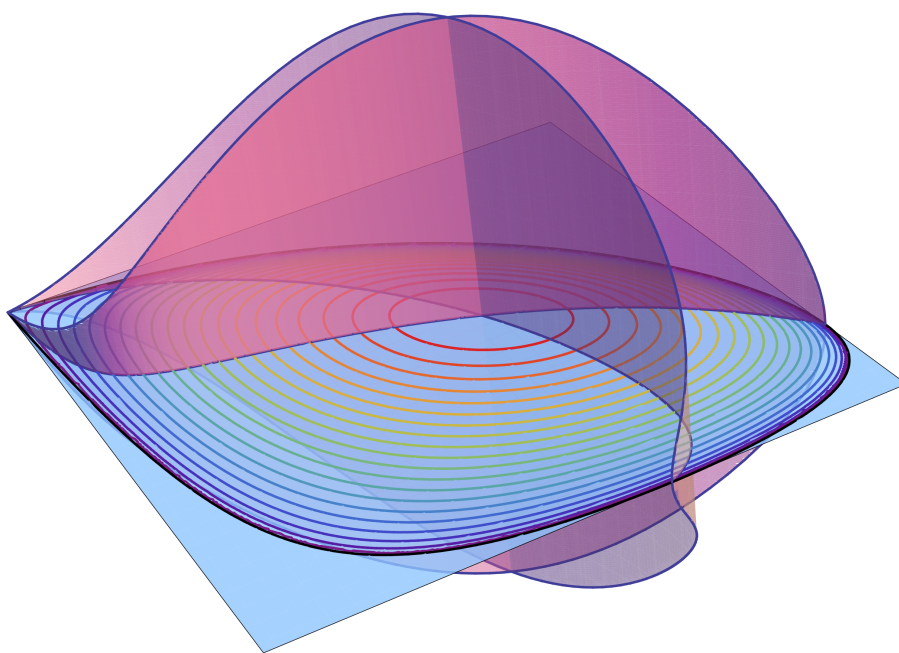


UNIVERSITÀ DEGLI STUDI DI PAVIA
DOTTORATO DI RICERCA IN FISICA – XXVI CICLO

**Single and collective dynamics
of discretized geometries**

Dimitri Marinelli



Tesi per il conseguimento del titolo



Università
degli Studi
di Pavia

Dipartimento di
Fisica
“A. Volta”



DOTTORATO DI RICERCA IN FISICA – XXVI CICLO

Single and collective dynamics of discretized geometries

dissertation submitted by

Dimitri Marinelli

to obtain the degree of

DOTTORE DI RICERCA IN FISICA

Supervisor: Prof. Annalisa Marzuoli

Referees: Prof. Robert Littlejohn, Prof. Patrizia Vitale

Cover: The plot represents the caustics of the Hamiltonian system described in Chapter 3. In particular, the pale blue plane represents the “screen” appearing in the study of the $6j$ symbol, and the blue larger contour is the $6j$ caustic. The two purple sections are plots of the two functions α_ℓ and $\alpha_{\tilde{\ell}}$. This particular choice of the parameters corresponds to the “twin” case (namely, when two quadrilaterals coincide under the action of the Regge symmetry). In this case the two sections meet both in their maxima and in the origin $\ell = \tilde{\ell} = 0$.

Single and collective dynamics of discretized geometries

Dimitri Marinelli

PhD thesis – University of Pavia

Printed in, 2013

ISBN: 978-88-95767-73-4

Contents

1	Introduction	3
2	Recoupling theory and discretized geometry	7
2.1	Recoupling theory of $SU(2)$ angular momentum	7
2.1.1	Ponzano–Regge asymptotic formula	9
2.1.2	Racah hypergeometric polynomial	10
2.2	Regge Calculus	11
2.2.1	Basic definitions	12
2.2.2	A heuristic viewpoint	15
2.2.3	Regge equations	17
2.3	Discretized geometries and Quantum Gravity	18
3	The volume operator and symmetric coupling of $SU(2)$ angular momenta	21
3.1	The Volume Operator	21
3.1.1	Formal definition	22
3.1.2	The eigenvalue problem	23
3.1.3	The three-term recurrence relations	24
3.2	The semiclassical limit and geometry of quadrilaterals	26
3.2.1	From three-term recurrence relations to second order finite difference equations	26
3.2.2	Schrödinger-like approach and semiclassical limit	27
3.2.3	Semiclassical geometry of the volume operator	28
3.2.4	Equations of motion and potential functions	29
3.2.5	Numerical studies	30
4	Regge Symmetries	33
4.1	Definition of Regge symmetry	34
4.2	The geometry of tetrahedra and associated quadrilaterals	36
4.2.1	Quadrilaterals and their Regge conjugate	37

4.2.2	The tetrahedron and its Regge conjugate	42
4.3	Quaternionic parametrizations and Regge symmetries	43
4.3.1	New variables	43
4.3.2	Conjugate quaternions	44
4.4	Regge symmetry for the volume operator	45
5	Discrete polynomials families from generalized coupling	49
5.1	Definition of the polynomials	49
5.1.1	Regge invariance	51
5.2	Algebraic approach to the Askey-scheme	52
5.2.1	Quadratic symmetry algebras	52
5.2.2	Generalized recoupling theory, Regge symmetry and duality	55
5.2.3	Classification of discrete polynomial families	57
5.2.4	Limiting cases	60
6	Lorentzian Regge Calculus	63
6.1	Peculiarities of the Lorentzian 4-simplex	63
6.2	Construction of foliated simplicial manifolds	67
6.2.1	Tent-like evolution for $S_3 \times I$	68
6.2.2	Symmetric triangulation of $S_3 \times I$	76
6.3	Some remarks on the dynamics	79
	Conclusions	81
	Bibliography	91

Chapter 1

Introduction

Motivations of this work are inspired by three papers: Regge’s “General Relativity without Coordinates” published in 1961 [1], Penrose’s “Angular Momentum: an Approach to Combinatorial Space-time” published in 1971 [2] and the contemporary paper by Ponzano and Regge “Semiclassical limits of Racah’s coefficients” [3]. While Regge Calculus, as the discrete approach to classical Einstein’s theory found by Regge has been called by Wheeler [4], started to be applied to quantum theory of gravity in the Euclidean path integral formulation in the 1980s, the ideas of Penrose (and, in the sense which will be reviewed in Chapter 2, also results found by Ponzano and Regge [3]) were truly innovative and far-reaching. In Penrose’s words [2]

My basic idea is to try and build up both space-time and quantum mechanics simultaneously – from combinatorial principles – but not (at least in the first instance) to try and change physical theory (...) One scarcely wants to take every concept in existing theory and try to make it combinatorial: there are too many things which look continuous in the existing theory. And to try to eliminate the continuum by approximating it by some discrete structure would be to change the theory. The idea, instead, is to concentrate only on things which, in fact, are discrete in existing theory and try and use them as primary concepts – then to build up other things using these discrete primary concepts as the basic building blocks. Continuous concepts could emerge in a limit, when we take more and more complicated systems.

Thus over the years classical and quantum ‘discretized geometries’, and in particular Penrose’s ‘spin networks’ in their variety of formulations and applications, have constituted a very active field of research for both theoretical physicists and geometers (it is worth recalling the Turaev–Viro model [5] which provides a regularized counterpart of Ponzano-Regge partition function for Euclidean 3-gravity and represents a topological invariant of closed 3-manifolds not recognized before).

Previous work on spin networks and Regge Calculus

In 1964 and 1965 Chakrabarti [6], Lèvy-Leblond and Lèvy-Nahas [7], looking for a symmetric treatment of the coupling of three angular momentum operators, independently introduced a new operator now called ‘volume operator’ as the triple product of the vector operators associated with the three angular momenta. They provided the matrix representation of the operator and studied its properties.

During the 1990s the volume operator became the fundamental ingredient of the loop approach to quantum gravity [8, 9, 10, 11] and for this reason many have studied its features and its spectrum [12, 13, 14, 15, 16, 17, 18] until very recently [19, 20, 21]. In loop quantum gravity the volume operator acts on the four-valent node of a graph. In this node resides the space of the intertwiners between the representations of the group $SU(2)$ associated with it [22]. Eigenstates of the volume operator form a convenient base for the space of the intertwiners.

The volume operator is strictly related to the $6j$ symbol, the recoupling coefficient between two binary coupled bases arising in the quantum theory of angular momenta. Ponzano and Regge [3] found the form of the $6j$ symbol in its semiclassical limit extending the previous analysis of Wigner [23]. This asymptotic analysis chains the $6j$ symbol to the geometry of an Euclidean tetrahedron. Other approaches, starting from the three terms recurrence relation for the $6j$ symbol and leading to the Ponzano-Regge formula were developed by Neville in 1971 [24] and by Schulten and Gordon [25], and a formal proof of the Ponzano-Regge formula was given by Roberts in 1999 [26].

This semiclassical analysis of the $6j$ symbol suggest to use similar tools for the volume operator along the lines established in Carbone et al. [12]. In this thesis the semiclassical analysis of the volume operator is based on the techniques introduced by Braum for the discrete WKB method [28, 29] and the analysis of the semiclassical mechanics of the $6j$ symbol by Aquilanti et al. [30]. Although the study of the volume operator by Haggard [31] and Haggard and Bianchi [19, 20] is compatible with our approach, it is conceptually very different: they quantize semiclassically the symplectic space associated with the “shape space” of polyhedra so that they follow a “classical to quantum” approach. Moreover, the geometric structure involved is associated with the dual tetrahedron, namely their “variables” are associated with areas of the faces of tetrahedra while for us the treatment is actually insensible to the choice of the role for the “variables”: they can be either areas or edge lengths, but we choose the second option to comply with the original spirit of Wigner and Ponzano–Regge. An important property that the study of $6j$ have revealed is its Regge symmetry [32]. We (see also [20]) found that volume operator possesses the same symmetry.

Finally, moving to the collective dynamics of discrete geometries, we based our treatment on the original paper by Regge [1] and the further developments

proposed by Wheeler in [33]. There has not been much work on classical Lorentzian Regge calculus, but only a few interesting sample calculations (*e.g.* [34, 35]).

Plan and main results of the thesis

- In Chapter 2, we review the standard recoupling theory for $SU(2)$ angular momenta and some basic facts about Regge Calculus.
- In Chapter 3 we develop the symmetric (re)-coupling theory for $SU(2)$ angular momenta, introducing the volume operator and evaluating its semiclassical limit through the associated three-term recurrence relation to be looked as a discrete Schrödinger equation. A mechanical analogue of the emerging dynamics is also provided.
- In Chapter 4 a definition of Regge symmetry is given and then generalized to quadrilaterals and tetrahedra. A new quaternion parametrization of quadrilaterals is provided. Regge symmetry is proved to act on quadrilaterals as a quaternionic conjugation. Finally, the proof of the invariance for Regge symmetry of the volume operator is completed.
- In Chapter 5 families of orthogonal polynomials associated with the volume operator are defined. An Askey-like classification of these orthogonal polynomials is given using the formalism of the quadratic algebras.
- In Chapter 6 we develop two different triangulations associated with a space-time of topology $S_3 \times \mathbb{R}$. We provide some preparatory tools apt to investigate Lorentzian aspects of discrete models of quantum gravity.

List of publications

- V. Aquilanti; D. Marinelli & A. Marzuoli “Hamiltonian dynamics of a quantum of space: hidden symmetries and spectrum of the volume operator, and discrete orthogonal polynomials” *Journal of Physics A: Mathematical and Theoretical*, IOP Publishing, 2013, **46**, 175303
- R. W. Anderson; V. Aquilanti; A. C. P. Bitencourt; D. Marinelli & M. Ragni “The screen representation of spin networks: 2D recurrence, eigenvalue equation for 6j symbols, geometric interpretation and hamiltonian dynamics” - *Computational Science and Its Applications–ICCSA 2013*, Lecture Notes in Computer Science - Springer, 2013, 46-59
- V. Aquilanti; D. Marinelli & A. Marzuoli “Symmetric coupling of angular momenta, quadratic algebras and discrete polynomials” - To appear in *J. Physics: Conference Series* (2013)
- G. Immirzi & D. Marinelli “A practical look at Regge Calculus” – to appear in *Springer Proceeding in Physics*
- V. Aquilanti; D. Marinelli & A. Marzuoli. - “Volume operator and the Askey scheme” – in preparation.

Chapter 2

Recoupling theory and discretized geometry

In this chapter we review some aspects of the recoupling theory for angular momenta and of the Regge Calculus. There is no intention of writing a self-contained introduction to these topics because that would lead us too far, but we use this chapter to fix the notation and to introduce the reader to the reference framework of this thesis. We refer to Messiah's textbook [36, Chapter XIII], Biedenharn and Louck [37, 38] and the recent review [27] for the first part of this chapter. On Lorentzian Regge calculus there isn't yet an ultimate reference we could use. On the other hand, the Euclidean Regge Calculus has been treated by many authors. A precious review we refer to for a comprehensive bibliography and a summary of the state of the art on Regge Calculus until the 1990s is [39].

2.1 Recoupling theory of $SU(2)$ angular momentum

Given three angular momentum operators $\mathbf{J}_1, \mathbf{J}_2, \mathbf{J}_3$ –associated with three kinematically independent quantum systems– the Wigner–coupled Hilbert space of the composite system is an eigenstate of the total angular momentum

$$\mathbf{J}_1 + \mathbf{J}_2 + \mathbf{J}_3 =: \mathbf{J} \quad (2.1.1)$$

and of its projection J_z along the quantization axis. The degeneracy can be completely removed by considering binary coupling schemes such as $(\mathbf{J}_1 + \mathbf{J}_2) + \mathbf{J}_3$ and $\mathbf{J}_1 + (\mathbf{J}_2 + \mathbf{J}_3)$, and by introducing intermediate angular momentum operators defined by

$$(\mathbf{J}_1 + \mathbf{J}_2) =: \mathbf{J}_{12}; \quad \mathbf{J}_{12} + \mathbf{J}_3 = \mathbf{J} \quad (2.1.2)$$

and

$$(\mathbf{J}_2 + \mathbf{J}_3) =: \mathbf{J}_{23}; \quad \mathbf{J}_1 + \mathbf{J}_{23} = \mathbf{J}, \quad (2.1.3)$$

respectively. In Dirac notation the simultaneous eigenspaces of the two complete sets of commuting operators $\{\mathbf{J}_1^2, \mathbf{J}_2^2, \mathbf{J}_{12}^2, \mathbf{J}_3^2, \mathbf{J}^2, J_z\}$ and $\{\mathbf{J}_1^2, \mathbf{J}_2^2, \mathbf{J}_3^2, \mathbf{J}_{23}^2, \mathbf{J}^2, J_z\}$ are spanned respectively by basis vectors

$$|j_1 j_2 j_{12} j_3; jm\rangle \text{ and } |j_1 j_2 j_3 j_{23}; jm\rangle, \quad (2.1.4)$$

where j_1, j_2, j_3 are labels corresponding to the eigenvalues $(j_i + 1)j_i$ of the operator \mathbf{J}_i^2 , and m is the total magnetic quantum number with range $-j \leq m \leq j$ in integer steps eigenvalue of the operator J_z . Note that j_1, j_2, j_3 run over $\{0, \frac{1}{2}, 1, \frac{3}{2}, 2, \dots\}$ (labels of $SU(2)$ irreducible representations), while $|j_1 - j_2| \leq j_{12} \leq j_1 + j_2$ and $|j_2 - j_3| \leq j_{23} \leq j_2 + j_3$ (all quantum numbers are in \hbar units).

The Wigner $6j$ symbol expresses the transformation between the two schemes (2.1.2) and (2.1.3), namely

$$|j_1 j_2 j_{12} j_3; jm\rangle = \sum_{j_{23}} [(2j_{12} + 1)(2j_{23} + 1)]^{1/2} \begin{Bmatrix} j_1 & j_2 & j_{12} \\ j_3 & j & j_{23} \end{Bmatrix} |j_1 j_2 j_3 j_{23}; jm\rangle \quad (2.1.5)$$

apart from a phase factor¹. It follows that the quantum mechanical probability

$$P = [(2j_{12} + 1)(2j_{23} + 1)] \begin{Bmatrix} j_1 & j_2 & j_{12} \\ j_3 & j & j_{23} \end{Bmatrix}^2 \quad (2.1.6)$$

represents the probability that a system, prepared in a binary coupled state (2.1.2), where j_1, j_2, j_3, j_{12}, j have definite magnitudes, will be measured to be in the state associated with the coupling scheme (2.1.3).

The $6j$ symbol may be written as sums of products of four Clebsch–Gordan coefficients or their symmetric counterparts, the Wigner $3j$ symbols. The relations between $6j$ and $3j$ symbols are given explicitly by (see *e.g.* [40])

$$\begin{Bmatrix} a & b & c \\ d & e & f \end{Bmatrix} = \sum (-)^{\Phi} \begin{pmatrix} a & b & c \\ \alpha & \beta & -\gamma \end{pmatrix} \begin{pmatrix} a & e & f \\ \alpha & \epsilon & -\varphi \end{pmatrix} \begin{pmatrix} d & b & f \\ -\delta & \beta & \varphi \end{pmatrix} \begin{pmatrix} d & e & c \\ \delta & -\epsilon & \gamma \end{pmatrix} \quad (2.1.7)$$

where $\Phi = d + e + f + \delta + \epsilon + \varphi$. Here Latin letters stand for j -type labels (integer or half-integers non-negative numbers) while Greek letters denote the associated magnetic quantum numbers (each varying in integer steps between $-j$ and j , $j \in \{a, b, c, d, e, f\}$). The sum is over all possible values of $\alpha, \beta, \gamma, \delta, \epsilon, \varphi$ but only three summation indices being independent by definition, the lower string of quantum numbers in each $3j$ is such that the summation of the values must give zero.

On the basis of the above decomposition it can be shown that the $6j$ symbol is invariant under any permutation of its columns or under interchange the upper and lower arguments in each of any two columns. These algebraic

¹ Actually this expression should contain the Racah W -coefficient $W(j_1 j_2 j_3 j; j_{12} j_{23})$ which differs from the $6j$ by the factor $(-)^{j_1 + j_2 + j_3 + j}$. Recall that $(2j_{12} + 1)$ and $(2j_{23} + 1)$ are the dimensions of the representations labeled by j_{12} and j_{23} , respectively.

2.1. Recoupling theory of $SU(2)$ angular momentum

relations involve $3! \times 4 = 24$ different $6j$ with the same value and are referred to as *classical symmetries* as opposite to “Regge” symmetries to be introduced and discussed in Chapter 4. These algebraic symmetries naturally reflect the *tetrahedral symmetry*. Note first that each $3j$ (or Clebsch–Gordan) coefficient vanishes unless its j -type entries satisfy the triangular condition, namely $|b - c| \leq a \leq b + c$, *etc.*. This suggests that each of the four $3j$'s in (2.1.7) can be associated with either a 3-valent vertex or a triangle. Accordingly, there are two graphical representation of the $6j$ exhibiting its symmetry properties. Here we adopt the three-dimensional picture introduced in the seminal paper by Ponzano and Regge [3], rather than Yutsis' “dual” representation as a complete graph on four vertices [41]. Then the $6j$ is thought of as the surface solid tetrahedron T with edge lengths $\ell_1 = a + \frac{1}{2}, \ell_2 = b + \frac{1}{2}, \dots, \ell_6 = f + \frac{1}{2}$ in \hbar units² and triangular faces associated with the triads $(abc), (aef), (dbf), (dec)$. This implies in particular that the quantities $q_1 = a + b + c, q_2 = a + e + f, q_3 = b + d + f, q_4 = c + d + e$ (sums of the edge lengths of each face), $p_1 = a + b + d + e, p_2 = a + c + d + f, p_3 = b + c + e + f$ are all integer with $p_h \geq q_k$ ($h = 1, 2, 3, k = 1, 2, 3, 4$). The conditions addressed so far are in general sufficient to guarantee the existence of a non-vanishing $6j$ symbol, but they are not enough to ensure the existence of a geometric tetrahedron T living in Euclidean 3-space with the given edges. More precisely, T exists in this sense if (*and only if*, see the discussion in the introduction of [3]) its square volume $V(T)^2 \equiv V^2$, evaluated by means of the Cayley–Menger determinant, is positive.

The features of the “quantum tetrahedron” outlined above represent the foundations of a variety of results, some of which were discovered in the golden age of quantum mechanics and have been widely used in old and present applications to atomic and molecular physics.

2.1.1 Ponzano–Regge asymptotic formula

The Ponzano–Regge asymptotic formula for the $6j$ symbol reads [3]

$$\left\{ \begin{matrix} a & b & d \\ c & f & e \end{matrix} \right\} \sim \frac{1}{\sqrt{24\pi V}} \cos \left\{ \left(\sum_{r=1}^6 \ell_r \theta_r + \frac{\pi}{4} \right) \right\} \quad (2.1.8)$$

where the limit is taken for all entries $\gg 1$ (recall that $\hbar = 1$) and $\ell_r \equiv j_r + 1/2$ with $\{j_r\} = \{a, b, c, d, e, f\}$. V is the Euclidean volume of the tetrahedron T and θ_r is the angle between the outer normals to the faces which share the edge ℓ_r .

From a quantum mechanical viewpoint, the above probability amplitude has the form of a semiclassical (wave) function since the factor $1/\sqrt{24\pi V}$ is slowly varying with respect to the spin variables while the exponential is a rapidly

²The $\frac{1}{2}$ -shift is shown to be crucial in the analysis developed in [3]: for high quantum numbers (*i.e.* in the semiclassical limit) $[j(j+1)]^{1/2} \sim j + \frac{1}{2}$.

oscillating dynamical phase. Such kind of asymptotic behavior complies with Wigner's semiclassical estimate for the probability, namely $\left\{ \begin{smallmatrix} a & b & d \\ c & f & e \end{smallmatrix} \right\}^2 \sim 1/12\pi V$, to be compared with the quantum probability given in (2.1.6).

2.1.2 Racah hypergeometric polynomial

The generalized hypergeometric series, denoted ${}_pF_q$, is defined for p real or complex numerator parameters a_1, a_2, \dots, a_p , q real or complex denominator parameters b_1, b_2, \dots, b_q and a single variable z by

$${}_pF_q \left(\begin{matrix} a_1 & \dots & a_p \\ b_1 & \dots & b_q \end{matrix} ; z \right) := \sum_{n=0}^{\infty} \frac{(a_1)_n \dots (a_p)_n}{(b_1)_n \dots (b_q)_n} \frac{z^n}{n!}, \quad (2.1.9)$$

where $(a)_n = a(a+1)(a+2)\dots(a+n-1)$ denotes a rising factorial with $(a)_0 = 1$. If one of the numerator parameter is a negative integer, as actually happens in the formula below, the series terminates and the resulting function is a polynomial in z .

The key expression for relating the $6j$ symbol to hypergeometric functions is given by the well-known Racah sum rule (see *e.g.* [37, 38], topic 11 and [40], Ch. 9 also for the original references). The final form of the so-called *Racah polynomial* is written in terms of the ${}_4F_3$ hypergeometric function evaluated at $z = 1$ according to

$$\left\{ \begin{matrix} a & b & d \\ c & f & e \end{matrix} \right\} = \Delta(abe) \Delta(cde) \Delta(acf) \Delta(bdf) (-)^{\beta_1} (\beta_1 + 1)! \\ \times \frac{{}_4F_3 \left(\begin{matrix} \alpha_1 - \beta_1 & \alpha_2 - \beta_1 & \alpha_3 - \beta_1 & \alpha_4 - \beta_1 \\ -\beta_1 - 1 & \beta_2 - \beta_1 + 1 & \beta_3 - \beta_1 + 1 & \end{matrix} ; 1 \right)}{(\beta_2 - \beta_1)! (\beta_3 - \beta_1)! (\beta_1 - \alpha_1)! (\beta_1 - \alpha_2)! (\beta_1 - \beta_3)! (\beta_1 - \alpha_4)!}, \quad (2.1.10)$$

where

$$\beta_1 = \min(a + b + c + d; a + d + e + f; b + c + e + f)$$

and the parameters β_2, β_3 are identified in either way with the pair remaining in the 3-tuple $(a + b + c + d; a + d + e + f; b + c + e + f)$ after deleting β_1 . The four α 's are identified with any permutation of $(a + b + e; c + d + e; a + c + f; b + d + f)$. Finally, the Δ -factors in front of ${}_4F_3$ are defined, for any triad (abc) as

$$\Delta(abc) = \left[\frac{(a + b - c)! (a - b + c)! (-a + b + c)!}{(a + b + c + 1)!} \right]^{1/2}$$

Such a seemingly complicated notation is indeed the most convenient for the purpose of listing further interesting properties of the Wigner $6j$ symbol.

- The Racah polynomial is placed at the top of the Askey hierarchy including all of hypergeometric orthogonal polynomials of one (discrete or

continuous) variable [42]. Most commonly encountered families of special functions in quantum mechanics are obtained from the Racah polynomial by applying suitable limiting procedures, as recently reviewed in [43]. Such an unified scheme provides in a straightforward way the algebraic *defining relations* of the Wigner $6j$ symbol viewed as an orthogonal polynomial of one discrete variable, *cfr.* (2.1.10). By resorting to standard notation from the quantum theory of angular momentum, such defining relations are:

the Biedenharn–Elliott identity ($R = a + b + c + d + e + f + p + q + r$):

$$\begin{aligned} \sum_x (-)^{R+x} (2x+1) \begin{Bmatrix} a & b & x \\ c & d & p \end{Bmatrix} \begin{Bmatrix} c & d & x \\ e & f & q \end{Bmatrix} \begin{Bmatrix} e & f & x \\ b & a & r \end{Bmatrix} \\ = \begin{Bmatrix} p & q & r \\ e & a & d \end{Bmatrix} \begin{Bmatrix} p & q & r \\ f & b & c \end{Bmatrix}; \end{aligned} \quad (2.1.11)$$

the orthogonality relation (δ is the Kronecker delta)

$$\sum_x (2x+1) \begin{Bmatrix} a & b & x \\ c & d & p \end{Bmatrix} \begin{Bmatrix} c & d & x \\ a & b & q \end{Bmatrix} = \frac{\delta_{pq}}{(2p+1)}. \quad (2.1.12)$$

- Given the relation (2.1.10), the unexpected new symmetry of the $6j$ symbol discovered in 1958 by Regge [44] (see also [37, 40]) is recognized as a “trivial” set of permutations on the parameters α, β that leaves ${}_4F_3$ invariant.
- The Askey hierarchy of orthogonal polynomials can be extended to a q -hierarchy [42], on the top of which the q - ${}_4F_3$ polynomial stands. It is worth noting that the deformation parameter q was originally assumed by physicists to be a real number related to Planck constant h by $q = e^h$, and therefore it is commonly referred to as a ‘quantum’ deformation, while the ‘classical’, undeformed Lie group symmetry is recovered at the particular value $q = 1$. In application to quantum gravity models and topological quantum field theory, q is taken to be a complex root of unity, the case $q = 1$ being considered as the “trivial” one. We refer to [45, 46] for accounts on the theory of q -special functions and q -tensor algebras, respectively.

2.2 Regge Calculus

Regge Calculus is a dynamical theory of space-time introduced in 1961 by Regge as a discrete approximation for the Einstein theory of gravity [1]. The basic idea is to replace a smooth space-time with a collection of simplices. The collective dynamics of these geometric objects is driven by the Regge action and the dynamical variables are their edge lengths (which play the role of

the metric tensor of General Relativity). Simplices are the n -dimensional generalization of triangles and tetrahedra and are formally defined below. For the moment it suffices to say that they are convex pieces of space and they can be suitably glued together to build an extended geometric object *e.g.* triangles (or 2-simplices) glued together can form a 2-dimensional surface. An important point is that even if simplices are flat (so are “pieces” of space of zero curvature) the spaces they may generate, in general, are not.

Coming back to General Relativity, from a heuristic point of view we can think to build a (discrete) space-time gluing together pieces of 4-dimensional Minkowski spaces getting thus a generic, non-globally-flat space-time. Namely, we are associating to a space-time a piecewise-linear simplicial manifold (PL-manifold in short).

2.2.1 Basic definitions

We start with some basic definitions referring to [47, 48] for a more detailed exposition of the topological construction of the triangulations.

Definition 1. A subspace σ^i of an n -dimensional vector space V over the real numbers is an i -simplex if is the convex hull of a set of $i + 1$ points $\{\mathbf{v}_0, \dots, \mathbf{v}_i\}$ with $i \leq n$ which do not lie in a $(i - 1)$ affine subspace. In other terms:

$$\sigma^i := \left\{ \sum_{j=0}^i \lambda_j \mathbf{v}_j \mid \lambda_j \geq 0, \sum_{j=0}^i \lambda_j = 1, \mathbf{v}_j \in V \right\}.$$

A *face* τ of an i -simplex is any simplex whose vertices are a subset of those of σ^i and is denoted by $\tau < \sigma^i$.

Definition 2. A *locally finite simplicial complex* is a (possibly infinite) collection K of simplices in \mathbb{R}^n such that

- $\sigma \in K$ and $\tau < \sigma \Rightarrow \tau \in K$;
- $\sigma \in K$ and $\tau \in K \Rightarrow \sigma \cap \tau < \sigma$ and $\sigma \cap \tau < \tau$;
- each point in the polyhedron $|K| := \bigcup_{\sigma \in K} \sigma$ has a neighborhood which intersects only a finite number of simplices of K .

Definition 3. The *star* of a simplex σ is the union of all simplices in K of which σ is a face, namely

$$\text{St}(\sigma, K) = \{\tau \in K \mid \sigma < \tau\}.$$

The *link* is the union of all faces $\tau \in \text{St}(\sigma, K)$ such that $\tau \cap \sigma = \emptyset$.

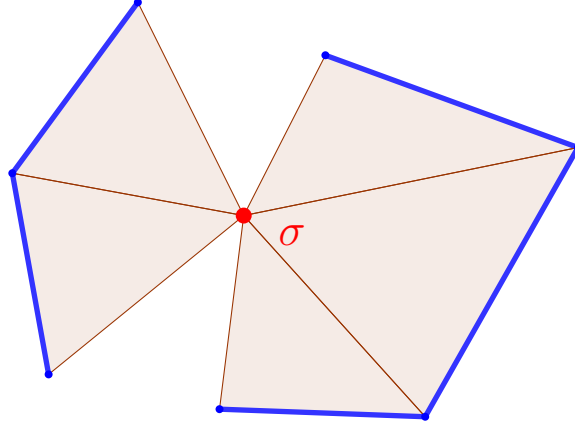


Figure 2.1: The link (in blue) of a 0-simplex (in red) in a 2-dimensional simplicial complex.

Definition 4. A map $f : K \rightarrow L$ of the simplicial complex K into the simplicial complex L is a triple $(|f|, K, L)$ where $|f| : |K| \rightarrow |L|$ is a continuous map of topological spaces.

The map $f : K \rightarrow L$ is said to be *linear* if it maps each simplex of K linearly into some simplex of L . The map is said *simplicial* if the image of each simplex of K is a simplex of L and a *simplicial isomorphism* if f^{-1} is also a simplicial map.

Definition 5. A *piecewise-linear homeomorphism* $f : K \rightarrow L$ is a map which is a simplicial isomorphism for some subdivision K' and L' of K and L .

Definition 6. A *piecewise-linear n -manifold* (or *PL-manifold*) is a polyhedron $\Delta_{\mathcal{M}} = |K|$ each point of which has a neighborhood, in $\Delta_{\mathcal{M}}$, PL-homeomorphic to an open set in \mathbb{R}^n .

As described above the PL-manifold is a fundamental ingredient for the Regge Calculus, but up to now this is only a topological object if we don't introduce a local metric in σ^n . A natural choice for \mathbb{R}^n would be the Euclidean metric $g_E(\mathbf{v}, \mathbf{w}) = (v^\mu - w^\mu)(v^\nu - w^\nu)\delta_{\mu\nu}$ (where the Einstein convention is adopted). This choice would lead to the Euclidean Regge Calculus. Recalling that the Minkowski space is a Lorentzian manifold whose underlying smooth manifold is \mathbb{R}^n and whose pseudo-Riemannian metric is at each point the Minkowski metric, we can locally endow each simplex with a Minkowski metric $g_\eta(\mathbf{v}, \mathbf{w}) = (v^\mu - w^\mu)(v^\nu - w^\nu)\eta_{\mu\nu}$ where $\eta = \text{diag}(-1, +1, +1, \dots, +1)$. In this way the PL-manifold inherits a global causal structure. We will focus on

the Lorentzian aspects of this manifold in Chapter 6. Once given everywhere a local metric, the structure of the PL-manifold can be determined by the set of the squared edge lengths of the simplicial complex $\{l_{e_i}^2\}_{e_i \in E}$ where E is the set of all 1-simplices in K . To introduce the remaining ingredients composing the Regge Calculus, in this section, we chose the Euclidean metric (from now we are tacitly assuming that $\Delta_{\mathcal{M}}$ is compact and without boundary).

In Regge view a space-time \mathcal{M} is treated as the polyhedron $\Delta_{\mathcal{M}}$ and the smooth geometry is replaced by a suitable PL geometry. Each n -simplex is flat and has a natural notion of n -dihedral angles which are functions of its (squared) edge lengths. Any n -simplex is itself endowed with an $(n-1)$ -dimensional PL-structure, so for each pair of $(n-1)$ -simplices there is a shared $(n-2)$ -simplex f . The dihedral angle θ_f is the angle between the normal vectors of the two $(n-1)$ -simplices that meet in f . In an n -dimensional simplicial complex an $(n-1)$ -simplex is shared by two n -simplices by definition; the $(n-2)$ -simplex is shared among several simplices so it is possible to define the deficit angle as follows

Definition 7. The *deficit angle* (or defect) ϵ_f at the $(n-2)$ -simplex f is

$$\epsilon_f := 2\pi - \sum_i \theta_f^i$$

where the sum is over all the n -simplices in $\text{St}(f, \Delta_{\mathcal{M}})$ and θ_f^i is the associated dihedral angle.

Now it is possible to introduce the Regge action, the counterpart of the Hilbert-Einstein action of General Relativity in Euclidean signature.

The Regge action is the functional associated with the simplicial PL-manifold $(\Delta_{\mathcal{M}}, \{l_j^2\})$ defined as

$$S_R [\{l_j^2\}] := \sum_f A_f \epsilon_f, \quad (2.2.1)$$

where the sum is over all the $(n-2)$ -simplices (in Regge Calculus literature called the “bones”), A_f is their natural volume of such a simplex evaluated with the Euclidean metric and ϵ_f is the deficit angle.

Finally we can say that a PL-manifold $(\Delta_{\mathcal{M}}, \{l_{e_i}\})$ in Regge Calculus represents a *discrete space-time* if it is an extremal of the Regge action plus possibly matter actions namely

$$\delta (S_R + S_M) = 0$$

where δ represents a suitable variation in the space of admissible lengths.

Jeff Cheeger, Werner Müller, and Robert Schrader in 1984 [49, 50] proved a local convergence in the sense of measures of the Regge action for an Euclidean PL-manifold to a scalar curvature of a smooth Riemannian manifold. They considered the Regge action as the scalar counterpart of the Lipschitz-Killing curvature [51].

2.2. Regge Calculus

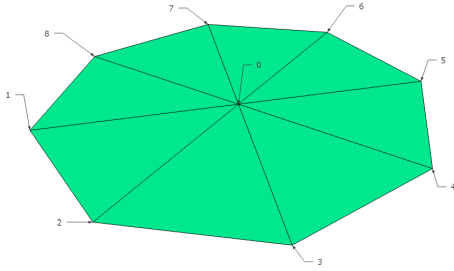


Figure 2.2: Simplicial tiling of a plane which form a 2-dimensional simplicial complex.

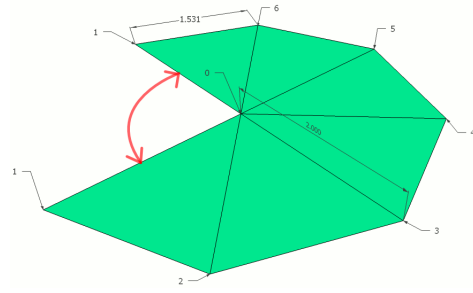


Figure 2.3: A geometric view of a simplicial complex with a non-null *deficit angle* at the central vertex (the two edges pointed by the arrow are identified).

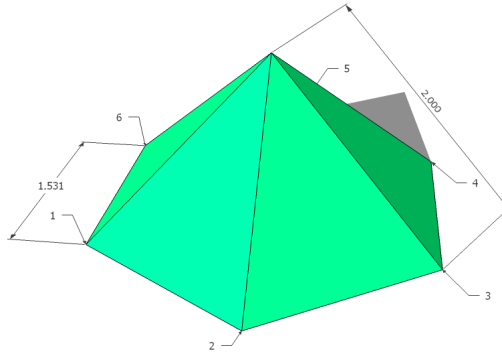


Figure 2.4: The simplicial complex of Fig. 2.3 embedded in \mathbb{R}^3

2.2.2 A heuristic viewpoint

Here we want to report an example proposed by Sorkin in 1974 [52] which gives a basic motivation of the assumption of Regge action 2.2.1 as the action for a discrete gravity. The idea is to evaluate the Einstein-Hilbert action for a four dimensional Minkowski space-time with a conic singularity residing in the tz -plane.

In a Minkowski space-time \mathcal{M} endowed with orthonormal coordinate base $\{t, x, y, z\}$ and flat metric $g_{\mu\nu} = \text{diag}(-, +, +, +)$ we can introduce a deficit angle in the xy -plane in the following way. It is convenient to move to polar coordinates

$$\begin{cases} x = r \cdot \cos(\gamma) & r \in [0, \infty); t, z \in \mathbb{R}. \\ y = r \cdot \sin(\gamma) & \gamma = [0, 2\pi) \end{cases}$$

Because of the periodicity of this coordinates for the γ variable, we have a natural identification of points with coordinate $\gamma = 0$ with points with coordinate $\gamma = 2\pi$. A conic singularity can be introduced identifying the points $\gamma = 0$

with $\gamma = 2\pi - \theta$, namely

$$\begin{cases} x = r \cdot \cos(k(\theta) \cdot \phi) & r \in [0, \infty); t, z \in \mathbb{R}. \\ y = r \cdot \sin(k(\theta) \cdot \phi) & \phi = [0, 2\pi) \end{cases}$$

where

$$k(\theta) \equiv 1 - \frac{\theta}{2\pi}.$$

It is now possible to evaluate the metric for this new manifold \mathcal{M}' , *i.e.*

$$g'_{\mu\nu} = g_{\rho\sigma} \frac{\partial x^\rho}{\partial x'^\mu} \frac{\partial x^\sigma}{\partial x'^\nu}$$

where

$$\begin{cases} x = r \cdot \cos(k(\theta) \cdot \phi) \\ y = r \cdot \sin(k(\theta) \cdot \phi) \end{cases} \quad \begin{cases} \frac{\partial x}{\partial r} = \cos(k \cdot \phi) \\ \frac{\partial x}{\partial \phi} = -k \cdot r \sin(k \cdot \phi) \\ \frac{\partial y}{\partial r} = \sin(k \cdot \phi) \\ \frac{\partial y}{\partial \phi} = r k \cos(k \cdot \phi) \end{cases}$$

and get $g'_{11} = g'_{rr} = \left(\frac{\partial x}{\partial r}\right)^2 + \left(\frac{\partial y}{\partial r}\right)^2 = \sin^2(k \cdot \phi) + \cos^2(k \cdot \phi) = 1$ $g'_{12} = g'_{r\phi} = \frac{\partial x}{\partial r} \frac{\partial x}{\partial \phi} + \frac{\partial y}{\partial r} \frac{\partial y}{\partial \phi} = -r \cos(k \cdot \phi) \sin(k \cdot \phi) + r \cos(k \cdot \phi) \sin(k \cdot \phi) = 0$ $g'_{22} = \left(\frac{\partial x}{\partial \phi}\right)^2 + \left(\frac{\partial y}{\partial \phi}\right)^2 = r^2 k^2$. The metric finally reads

$$g' = \begin{pmatrix} -1 & 0 & 0 & 0 \\ 0 & 1 & 0 & 0 \\ 0 & 0 & r^2 k^2 & 0 \\ 0 & 0 & 0 & 1 \end{pmatrix} = \begin{pmatrix} -1 & 0 & 0 & 0 \\ 0 & 1 & 0 & 0 \\ 0 & 0 & \left(1 - \frac{\theta}{2\pi}\right)^2 r^2 & 0 \\ 0 & 0 & 0 & 1 \end{pmatrix}.$$

This metric has a cuspid in the origin $r = 0$.

We can regularize the metric in $r \rightarrow 0$ introducing the function

$$e^{2\lambda(r)} = \begin{cases} r^2 & \text{if } r \rightarrow 0 \\ r^2 \left(1 - \frac{\theta}{2\pi}\right)^2 & \text{if } r \gg 0 \end{cases} \quad g' = \begin{pmatrix} -1 & 0 & 0 & 0 \\ 0 & 1 & 0 & 0 \\ 0 & 0 & e^{2\lambda(r)} & 0 \\ 0 & 0 & 0 & 1 \end{pmatrix}$$

and smoothing the cusp in $r \rightarrow 0$.

Christoffel symbols and curvature tensors can be easily calculated to arrive to the Ricci scalar

$$R = 2 \left(\lambda''(r) + (\lambda'(r))^2 \right) \\ \sqrt{-\det g'} = e^{\lambda(r)}.$$

The Einstein-Hilbert action

$$S_{EH} = \int_{\mathcal{M}} d^4x R \sqrt{-\det g'}$$

$$= -\frac{1}{16\pi} \int_{\mathcal{M}} d^4x \left[2e^\lambda \left(\lambda'' + (\lambda')^2 \right) \right] = -\frac{1}{16\pi} \int_{\mathcal{M}} d^4x \left[2 \frac{d^2 e^\lambda}{dr^2} \right]. \quad (2.2.2)$$

This integral can be solved by parts

$$\begin{aligned} & -\frac{1}{2} \int_0^\infty \int_0^{2\pi} dr d\phi 2 \cdot (e^{\lambda(r)})'' = -2\pi \int_0^\infty (e^{\lambda(r)})' dr \\ & = -2\pi (e^{\lambda(r)})' \Big|_0^\infty \Rightarrow \begin{cases} r=0 & e^\lambda = r \\ r \rightarrow \infty & e^\lambda = (1 - \frac{\theta}{2\pi}) \end{cases} \\ & = -2\pi \left(-1 + 1 - \frac{\theta}{2\pi} \right) = \theta \end{aligned}$$

so that

$$S_{EH} = -\frac{1}{16\pi} \iiint d\phi dr dz dt R \sqrt{-\det g'} = \frac{1}{8\pi} \theta \iint dz dt.$$

If the singularity were confined in a compact region, this action would not diverge and $\iint dz dt =: A$ would be the Euclidean area of the compact region.

Since any PL-manifold is flat almost everywhere, and the action is an additive quantity, we have a contributions to the Einstein-Hilbert action only from triangles with non-null deficit angle, so we can write the 4-dimensional *Regge Action* as

$$S_R = \frac{1}{8\pi} \sum_i A_i \varepsilon_i \quad (2.2.3)$$

where A_i is the (positive) area of the triangle i in the PL-manifold and ε_i is the deficit angle (or defect) associated to it .

2.2.3 Regge equations

In General Relativity the dynamical field is the metric tensor while in Regge Calculus its role is played by the collections of the squared edge lengths. In fact, the metric tensor is a symmetric tensor with $n(n-1)/2$ independent entries (where n is the dimension of the space-time) and $n(n-1)/2$ are also the number of edges in a n -simplicial complex (it coincides with the number of links in a complete graph because each vertex of a simplex is connected to all the other vertices by an edge). In particular, 4-simplex is completely determined by its 10 edge lengths. Thus the action has to be variated with respect to these (square) edge lengths of the simplicial complex, formally

$$\delta S_R + \delta S_M = 0 \quad \frac{1}{8\pi} \left(\sum_t \delta A_t \epsilon_t + \sum_t A_t \delta \epsilon_t \right) + \delta S_M$$

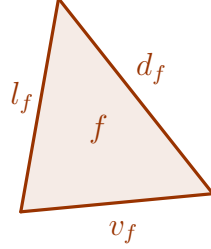


Figure 2.5: The triangle f with edge lengths $\{v_f, l_f, d_f\}$

where areas in terms of the edge lengths $\{v_t, l_t, d_t\}$ reads (Fig. 2.5)

$$A_{t.vld}^2 = \frac{1}{16} \left[(v_t^2 + l_t^2 - d_t^2)^2 - 4v_t^2 l_t^2 \right].$$

We get three implicit equations for each triangle of the simplicial complex.

$$\frac{1}{8\pi} \frac{\partial A}{\partial v_i} \epsilon_t = \frac{v_t}{16\pi A_t} (d_t^2 + l_t^2 - v_t^2) \epsilon_t \quad (2.2.4)$$

The second term (the variation of the defect ϵ_t) vanish as proved by Regge [1] thanks to the Schlafli identity which in Euclidean 4-space reads

$$\sum_t A_t (\delta \epsilon_t) = 0.$$

This leads to a overdetermined system of implicit equations, the solutions of which would be the set of edge lengths which fix the geometry of the discrete space-time. Such set of implicit equations are the discrete counterpart of the Einstein's differential equations, the equations of the gravitational field in General Relativity.

2.3 Discretized geometries and Quantum Gravity

Regge Calculus inspired and is at the base of almost all the present discretized model for a quantum theory of gravity for at least two reasons: firstly it is a discretized model, thus it represents a possible atomistic system typical of the quantum systems, in Einstein's words, from a letter to Hans Walter Dällenbach (one of his former students) written in 1916 [53]

But you have correctly grasped the drawback that the continuum brings. If the molecular view of matter is the correct (appropriate) one, i.e., if a part of the universe is to be represented by a finite

2.3. Discretized geometries and Quantum Gravity

number of moving points, then the continuum of the present theory contains too great a manifold of possibilities. I also believe that this too great is responsible for the fact that our present means of description miscarry with the quantum theory. The problem seems to me how one can formulate statements about a discontinuum without calling upon a continuum (space-time) as an aid; the latter should be banned from the theory as a supplementary construction not justified by the essence of the problem, which corresponds to nothing “real”. But we still lack the mathematical structure unfortunately. How much have I already plagued myself in this way!

Secondly, Regge himself with Ponzano noticed a deep connection between the Regge action (2.2.1), the asymptotic of the $6j$ symbol (2.1.8) and a path-integral formulation of gravity. In [3] (we refers to [54, 27, 55], for recent reviews) they defined the following *state sum*:

we denote by $\mathcal{T}^3(j) \rightarrow \mathcal{M}^3$ a particular triangulation of a closed 3-dimensional simplicial manifold \mathcal{M}^3 (of fixed topology) obtained by assigning $SU(2)$ spin variables $\{j\}$ to the edges of \mathcal{T}^3 . The assignment must satisfy a number of conditions, better illustrated if we introduce the *state functional* associated with $\mathcal{T}^3(j)$, namely

$$\mathbf{Z}[\mathcal{T}^3(j) \rightarrow \mathcal{M}^3; L] = \Lambda(L)^{-N_0} \prod_{A=1}^{N_1} (-1)^{2j_A} \mathbf{w}_A \prod_{B=1}^{N_3} \phi_B \left\{ \begin{matrix} j_1 & j_2 & j_3 \\ j_4 & j_5 & j_6 \end{matrix} \right\}_B \quad (2.3.1)$$

where N_0, N_1, N_3 are the number of vertices, edges and tetrahedra in $\mathcal{T}^3(j)$, $\Lambda(L) = 4L^3/3C$ (L is a fixed length and C an arbitrary constant), $\mathbf{w}_A = (2j_A + 1)$ are the dimensions of irreducible representations of $SU(2)$ which weigh the edges, $\phi_B = (-1)^X$, $X = \sum_{p=1}^6 j_p$ and $\{:::\}_B$ are $6j$ symbols to be associated with the tetrahedra of the triangulation. Finally, the Ponzano–Regge *state sum* is obtained by summing over triangulations corresponding to all assignments of spin variables $\{j\}$ bounded by the cut-off L

$$\mathbf{Z}_{PR}[\mathcal{M}^3] = \lim_{L \rightarrow \infty} \sum_{\{j\} \leq L} \mathbf{Z}[\mathcal{T}^3(j) \rightarrow \mathcal{M}^3; L], \quad (2.3.2)$$

where the cut-off is formally removed by taking the limit in front of the sum.

The state sum 2.3.2 can be approximated replacing the sum by an integral and the $6j$ with its asymptotic formula (2.1.8):

$$\mathbf{Z}_{PR}[\mathcal{M}^3] \approx \frac{1}{\sqrt{24\pi}} \int \prod_A^{N_1} dj_A (2j_A + 1) (-1)^{2j_A} \prod_{B=1}^{N_3} \phi_B \frac{1}{\sqrt{V_k}} \cos \left(\sum_{l \in B} j_l \theta_l^B + \frac{\pi}{4} \right). \quad (2.3.3)$$

the dominant contribution to the integral comes from the points of stationary phase, which are given by

$$\sum_B (\pi - \theta_i^B) = 2\pi$$

where the sum is over all tetrahedra B meeting on edge i , namely $B \in \text{Sr}(i)$. Now (2.3.3) contains a term of the form

$$\int \prod_A^{N_1} dj_A (2j_A + 1) \exp \left(i \sum_{A'}^{N_1} j_l \left(2\pi - \sum_{B \in \text{Sr}(i)} (\pi - \theta_l^B) \right) \right) =$$

$$\int \prod_A^{N_1} dj_A (2j_A + 1) \exp \left(i \sum_{A'}^{N_1} j_l \epsilon_l \right)$$

which looks precisely like a Feynman path-integral (sum over histories) with in the exponent the Regge Calculus action in three dimension:

$$\int \prod_A^{N_1} d\mu_A \exp(i S_R)$$

with $S_R := \sum_{A'}^{N_1} j_A \epsilon_A$

the 3-dimensional counterpart of (2.2.1) with an appropriate measure in the space of edge lengths $d\mu_i(j_i)$. Once realized that this Ponzano-Regge approach can be related to a theory of three-dimensional gravity started many attempts to generalize it to four-dimension. Barrett-Crane model or spin-foam model have been formulated. We have to notice that these Ponzano-Regge-like models cannot be considered complete theories of quantum gravity. Most of the studies have been developed in an Euclidean gravity framework (the gauge group is in fact $SU(2)$ rather than the complexified Lorentz group $SL(2, \mathbb{C})$) and a generalizations to the Lorentzian case is at the moment not fully accomplished. Related to this, Ponzano-Regge-like models does not involve the causal structure typical of General Relativity, in fact the the cosine in expression (2.3.3) generates also other contributes to the path-integral of the form $\int \prod_A^{N_1} d\mu_A \exp(-i S_R)$ which have not a straightforward interpretation in a causal theory. This issue infects also recent Lorentzian spinfoam and has to be considered an open problem (see *e.g.* [56]). Lorentzianity and causality are basically also the motivations for our last Chapter 6 where we build simple triangulations and develop their Lorentian structure.

Chapter 3

The volume operator and symmetric coupling of $SU(2)$ angular momenta

3.1 The Volume Operator

Historically, the volume operator was introduced to find convenient symmetric bases for three-particle states as alternative to the binary coupling schemes of section 2.1. The total angular momentum of the system is a self-adjoint operator defined here as

$$\mathbf{J}_T := \mathbf{J}_1 + \mathbf{J}_2 + \mathbf{J}_3, \quad (3.1.1)$$

where \mathbf{J}_1 , \mathbf{J}_2 and \mathbf{J}_3 are the operators associated to the angular momentum of each of the three particles subsystems. Chakrabarti and then Lèvy-Leblond, Lèvy-Nahas [6, 7] proposed a fifth operator

$$K := \mathbf{J}_1 \cdot (\mathbf{J}_2 \times \mathbf{J}_3) \quad (3.1.2)$$

which commutes with \mathbf{J} and has been proven [7] to form a complete set of commuting observables together with the operators: $(\mathbf{J}_1)^2$, $(\mathbf{J}_2)^2$, $(\mathbf{J}_3)^2$, $(\mathbf{J}_T)^2$ and \mathbf{J}_z (the component of the total angular momentum with respect to the quantization axis). In this way K would substitute the operator $(\mathbf{J}_{12})^2$ or the operator $(\mathbf{J}_{23})^2$ which are the squares of the observables $\mathbf{J}_{12} := \mathbf{J}_1 + \mathbf{J}_2$ and $\mathbf{J}_{23} := \mathbf{J}_2 + \mathbf{J}_3$ in solving the degeneracy in the total space (\mathbf{J}_T, J_z) . Quantum numbers j_{12} and j_{23} associated with eigenvalues of these operators correspond to the standard binary coupling of section 2.1. On the other hand, the eigenstates of the operator K provide a basis for the Hilbert space in which all the components of the system are treated all on the same footing.

3.1.1 Formal definition

The Hilbert space where the operators will act is a subspace of $\mathcal{H} = \bigotimes_{i=1}^4 \mathcal{H}_i$. Each Hilbert space is determined by the highest-weight j_i representation of the group $SU(2)$ of dimension $(2j_i + 1)$. For future use we redefine the total angular momenta as $\mathbf{J}_T \equiv -\mathbf{J}_4$ and define each operator in this Hilbert space as:

$$\mathbf{J}_i := \bigotimes_{j=1}^4 \mathbb{I} (1 - \delta_{ij} + \delta_{ij} \mathbf{J})$$

(e.g. $\mathbf{J}_3 = \mathbb{I} \otimes \mathbb{I} \otimes \mathbf{J} \otimes \mathbb{I}$). The definition given in (3.1.1) now becomes a closure relation which reduces the Hilbert space to be

$$\ker \left(\sum_{i=1}^4 \mathbf{J}_i \right) =: \mathcal{H} \subset \mathcal{H}.$$

Definition 8. The *volume operator* K is a linear operator acting on the Hilbert space \mathcal{H} according to

$$K := \mathbf{J}_1 \cdot (\mathbf{J}_2 \times \mathbf{J}_3) = \sum_{\mu\nu\gamma} \epsilon_{\mu\nu\gamma} J_1^\mu J_2^\nu J_3^\gamma.$$

where $\epsilon_{\mu\nu\gamma}$ is the 3-dimensional completely antisymmetric Levi-Civita symbol.

Remark 9. K is a scalar operator so it is invariant under spatial rotations and under the action of the $SU(2)$ group. The eigenstates of this operator span the intertwiner space of the four representation spaces (in fact, the spectrum is non-degenerate [7]).

Using the binary coupling scheme described in Chapter 2, namely projecting the operator on an intermediate basis $\mathbf{J}_{12} := \mathbf{J}_1 + \mathbf{J}_2$, the volume operator K is represented as a tridiagonal matrix. This matrix picture plays a fundamental role and allows a direct numerical inspection as provided in Section 3.2.5.

Theorem 10. *The volume operator expressed in the binary basis of the intermediate operator \mathbf{J}_{12} is an antisymmetric tridiagonal matrix*

$$\begin{aligned} \mathcal{M}_{\mathbf{J}_{12}\mathbf{J}_{12}}(K) &\equiv \langle j'_{12} | K | j_{12} \rangle = \\ &= \begin{bmatrix} 0 & i\alpha_{\ell_{\min}+1} & & & \\ -i\alpha_{\ell_{\min}+1} & \ddots & \ddots & & \\ & \ddots & 0 & i\alpha_{\ell_{\max}} & \\ & & -i\alpha_{\ell_{\max}} & 0 & \end{bmatrix} \end{aligned} \quad (3.1.3)$$

where

$$\alpha_\ell = \frac{F(\ell; j_1 + \frac{1}{2}; j_2 + \frac{1}{2}) F(\ell; j_3 + \frac{1}{2}; j_4 + \frac{1}{2})}{\sqrt{(2\ell + 1)(2\ell - 1)}}, \quad (3.1.4)$$

with $F(a, b, c) = \frac{1}{4} \sqrt{(a+b+c)(a+b-c)(a-b+c)(-a+b+c)}$ is the Heron's formula for the area of a triangle having edge lengths a, b, c .

3.1. The Volume Operator

Proof. see [7] for a proof of the theorem. □

3.1.2 The eigenvalue problem

The eigenstates of the volume operator are found as solutions of the formal equation

$$K \left| \begin{array}{cc} j_1 & j_2 \\ j_3 & j_4 \end{array} ; k \right\rangle = \lambda \left(\begin{array}{cc} j_1 & j_2 \\ j_3 & j_4 \end{array} ; k \right) \left| \begin{array}{cc} j_1 & j_2 \\ j_3 & j_4 \end{array} ; k \right\rangle \quad (3.1.5)$$

where here $\lambda(k)$ denotes the eigenvalue associated to the k th eigenstate. A ‘generalized’ recoupling coefficients can be defined as a unitary map relating the binary coupling j_{12} to the symmetric coupling k . Note that in (3.1.5) (and in the rest of the thesis) the magnetic quantum number m (eigenvalue of J_4^z) is dropped since all matrix elements of (scalar, vector) operators are invariant owing to the Wigner-Eckart theorem. Moreover, once the Hilbert space is fixed, we use $\lambda(k)$ and $|k\rangle$ in place of those in (3.1.5), omitting the labels of the representations

Definition 11. A *generalized recoupling coefficient* $\Psi_{j_{12}}^k$ is a unitary map such that

$$|k\rangle = \sum_{j_{12}} \Psi_{j_{12}}^k |j_{12}\rangle$$

where the sum is over admissible values of j_{12} restricted by suitable triangular conditions.

This map is simply the matrix of the eigenstates of K expanded in the j_{12} -basis and, for a direct calculation, we just have to diagonalize the matrix (3.1.3). In fact,

$$\sum_{j'_{12}} \langle j_{12} | K | j'_{12} \rangle \Psi_{j'_{12}}^k = \lambda(k) \Psi_{j_{12}}^k \quad (3.1.6)$$

with

$$\Psi_{j_{12}}^k = \langle j_{12} | k \rangle. \quad (3.1.7)$$

The binary coupling j_{12} is actually equivalent to the binary coupling j_{23} in the sense that:

Theorem 12. *The generalized recoupling coefficient referred to the binary coupling j_{23} is*

$$\overline{\Psi_{j_{23}}^k} = \sum_{j_{12}} \langle k | j_{12} \rangle \langle j_{12} | j_{23} \rangle = \sum_{j_{12}} \overline{\Psi_{j_{12}}^k} \langle j_{12} | j_{23} \rangle \quad (3.1.8)$$

Proof. The proof is straightforward: we use the identity for j_{23} on (3.1.7), $\Psi_{k_{12}}^k = \langle k | j_{12} \rangle = \sum_{j_{23}} \langle k | j_{23} \rangle \langle j_{23} | j_{12} \rangle$, then we can verify directly (3.1.8) through the identity:

$$\langle k | j_{12} \rangle = \sum_{j_{23}} \sum_{j'_{12}} \langle k | j'_{12} \rangle \langle j'_{12} | j_{23} \rangle \langle j_{23} | j_{12} \rangle \quad (3.1.9)$$

□

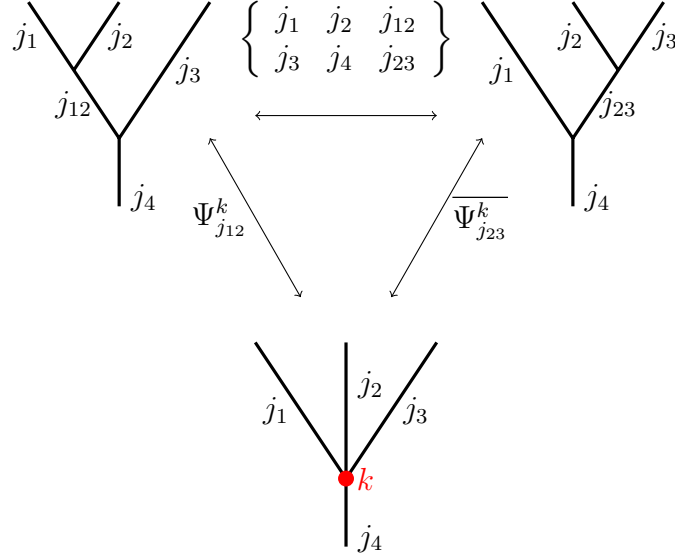


Figure 3.1: Symmetric re-coupling scheme

In Eq. (3.1.8), $\langle j_{12}|j_{23} \rangle$ is the usual $6j$ symbol (as introduced in (2.1.5)) up to a normalization factor:

$$\begin{aligned} \langle j_1, j_2 j_3, j_{23}, j_4, m | j_1, j_2 j_{12} j_3, j_4, m' \rangle &= \\ &= \delta_{mm'} \sqrt{(2j_{12} + 1)(2j_{23} + 1)} (-1)^{\sum_i j_i} \left\{ \begin{array}{ccc} j_1 & j_2 & j_{12} \\ j_3 & j_4 & j_{23} \end{array} \right\} \end{aligned}$$

and we could use either the resolution of the identity for j_{12} -basis and j_{23} -basis or the orthogonality of $6j$ symbols. Eq. (3.1.9) reveals another interesting aspect of the symmetric recoupling, namely

$$\sum_k \Psi_{j_{12}}^k \overline{\Psi_{j_{23}}^k} = \langle j_{12}|j_{23} \rangle \quad (3.1.10)$$

as illustrated in the diagram of Fig. 3.1.

3.1.3 The three-term recurrence relations

The eigenvalue problem for the operator K expressed in one of the binary basis is equivalent to find a solution for the three-term recursion relation [57, 12] ($i = \sqrt{-1}$)

$$\lambda_k \Psi_\ell^k + i \alpha_{\ell+1} \Psi_{\ell+1}^k - i \alpha_\ell \Psi_{\ell-1}^k = 0 \quad (3.1.11)$$

once the eigenvalue in (3.1.5) $\lambda(k) =: -\lambda_k$ is known and the boundary condition are provided. This equivalence between the two problems is straightforward when the matrix representation of the operator in question is tridiagonal. In this case (3.1.11) follows directly from (3.1.6) and (3.1.3).

3.1. The Volume Operator

The correct boundary conditions are found noticing that the coefficient (3.1.4) are bounded by the vanishing value

$$\alpha_{\ell_{\min}} = \alpha_{\ell_{\max}+1} = 0, \quad (3.1.12)$$

where

$$\ell_{\min} := \max(|j_1 - j_2|, |j_3 - j_4|) \leq \ell \leq \min(j_1 + j_2 + 1, j_3 + j_4 + 1). \quad (3.1.13)$$

Then the following boundary conditions

$$\begin{cases} \Psi_{\ell_{\min}-1} = \Psi_{\ell_{\max}+1} = 0 \\ \Psi_{\ell_{\min}} = \Psi_0 \end{cases} \quad \Psi_0 \in \mathbb{C}$$

have to hold, where Ψ_0 is an arbitrary constant corresponding to the freedom in the choice of the normalization of the eigenvectors.

Note that the second zero of α_ℓ in (3.1.12) does not fix the dimension of the vector space where Ψ_ℓ^k lives. In fact, the last two relations reduce to

$$\begin{aligned} \Psi_{\ell_{\max}}^k &= \frac{i \alpha_{\ell_{\max}}}{\lambda_k} \Psi_{\ell_{\max}-1}^k \\ \Psi_{\ell_{\max}+1}^k &= \frac{i \alpha_{\ell_{\max}+2}}{\lambda_k} \Psi_{\ell_{\max}+2}^k \end{aligned}$$

so that, if the number of equations in (3.1.11) is not fixed, the equivalence with the matrix representation (3.1.3) must be imposed through the boundary condition $\Psi_{\ell_{\max}+1} = 0$.

The next step consists in introducing a very useful change of phase. The relation (3.1.11) can be transformed into a real three-term recurrence relation with the following changes of phases

$$\Psi_\ell^k = (i)^{\ell-\ell_{\min}} \psi_\ell^k.$$

ψ_ℓ^k can also be seen as the eigenfunction of an operator results of the action of a suitable unitary (diagonal) transformation on the volume operator. Then (3.1.11) becomes

$$\lambda_k \psi_\ell^k + \alpha_{\ell+1} \psi_{\ell+1}^k + \alpha_\ell \psi_{\ell-1}^k = 0. \quad (3.1.14)$$

A different transformation already well known in literature [6, 7], related to the time-reversal symmetry of the system [30, 19] is

$$\begin{aligned} \psi_\ell^k &= (-1)^{\ell-\ell_{\min}} \phi_\ell^k \quad (3.1.15) \\ \lambda_k (-1)^{\ell-\ell_{\min}} \phi_\ell^k &= -\alpha_{\ell+1} (-1)^{\ell-\ell_{\min}} \phi_{\ell+1}^k - \alpha_\ell (-1)^{\ell-\ell_{\min}} \phi_\ell^k \\ -\lambda_k \phi_\ell^k &= \alpha_{\ell+1} \phi_{\ell+1}^k + \alpha_\ell \phi_\ell^k. \end{aligned}$$

Then, if λ_k is an eigenvalue of the system, also $-\lambda_k$ is an eigenvalue and the corresponding eigenfunction is $\phi_\ell = (-1)^{\ell-\ell_{\min}} \Psi_\ell$. Therefore when the dimension of the volume operator is odd a couple of eigenvalues have to coincide and also zero is an eigenvalue of the system.

It is convenient now to fix a convention for the index k .

3. The volume operator and symmetric coupling of $SU(2)$ angular momenta

- If present, let fix the index $k = 0$ for the zero eigenvalue $\lambda_0 = 0$ and let $k > 0$ if $\lambda_k > 0$.
- Using the symmetry (3.1.15) we can impose $\lambda_k = -\lambda_{-k}$.
- Finally, we chose to sort the monotonic increasing sequences of the positive eigenvalues so that

$$\lambda_1 = \min \{\lambda_k\}_{k=1}^{k_{\max}} \quad \text{and} \quad \lambda_{k_{\max}} = \max \{\lambda_k\}_{k=1}^{k_{\max}}$$

where k_{\max} is $D/2$ for a volume operator of even dimension D or $(D-1)/2$ for a volume operator of odd dimension D .

3.2 The semiclassical limit and geometry of quadrilaterals

We are going to look for the geometrical features shared by volume operator by studying the semiclassical limit of the three-term recurrence relation established in the previous section using a suitable WKB method introduced by Braun [29] for the analysis of discrete systems.

3.2.1 From three-term recurrence relations to second order finite difference equations

Starting from a symmetric three-term recurrence relation as given in (3.1.14), we can introduce a set of operators which turn the relation into a finite difference equation defined on an evenly-spaced lattice $\ell = 0, 1, \dots$

We can introduce the first order finite difference operators

$$\Delta := (\hat{T}_+ - \mathbb{I}) := \psi_\ell \mapsto \psi_{\ell+1} - \psi_\ell \quad \nabla := (\mathbb{I} - \hat{T}_-) := \psi_\ell \mapsto \psi_\ell - \psi_{\ell-1}$$

where \hat{T}_\pm are the shift operators $\psi_\ell \mapsto \psi_{\ell\pm 1}$, and the second order finite difference operator

$$\nabla\Delta := (\hat{T}_+ - 2 \cdot \mathbb{I} + \hat{T}_-) := \psi_\ell \mapsto \psi_{\ell+1} - 2\psi_\ell + \psi_{\ell-1}.$$

Finally, we can write the corresponding difference equation according to

$$\begin{aligned} (f_2 \nabla\Delta + f_1 \Delta + f_0) \psi_\ell^k &= 0 \\ \text{with } f_2 &\equiv \alpha_{\ell-1}; \quad f_1 \equiv \alpha_{\ell+1} - \alpha_{\ell-1}; \quad f_0 \equiv -\lambda_k + \alpha_{\ell+1} + \alpha_{\ell-1} \\ [\alpha_{\ell-1} \nabla\Delta + (\alpha_{\ell+1} - \alpha_{\ell-1}) \Delta + (\alpha_{\ell+1} + \alpha_{\ell-1})] \psi_\ell^k &= -\lambda_k \psi_\ell^k \end{aligned} \quad (3.2.1)$$

and thus we recover an eigenvalue problem with real (not purely imaginary as they were originally) operator.

3.2.2 Schrödinger-like approach and semiclassical limit

Recalling that momentum operators in quantum mechanics are the generator of translations, Braun [29] suggested the introduction of a momentum operator in a discrete setting as the generator of (evenly spaced) shifts, and the associated exponential map as the shift operator:

$$\hat{\varphi} = -i \frac{\partial}{\partial \ell} \quad \hat{T}_{\pm} = e^{\pm i \hat{\varphi}}.$$

From the three-term relation (3.1.14), using the above definition, we can extract a Hamiltonian operator. In this way the study of the volume operator becomes a stationary Schrödinger-like problem for

$$\hat{H} = (\alpha_{\ell} e^{-i \hat{\varphi}} + \alpha_{\ell+1} e^{i \hat{\varphi}}). \quad (3.2.2)$$

whose operatorial form will allow a direct inspection of the semiclassical limit.

The system described by the Hamiltonian operator (3.2.2) is one dimensional and (ℓ, φ) are the associated canonical coordinates. We should remember that j_i s and ℓ are quantum numbers associated to angular momenta, namely they would be expressed in units of \hbar , the Plank constant. The conditions $\{j_i \gg 1\}_{i=1}^4$ and $\ell \gg 1$ denote the regime where macroscopic effects occur. In particular, we can consider it a consistent semiclassical limit if the operator acting on a well behaved function is slowly varying, and this is actually the case:

Lemma 13. *In the limit $\ell \gg 1$, α_{ℓ} is a slowly varying function, given by*

$$\frac{\alpha_{\ell}}{\alpha_{\ell+1}} = 1 - 3 \left(\frac{1}{\ell} \right) + 6 \left(\frac{1}{\ell} \right)^2 + O \left(\left(\frac{1}{\ell} \right)^3 \right). \quad (3.2.3)$$

Lemma 13 allows to replace α_{ℓ} and $\alpha_{\ell+1}$ with their midpoint value, so the Eq. 3.2.2 becomes

$$\hat{H} = \alpha_{\ell+\frac{1}{2}} \left(\frac{\alpha_{\ell}}{\alpha_{\ell+\frac{1}{2}}} e^{-i \hat{\varphi}} + \frac{\alpha_{\ell+1}}{\alpha_{\ell+\frac{1}{2}}} e^{i \hat{\varphi}} \right) \approx \alpha_{\ell+\frac{1}{2}} (e^{-i \hat{\varphi}} + e^{i \hat{\varphi}}). \quad (3.2.4)$$

Therefore in the continuous limit when $\{j_i \gg 1\}_{i=1}^4$ and $\ell \gg 1$ the Hamiltonian operator (3.2.2) can be associated to the classical Hamiltonian function

$$\begin{aligned} H'(\ell, \varphi) &= 2 \alpha_{\ell+\frac{1}{2}} \cos \varphi = \\ H'(\ell, \varphi) &= \frac{\cos \varphi}{\ell \sqrt{1 + \frac{1}{\ell}}} F\left(\ell + \frac{1}{2}; j_2 + \frac{1}{2}; j_1 + \frac{1}{2}\right) F\left(\ell + \frac{1}{2}; j + \frac{1}{2}; j_3 + \frac{1}{2}\right) \end{aligned} \quad (3.2.5)$$

where $F(a, b, c)$ is the Heron's formula.

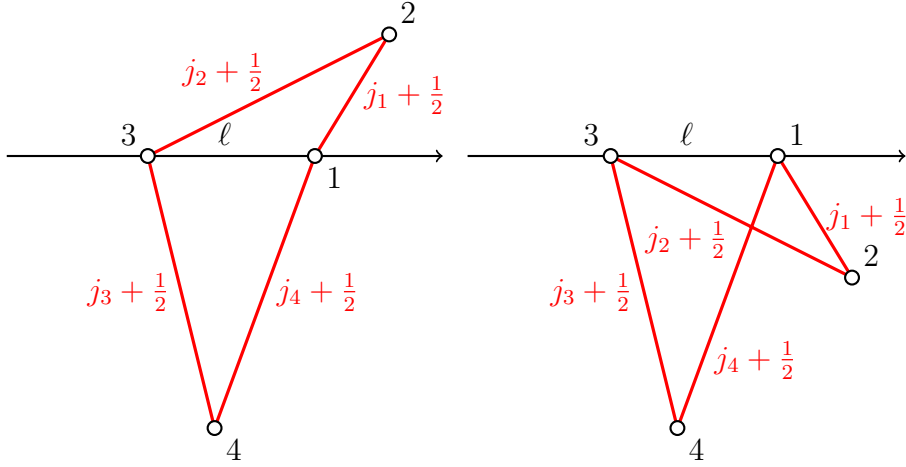


Figure 3.2: Planar quadrilaterals associated with α_ℓ . Here $j_1 = 14$, $j_2 = 27$, $j_3 = 28$, $j_4 = 29$; $\ell = 17$

Remark. It is worth to stress that, up to the third order, the expansion (3.2.3) does not depend on the value of the other parameters $\{j_i\}_{i=1}^4$: Lemma 13 does not need the condition $\{j_i \gg 1\}_{i=1}^4$, thus we might think that this condition is not needed to study the semiclassical regime. Since the range of ℓ is not arbitrary but given by (3.1.13), the condition $\ell \gg 1$ restrict the admissible values of the parameters $\{j_i\}_{i=1}^4$. They have to satisfy the conditions $\min(j_1 + j_2 + 1, j_3 + j_4 + 1) \gg 1$ and $\max(|j_1 - j_2|, |j_3 - j_4|) \gg 1$. In case $\{j_i \gg 1\}_{i=1}^4$ the first condition is always satisfied while the second must be imposed. There are still cases in which this semiclassical limit hold e.g. when $j_1, j_3 \gg 1$ and $j_2, j_4 \not\gg 1$: these cases will be treated in Chapter 5.

3.2.3 Semiclassical geometry of the volume operator

As shown in Chapter 2, the recoupling theory of $SU(2)$ group is pervaded by Euclidean geometry and the symmetric recoupling is not an exception. The coefficients α_ℓ defined in (3.1.4) and considered as functions of the parameters $\{j_i\}_{i=1}^4$ and ℓ (i.e. $\alpha(j_1, j_2, j_3, j_4; \ell)$), can be associated with quadrilaterals represented in Fig.3.2. In fact, if we restrict to values of α_ℓ real (that is the case for the volume operator for $SU(2)$ group), the Heron's formulas are areas of two triangles: one with edge lengths $j_1 + \frac{1}{2}$, $j_2 + \frac{1}{2}$ and ℓ ; the other with $j_3 + \frac{1}{2}$, $j_4 + \frac{1}{2}$ and ℓ (see (3.2.5)). Thus, up to isometries of the plane, four quadrilateral can be associated to α_ℓ (Fig. 3.2) which reduce to two once conveying that the edge j_i and j_{i+2} ($i \in \mathbb{N} \pmod{4}$) share no vertices (namely, they are opposite). Zeros of α_ℓ occur when at least one of the triangle is degenerate.

The quadrilateral introduced above determines the domain of definition of the function in the space of parameters $\{j_i\}_{i=1}^4$: they have to satisfy quadrilat-

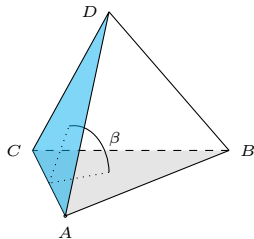


Figure 3.3: Tetrahedron with dihedral angle β .

eral inequalities. Of course, triangular inequalities set the range of ℓ to be as in Eq. (3.1.13).

The volume of a tetrahedron, being a function of six parameters, can be expressed in several ways. For the tetrahedron in Fig. 3.3 the 'orientated' volume is given by the well known formula

$$V_{ABCD} = \frac{2}{3} \mathcal{A}_{ABC} \mathcal{A}_{ACD} \frac{\sin(\beta)}{\ell_{AC}} \quad (3.2.6)$$

where \mathcal{A}_{ABC} and \mathcal{A}_{ACD} are respectively the areas of the triangles ABC and ACD , ℓ_{AC} is the length of the common edge and β is the dihedral angle between these two faces. The classical Hamiltonian (3.2.5) ($\ell \gg 1$) is seen to be necessarily proportional to the Euclidean volume of the tetrahedron up to a switch of the angular variable. Actually, the two triangles form a quadrilateral which does not lie in a plane, but rather creased along the edge ℓ of a dihedral angle $(\frac{\pi}{2} - \varphi) =: \beta$. Adding the edge opposite to ℓ , the quadrilateral becomes a geometric tetrahedron. Clearly, the two quadrilaterals in Fig. 3.2 would represent two degenerate cases for the volume of the tetrahedron occurring *e.g.* when $\varphi = \frac{\pi}{2}$ or $\varphi = \frac{3\pi}{2}$.

Note that the same geometrical analysis and semiclassical construction hold had we chosen the binary basis j_{23} to expand the volume operator. The main difference is that the two triangles form creasing the quadrilateral along the other diagonal and thus different triangular relations have to be satisfied.

3.2.4 Equations of motion and potential functions

Now we have the geometrical picture to control and understand the volume operator in terms of a classical dynamical system.

The classical canonical variables (ℓ, φ) obey the Hamilton's equations

$$\frac{d\ell}{dt} = \frac{\partial H'}{\partial \varphi} = -2\alpha_{\ell+\frac{1}{2}} \sin \varphi \quad \frac{d\varphi}{dt} = -\frac{\partial H'}{\partial \ell}. \quad (3.2.7)$$

During the classical motion, the diagonal ℓ and the dihedral angle φ change their value preserving the "energy" of the system. The result is a geometric

configuration (the hall of a tetrahedron, so to speak) changing continuously its shape but preserving its volume as a constant of motion.

Quantum mechanics extends the domain of the canonical variables to regions of phase space classically not allowed. Boundaries of these regions are the so-called potential-energy curves particularly important in applications. They are defined as turning points, namely the points where for each value of energy the classical “speed” changes sign. From (3.2.7) this happens when the momentum φ is either 0 or π

$$U^+(\ell) = H'(\ell, 0) = -U^-(\ell) = H'(\ell, \pi) = 2\alpha_\ell. \quad (3.2.8)$$

We will see in the next section that the above conditions define closed curved in the ℓ -energy plane. These curves have the physical meaning of torsional-like potential functions viewing the quadrilaterals in Fig. 3.2 as a three dimensional mechanical systems.

At each value of ℓ , the possible values E' of the Hamiltonian are bounded by

$$U^- \leq E' \leq U^+$$

and the eigenvalues λ_k of the quantum system are bounded by

$$\min U^- \leq \lambda_k \leq \max U^+ \quad (3.2.9)$$

as proven in [28].

3.2.5 Numerical studies

Through a numerical simulation developed in Python using the SciPy libraries [58] (in particular NumPy), it is possible to directly explore the behaviour of the quantum operator (3.2.2). In Fig. 3.4 are reported two example of spectra of the volume operator. The horizontal lines represent the eigenvalue λ_k , the curves are the caustics (the turning points of the semiclassical analysis) defined in (3.2.8), which limit the classically allowed region (in red U_ℓ^+ , in blue U_ℓ^-).

As can be seen, the eigenvalues are symmetrically distributed with respect to the $E' = 0$ value (which is itself an eigenvalue if the dimension of the volume operator is odd) as a consequence of the transformation (3.1.15). This transformation implies also the oscillatory behaviour of the eigenvector associated to the maximum of the eigenvalues, namely $= (-1)^{\ell - \ell_{\min}} \psi_\ell^{-k_{\max}}$.

The extrema of U_ℓ^+ and U_ℓ^- bound the spectrum, as discussed in the previous section (3.2.9).

Regions of parameter space where the semiclassical limit described in subsection 3.2.2 does not apply, manifest irregular behaviour of the potential functions such as the appearance of cusps as documented in Fig. 3.5. We will see later that this behaviour correspond to particular cases of the parameter space in which the action of the Regge symmetry is trivial.

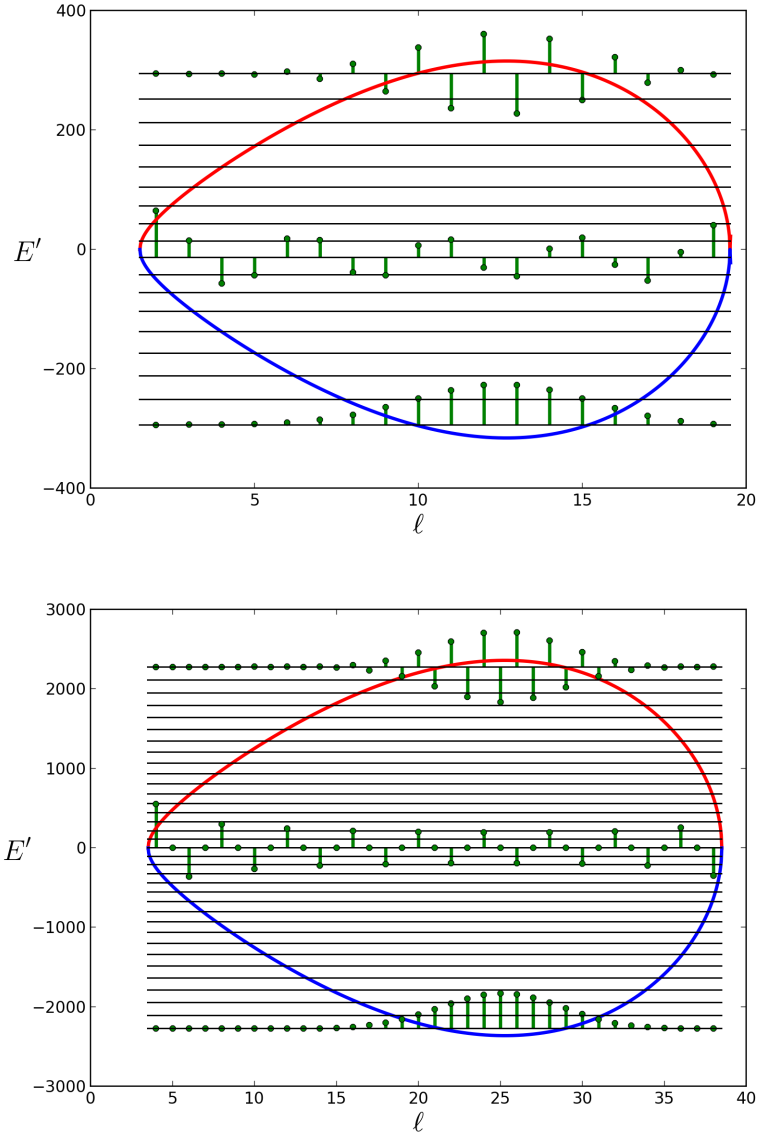


Figure 3.4: Plot of the spectra of the volume operator, three of the eigenvectors and potential-energy functions.

Upper: parameters $j_1, j_2, j_3, j_4 = 8.5, 10.5, 13.5, 14.5$ or $s, u, r, v = 23.5, -4.5, 1.5, 0.5$. (variables s, u, r, v are defined in Chap. 4.) Lower: all four parameters are doubled. In green the stick graph of the eigenfunctions (unnormalized). In red U_ℓ^+ , in blue U_ℓ^- defined in (3.2.8).

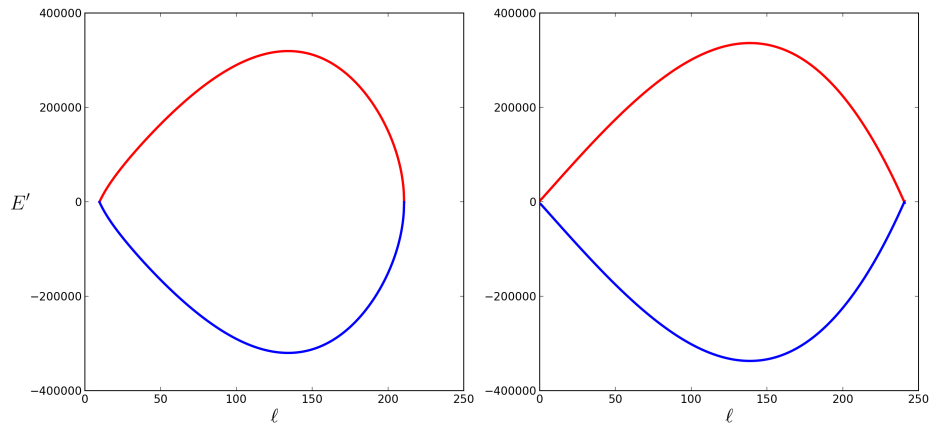


Figure 3.5: Potential functions U^+ and U^- are shown for two particular cases. In the left panel, $j_1, j_2, j_3, j_4 = 100.0, 110.0, 130.0, 140.0$, $v = 0$, the so called “tangential” quadrilateral, while on the right $j_1 = j_2 = j_3 = j_4 = 120.0$ the “ex-tangential” quadrilateral.

Chapter 4

Regge Symmetries

In 1958 Regge [44] found that Clebsch-Gordan coefficients possess a discrete symmetry group of 72 elements, much bigger than the group of 12 elements which was already known and have a manifest physical meaning. A few months later, Regge [32] found that also the $6j$ symbol has a discrete symmetry group wider than the one we introduced in Chap 2. The new transformations he introduced are now called Regge symmetries. Since it is possible to consider any Clebsch-Gordan coefficients as a particular limit of the parameters of the $6j$ symbols, defining Regge symmetries for the latter is actually sufficient. In the original notation [32]:

$$\begin{aligned}
 \left\{ \begin{array}{ccc} a & b & c \\ d & e & f \end{array} \right\} &= \left\{ \begin{array}{ccc} a & \frac{b+c+e-f}{2} & \frac{b+c+f-e}{2} \\ d & \frac{b+c+f-e}{2} & \frac{b+c-f+e}{2} \end{array} \right\} = \\
 &= \left\{ \begin{array}{ccc} \frac{a+c+f-d}{2} & b & \frac{a+c+f-f}{2} \\ \frac{c+d+f-a}{2} & e & \frac{a+d+f-e}{2} \end{array} \right\} = \left\{ \begin{array}{ccc} \frac{a+b+e-d}{2} & \frac{a+b+d-e}{2} & c \\ \frac{b+d+e-a}{2} & \frac{a+d+e-b}{2} & f \end{array} \right\} = \\
 &= \left\{ \begin{array}{ccc} \frac{b+e+c-f}{2} & \frac{a+f+c-d}{2} & \frac{a+d+b-e}{2} \\ \frac{b+f+e-c}{2} & \frac{c+d+f-a}{2} & \frac{a+d+e-b}{2} \end{array} \right\} = \left\{ \begin{array}{ccc} \frac{b+c+f-e}{2} & \frac{a+c+d-f}{2} & \frac{a+b+e-d}{2} \\ \frac{f+e+c-b}{2} & \frac{a+d+f-e}{2} & \frac{d+e+b-a}{2} \end{array} \right\}.
 \end{aligned} \tag{4.0.1}$$

Later, Ponzano and Regge in [3] introduced the asymptotic formula for the $6j$ symbol (2.1.8). This formula, as reviewed in subsection 2.1.1, links a $6j$ with an Euclidean tetrahedron and the classical symmetries of the $6j$ s are just relabeling of the edges of the Euclidean tetrahedron. The Regge symmetry, on the other hand, changes the values of the entries of a $6j$ so it involves two different tetrahedra (tetrahedra are uniquely determined by their edge lengths).

Ponzano and Regge found that the two tetrahedra corresponding to two $6j$ s related by a Regge symmetry, have the same volume (in this way they found a new set of equivolume tetrahedra). Moreover, they proved that the phase of the asymptotic formula, namely the argument of the cosine in (2.1.8) (the Regge action for the tetrahedra), is also the same for the two tetrahedra.

Roberts in 1999 [26] recognized that these two properties are sufficient to prove that two tetrahedra related by a Regge symmetry are scissor congruent¹.

To better understand this symmetry we start studying its action on the geometry of quadrilaterals.

4.1 Definition of Regge symmetry

Let us consider a real parameter space of dimension 4, namely the space of vectors $\mathbf{v} = (a, b, c, d)$.

Definition 14. The Regge symmetry, or Regge transformation, is the map

$$\mathcal{R} : (a, b, c, d) \mapsto (s - a, s - b, s - c, s - d) \quad (4.1.1)$$

$$\text{where } s := \frac{1}{2}(a + b + c + d), \quad (4.1.2)$$

s is called the semi-perimeter.

A first interesting feature of this transformation is that it maps integers to integers and half-integers to half-integers.

Moreover, being the Regge symmetry a linear transformation in the parameter space, it has a matrix representation which turns out to be very useful in what follows, namely

$$R := \frac{1}{2} \begin{pmatrix} -1 & 1 & 1 & 1 \\ 1 & -1 & 1 & 1 \\ 1 & 1 & -1 & 1 \\ 1 & 1 & 1 & -1 \end{pmatrix}$$

so that

$$R\mathbf{v} = \mathbf{v}' = \begin{pmatrix} s - a \\ s - b \\ s - c \\ s - d \end{pmatrix}.$$

R is a symmetric orthogonal matrix ($\in O(4)$); its determinant is -1 and it is obviously an involution, namely

$$RR = \mathbb{I}$$

For a 6-dimensional parameter space, the case associated with the analysis of the $6j$ symbol, the Regge transformation actually keeps a subspace invariant. In fact, the first two lines of the collection of equalities in (4.0.1) can be

¹Two polyhedra are scissors congruent if one may be dissected into finitely-many sub-polyhedra which may be reassembled to form the other.

4.1. Definition of Regge symmetry

obtained applying by the transformations

$$\begin{aligned}
 R_3 &:= \frac{1}{2} \begin{pmatrix} -1 & 1 & 1 & 1 & 0 & 0 \\ 1 & -1 & 1 & 1 & 0 & 0 \\ 1 & 1 & -1 & 1 & 0 & 0 \\ 1 & 1 & 1 & -1 & 0 & 0 \\ 0 & 0 & 0 & 0 & 2 & 0 \\ 0 & 0 & 0 & 0 & 0 & 2 \end{pmatrix} & R_2 &:= \frac{1}{2} \begin{pmatrix} -1 & 1 & 0 & 0 & 1 & 1 \\ 1 & -1 & 0 & 0 & 1 & 1 \\ 0 & 0 & 2 & 0 & 0 & 0 \\ 0 & 0 & 0 & 2 & 0 & 0 \\ 1 & 1 & 0 & 0 & -1 & 1 \\ 1 & 1 & 0 & 0 & 1 & -1 \end{pmatrix} \\
 R_1 &:= \frac{1}{2} \begin{pmatrix} 2 & 0 & 0 & 0 & 0 & 0 \\ 0 & 2 & 0 & 0 & 0 & 0 \\ 0 & 0 & -1 & 1 & 1 & 1 \\ 0 & 0 & 1 & -1 & 1 & 1 \\ 0 & 0 & 1 & 1 & -1 & 1 \\ 0 & 0 & 1 & 1 & 1 & -1 \end{pmatrix} & & (4.1.3)
 \end{aligned}$$

acting on the vector $\tilde{\mathbf{v}} = (a, d, b, e, c, f)$.

In this vector space, the classical symmetries (associated with the tetrahedral group, see Chapter 2) can be implemented as permutation matrices, *e.g.* the exchange of the first and the second column

$$\begin{Bmatrix} a & b & c \\ d & e & f \end{Bmatrix} \rightarrow \begin{Bmatrix} b & a & c \\ e & d & f \end{Bmatrix}$$

reads

$$P_{12}^{col} = \begin{pmatrix} 0 & 0 & 1 & 0 & 0 & 0 \\ 0 & 0 & 0 & 1 & 0 & 0 \\ 1 & 0 & 0 & 0 & 0 & 0 \\ 0 & 1 & 0 & 0 & 0 & 0 \\ 0 & 0 & 0 & 0 & 1 & 0 \\ 0 & 0 & 0 & 0 & 0 & 1 \end{pmatrix}.$$

We can easily see that the Regge transformations R_2 and R_3 are direct consequence of the classical symmetries plus the transformation R_1 in (4.1.3). In fact it can be easily checked that

$$R_2 = P_{12}^{col} R_1 (P_{12}^{col})^T,$$

and the same holds for R_3 once defined the permutation matrix P_{13}^{col} which exchanges the first and the third column. Note that P_{23}^{col} is not independent and can be expressed as $P_{23}^{col} = P_{13}^{col} P_{12}^{col} P_{13}^{col} = P_{12}^{col} P_{13}^{col} P_{12}^{col}$.

The functional equalities of the $6j$ written in the last line of (4.0.1) (defining the associated transformations R_4 and R_5) cannot be obtained through a classical symmetry plus a Regge transformation but they would correspond to a pair of Regge transformations. Introducing the classical symmetry transformation P_{12}^{row} which exchange the rows of two elements

$$P_{12}^{row} \triangleright \begin{Bmatrix} a & b & c \\ d & e & f \end{Bmatrix} \rightarrow \begin{Bmatrix} d & e & c \\ a & b & f \end{Bmatrix},$$

the transformation R_4 is expressed as

$$R_4 = P_{13}^{col} P_{12}^{col} P_{12}^{row} R_1 R_2 = P_{13}^{col} P_{12}^{col} P_{12}^{row} R_1 P_{12}^{col} R_1 P_{12}^{col}.$$

It worth noting that the following commutation relations hold for the Regge transformations on the six dimensional parameter space:

$$[P_{ij}^{row}, R_k] = 0 \quad [P_{ij}^{row}, P_{ij}^{col}] = 0 \quad \forall i, j, k = 1, 2, 3 \quad (4.1.4)$$

$$[P_{lm}^{col}, R_n] = 0 \quad \forall l, m, n = 1, 2, 3 \quad \vee l \neq m \neq n \neq l. \quad (4.1.5)$$

For completeness we report that the matrix R_5 is

$$R_5 \sim R_2 R_1$$

where the symbol \sim means: up to classical symmetries acting on the transformation from the left.

The algebra defined in formula (4.1.4) and (4.1.5) is a matrix realization in the space of parameters of the symmetry group (with 144 elements) of the $6j$ symbol. Regge [32] found that this group is isomorphic to the direct product of the symmetric group on four and three elements, namely $S_4 \times S_3$ (see [32]).

Using the notation introduced in Definition 14, we can express the $6j$ s in the last line of (4.0.1) in terms of three semi-perimeters. This simplifies the formula according to

$$\left\{ \begin{array}{ccc} s_1 - f & s_2 - d & s_3 - e \\ s_1 - c & s_2 - a & s_3 - b \end{array} \right\} = \left\{ \begin{array}{ccc} s_1 - e & s_2 - f & s_3 - d \\ s_1 - b & s_2 - c & s_3 - a \end{array} \right\}$$

where

$$s_1 := \frac{1}{2}(b + c + e + f), \quad s_2 := \frac{1}{2}(a + c + d + f) \quad s_3 := \frac{1}{2}(a + b + d + e).$$

4.2 The geometry of tetrahedra and associated quadrilaterals

The geometry underlying the Regge symmetry has at present no satisfactory geometric explanation. What follows is an analysis of some basic features associated with Euclidean aspects of this symmetry. In Chapter 2 we have described the relation between $6j$ and the geometry of a tetrahedron. A Regge transformation as in Definition 14 acts on a subset of the parameter space of the $6j$ which corresponds indeed to a quadrilateral (two opposite edges, namely that they don't share a vertex, are invariant under the symmetry action).

4.2. The geometry of tetrahedra and associated quadrilaterals

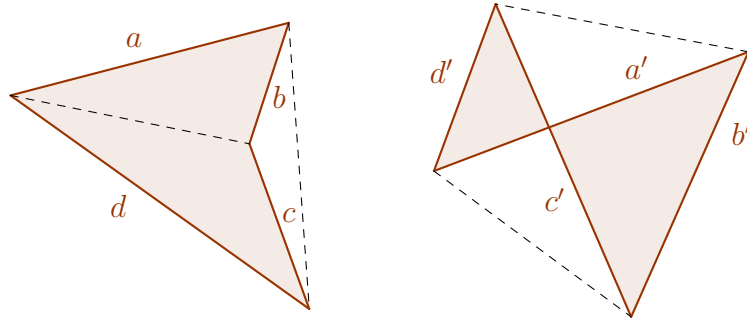


Figure 4.1: On the left, a simple quadrilateral; on the right, a non simple one.

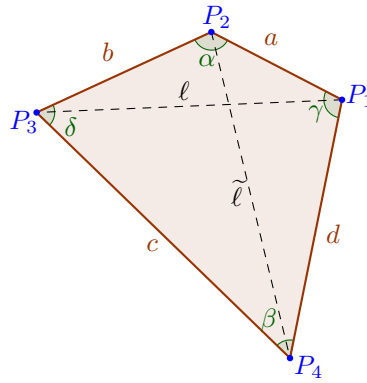


Figure 4.2: Convex quadrilateral

4.2.1 Quadrilaterals and their Regge conjugate

Planar quadrilaterals are quadrilaterals, namely sets of 4 edges and 4 vertices where each vertex is shared by two edges, embedded in an Euclidean plane and can be classified in two different categories [59]: *simple* and *not simple* (Fig. 4.1). *Simple quadrilaterals* are those without consecutive edges lying on the same line (we call the latter *degenerate* or *triangular* case) and without two edges intersecting (these configurations can be better understood as being part of a degenerate, flattened tetrahedron). All other quadrilaterals in the plane are termed *not simple*.

In this section we will consider only *simple* quadrilaterals.

We have already mentioned that, given four edge lengths, there exist an infinite number of planar quadrilaterals. In general, they cannot be always smoothly deformed into each other, so the space of shapes of quadrilaterals is a very interesting mathematical object (see *e.g.* [60, 61, 62]).

The (squared) area of the convex planar quadrilateral represented in Fig. 4.2 is given by the Bretschneider's Formula [63]:

$$\begin{aligned} (\mathcal{A}_{1234})^2 &= (s-a)(s-b)(s-c)(s-d) - abcd \cos^2\left(\frac{\gamma+\delta}{2}\right) = \\ &= (s-a)(s-b)(s-c)(s-d) - abcd \cos^2\left(\frac{\alpha+\beta}{2}\right), \end{aligned}$$

where $s = \frac{1}{2}(a+b+c+d)$ is indeed the semi-perimeter. The Regge transformation acting on the edge lengths of this quadrilateral (keeping the angle γ, δ fixed) is $\mathcal{R} : (a, b, c, d) \mapsto (a', b', c', d')$ and we will prove that it generates another quadrilateral (Sec. 4.2.1.1). This new quadrilateral has the same semi-perimeter of the previous one and area given by

$$(\mathcal{A}'_{1'2'3'4'})^2 = a'b'c'd' \cos^2\left(\frac{\gamma+\delta}{2}\right)$$

Therefore the two areas are equal only if (and only if)

$$\begin{aligned} a'b'c'd' &= abcd \\ (a+b-c-d)(a-b+c-d)(a-b-c+d)(a+b+c+d) &= 0 \end{aligned} \quad (4.2.1)$$

(this expression will be used and clarified later).

Theorem 15. *The action of the Regge transformation on the shape of a planar quadrilateral with edge lengths (a, b, c, d) and diagonal ℓ , assuming ℓ fixed, keeps invariant the second diagonal $\tilde{\ell}$ of the quadrilateral. the semi-perimeter s is invariant too.*

The proof of the theorem is postponed to the end of this section.

An alternative formula for the squared area of quadrilaterals is the Coolidge's formula, written in terms of the diagonals of the quadrilateral [63], here recasted in a convenient way as

$$(\mathcal{A}_{1234})^2 = (s-a)(s-b)(s-c)(s-d) - \frac{1}{4}(ac+bd)^2 + \frac{1}{4}(\tilde{\ell})^2 \quad (4.2.2)$$

Theorem 16. *The action of the Regge transformation on the squared area of a quadrilateral reads*

$$\mathcal{R} \triangleright (\mathcal{A}_{1234})^2 = (\mathcal{A}'_{1'2'3'4'})^2 + s u r v,$$

where the new variables u, r and v are defined as follows:

$$\begin{cases} s := \frac{1}{2}(a+b+c+d) \\ u := \frac{1}{2}(a+b-c-d) \\ v := \frac{1}{2}(a-b-c+d) \\ r := \frac{1}{2}(a-b+c-d) \end{cases} \cdot \quad (4.2.3)$$

4.2. The geometry of tetrahedra and associated quadrilaterals

Remark 17. In terms of the new variables (4.2.3), expression (4.2.1) can be recasted as

$$a' b' c' d' - a b c d = s u r v,$$

and Theorem 16 and expression (4.2.1) together imply that the area of the Regge transformed quadrilateral coincides with the area of the original one if at least one of the new variables (4.2.3) is zero.

We will see later further algebraic and geometrical properties of these new variables and how they are crucial to get insight into the Regge transformation.

Theorem 18. *The product of the area of two triangles sharing an edge ℓ is invariant under the action of the Regge transformation on its edges, namely*

$$F(a, b, \ell) F(c, d, \ell) = F(a', b', \ell) F(c', d', \ell) \quad (4.2.4)$$

Proof. The term on the right-hand side of the equation (4.2.4), making the Heron's formula explicit, reads

$$\begin{aligned} & \frac{1}{16} [(2s - a - b + \ell)(2s - a - b - \ell)(-a + b + \ell)(a - b + \ell) \times \\ & \quad \times (2s - c - d + \ell)(2s - c - d - \ell)(-c + d + \ell)(c - d + \ell)]^{1/2} = \\ & = \frac{1}{16} [(c + d + \ell)(c + d - \ell)(-a + b + \ell)(a - b + \ell) \times \\ & \quad \times (a + b + \ell)(a + b - \ell)(-c + d + \ell)(c - d + \ell)]^{1/2} \end{aligned}$$

that coincides with the left hand side. \square

4.2.1.1 Quadrilateral inequalities

From here on, we generalize our analysis to not necessarily planar quadrilateras, namely quadrilaterals embedded in Euclidean space with dimension $d \geq 3$.

Given four real numbers, they cannot in general be associated to the edge lengths of a quadrilateral because they have to satisfy the quadrilateral inequalities [64, 30], namely an edge length cannot be larger than the sum of all the other edge lengths (actually, this is true for any polyhedron in Euclidean spaces of any dimension). Let's denote the real numbers $\{l_i\}_{i=1}^4$: the quadrilateral inequality reads

$$l_j \leq \sum_{\substack{i=1 \\ i \neq j}}^4 l_i \Rightarrow l_j \leq p - l_j \Rightarrow l_j \leq s \quad j = 1, \dots, 4 \quad (4.2.5)$$

where p is the perimeter and s the semi-perimeter. If the four real numbers $\{l_i\}_{i=1}^4$ which satisfy (4.2.5) are changed by a Regge transformation into $\{l_i^R\}_{i=1}^4 = \mathcal{R} \triangleright \{l_i\}_{i=1}^4$, these new quantities can be associated to another quadrilateral, in fact $l_j^R = s - l_j \leq s$, and this holds if $\{l_i\}_{i=1}^4$ are positive.

4.2.1.2 A convention

It is now convenient to introduce a convention for the labels associated to the edges of the quadrilaterals. This convention will simplify (with no loss of generality) all calculations in the next sections.

- Assume we have four edge lengths $\{l_i\}_{i=1}^4$ and the following “opposition relation”: edge i is opposed to edge $j = i + 2, \pmod 4$. Let’s call $\{l_i^R\}_{i=1}^4 := \mathcal{R} \triangleright \{l_i\}_{i=1}^4$ with the same opposition relation. Define

$$a := \min \left(\{l_i\}_{i=1}^4, \{l_i^R\}_{i=1}^4 \right) \quad (4.2.6)$$

and denote the Regge transformed edge length by $a' = s - a$. In this way we choose to associate unprimed labels with edges of the quadrilateral having the shorter edge. Primed letters are assigned to the Regge transformed edges.

- The second step consists in associating the label c to the edge opposite to a (from here on, with an abuse of language, we will use the label of the edge also to express its edge length).
- Finally, d is chosen to be the edge with maximum length between the two remaining edges.

So we have the following set of inequalities

$$a \leq b \leq d \leq s,$$

where $s = \frac{1}{2}(a + b + c + d)$ and in particular the last inequality derives from (4.2.5).

Theorem 19. *Given a, b, d and adopting the convention above, c is constrained by*

$$d - (b - a) \leq c \leq d + (b - a) \quad (4.2.7)$$

Proof. From (4.2.6) we have that $c' \geq a$ and $d' \geq a$ (constraints given by $b' \geq a$ are weaker).

$$\begin{aligned} a + b - c + d &\geq 2a \Rightarrow c \leq d + b - a \\ a + b + c - d &\geq 2a \Rightarrow c \geq d - b + a \end{aligned}$$

□

The quadrilateral depicted in Fig. 4.2 is labeled following the above convention.

Note that we can also write (4.2.7) in the form $b' \leq c \leq a'$. If c is not in this range we simply have that (4.2.6) is not true, thus we are not really applying the convention. Another trivial consequence of the convention is that

$$a' \geq b' \geq d'.$$

We will see in the next subsection that the constraints on c , having considered also the Regge transformed quadrilateral, are crucial in the search for further geometric features.

4.2. The geometry of tetrahedra and associated quadrilaterals

4.2.1.3 Triangular inequalities

In section 3.2.3 we have been interested in quadrilaterals embedded in three dimensional Euclidean space formed by two triangles sharing an edge. Here we revise the analysis in [30] in terms of the convention 4.2.1.2 to study the not planar quadrilateral and which are the constraints its edges have to satisfy. To this end, consider the two triangles $\{a, b, \ell\}$ and $\{c, d, \ell\}$ glued together along the edge ℓ and assume a opposite to c .

Here we require that a, b, c, d respect the convention introduced in the previous subsection and we will see later how to make it completely general, namely true also in the cases which do not comply with the convention itself. If we complete the tetrahedron with the edge $\tilde{\ell}$, the same quadrilateral can be formed by two different triangles $\{d, a, \tilde{\ell}\}$ and $\{b, c, \tilde{\ell}\}$, still with a opposite to c .

Triangular inequalities constrain the edges ℓ and $\tilde{\ell}$ to be

$$\begin{aligned} \ell_{\min} &\leq \ell \leq \ell_{\max} \\ \tilde{\ell}_{\min} &\leq \tilde{\ell} \leq \tilde{\ell}_{\max} \end{aligned}$$

where

$$\begin{aligned} \ell_{\min} &= \max(|b - a|, |d - c|); & \ell_{\max} &= \min(b + a, c + d) \\ \tilde{\ell}_{\min} &= \max(|c - b|, |d - a|); & \tilde{\ell}_{\max} &= \min(c + b, d + a). \end{aligned}$$

Thus for ℓ_{\min} we have $b - a > d - c$ which can be read in terms of primed lengths $a' - b' > c' - d'$.

Theorem 20. $\ell_{\min} = b - a$ and $\ell_{\max} = b + a$

Proof. In our convention $b > a$ so we have

$$\begin{cases} b - a > d - c & \text{if } d > c \\ b - a > c - d & \text{if } c > d \end{cases}$$

using (4.2.7) we get

$$\begin{cases} d - c < b - a \\ c - d < b - a \end{cases} \Rightarrow |d - c| \leq b - a.$$

while $b + a < c + d$ by definition. □

Theorem 21. $\tilde{\ell}_{\min} = d - a$ and $\tilde{\ell}_{\max} = d + a$

Proof. In our convention $d > a$ so we have

$$\begin{cases} c - b < d - a & c > b \\ b - c < d - a & c < b \end{cases} \Rightarrow \begin{cases} c - d < b - a & c > b \\ b + a < d + c & c < b. \end{cases}$$

The first line is always satisfied by (4.2.7) while the second one is granted by definition. \square

As a consequence of Theorems 20 and 21 we have that both the ranges of ℓ and $\tilde{\ell}$ are given by $2a$.

Appendix: proof of Theorem 15

Proof. The area of a convex planar quadrilateral in terms of its edges and a diagonal ℓ is simply the sum of the areas of the two triangles $F(a, b, \ell) + F(c, d, \ell)$ and must be equal to (4.2.2), so that

$$\begin{aligned} (\mathcal{A}_{1234})^2 &= F(a, b, \ell)^2 + F(c, d\ell)^2 + 2F(a, b, \ell)F(c, d\ell) = \\ &= (s-a)(s-b)(s-c)(s-d) - \frac{1}{4} \left(ac + bd + \tilde{\ell} \right) \left(ac + bd - \tilde{\ell} \right). \end{aligned}$$

Since it is possible to write $\tilde{\ell}$ as

$$\begin{aligned} \tilde{\ell}^2 &= -\frac{8}{\ell^2} F(a, b, \ell)F(c, d\ell) + \\ &\quad - \frac{1}{2\ell^2} \left((a-b)(a+b)(c-d)(c+d) + (a^2 + b^2 + c^2 + d^2)\ell^2 - \ell^4 \right), \end{aligned}$$

We get

$$\begin{aligned} (a+b)(c+d) &= (a'+b')(c'+d') \\ a^2 + b^2 + c^2 + d^2 &= a'^2 + b'^2 + c'^2 + d'^2 = \mathbf{v}^2 \end{aligned} \quad (4.2.8)$$

which implies that $\tilde{\ell}$ is invariant under the Regge transformation. \square

4.2.2 The tetrahedron and its Regge conjugate

Let's see now how the Regge transformation acts on a tetrahedral shape. Formulas (4.0.1) and the association between $6j$ symbol and an Euclidean tetrahedron tell us that any Regge transformation acts on four edges of a tetrahedron keeping a pair of opposite edges unchanged. The Regge-transformed tetrahedra is called 'conjugate' for the reason explained in the next section.

Theorem 22. *Consider a tetrahedron with edge lengths $(a, b, c, d; \ell, \tilde{\ell})$. The dihedral angle at the edge ℓ , denoted Θ_ℓ , between two triangles $\{a, b, \ell\}$ and $\{c, d, \ell\}$ is invariant under the action of the Regge transformation*

$$\mathcal{R}_1 \triangleright (a, b, c, d; \ell, \tilde{\ell}) = (s-a, s-b, s-c, s-d; \ell, \tilde{\ell}).$$

4.3. Quaternionic parametrizations and Regge symmetries

Proof. The proof of the theorem follows from a direct calculation made with a computer algebra system (Mathematica) and using the formula for the cosine of the dihedral angle as function of the internal angles of the three triangles insisting on a vertex of the tetrahedra

$$\cos \Theta_\ell = \frac{\cos \varphi_{al} \cos \varphi_{dl} - \cos \varphi_{ad}}{\sin \varphi_{al} \sin \varphi_{dl}},$$

where the angle φ_{ij} is the angle between edge i and edge j and its cosine can be expressed as a function of the squared edge lengths using the law of cosines. \square

Theorem 23. *The volume of a tetrahedron is invariant under the Regge transformation of four consecutive edges.*

Proof. Four consecutive edges belonging to a tetrahedron have to form a polygon. Indeed it is a quadrilateral composed of two triangles hinged at the edge ℓ which is invariant under the Regge transformation. For Theorem 22, we know that its dihedral angle is kept invariant by the Regge transformation and for Theorem 18, it is also true for the product of the areas of the two triangles. Finally, using the formula for the volume introduced in the previous chapter (3.2.6) we have proved the invariance. \square

4.3 Quaternionic parametrizations and Regge symmetries

4.3.1 New variables

In (4.2.3) we have introduced a new set of variables playing the role of parameters for the quadrilateral. Here we study their behavior under the action of the Regge transformation. Recall that

$$\begin{aligned} s &= (a + b + c + d)/2 \\ u &= (a + b - c - d)/2 \\ v &= (a - b - c + d)/2 \\ r &= (a - b + c - d)/2, \end{aligned} \tag{4.3.1}$$

where the semi-perimeter s of the quadrilateral has been already explicitly introduced. This transformation, in the four dimensional parameter space $\mathbf{v} = (a, b, c, d)$, is associated with the matrix

$$W = \frac{1}{2} \begin{pmatrix} 1 & 1 & 1 & 1 \\ 1 & 1 & -1 & -1 \\ 1 & -1 & -1 & 1 \\ 1 & -1 & 1 & -1 \end{pmatrix} \tag{4.3.2}$$

namely,

$$W \mathbf{v} = \mathbf{u} := (s, u, v, r).$$

W is a symmetric and orthogonal matrix; its determinant is 1 and it is an involution, thus belonging to the real orthogonal group $SO(4)$.

The action of the Regge transformation on the new variables can be evaluated acting adjointly on the matrix R

$$W R W^T =: Q = \text{diag}(1, -1, -1, -1) \quad (4.3.3)$$

thus getting $\mathcal{R} \triangleright \mathbf{u} = \mathbf{u}' := (s, -u, -v, -r)$.

Remark. The area of a quadrilateral expressed in formula (4.2.2) parametrized by the new variables (s, u, v, r) and having diagonals ℓ and $\tilde{\ell}$ simplifies to

$$(\mathcal{A}_{1234})^2 = \frac{1}{4} (\ell \tilde{\ell})^2 - \frac{1}{4} (r s + u v)^2.$$

Adopting the convention of Subsection 4.2.1.2 on the parameter space, it is possible to study the allowed ranges of the new variables. It is possible to use the constraint on c to simplify the system of inequalities to get

$$\begin{aligned} u_{\min} &= \frac{1}{2} (a_{\min} + b_{\min} - c_{\max} - d_{\max}) = \frac{1}{2} (2a_{\min} - 2d_{\max}) = -d_{\max} \\ u_{\max} &= \frac{1}{2} (a_{\max} + b_{\max} - c_{\min} - d_{\min}) = \frac{1}{2} (2b_{\max} - 2d_{\min}) = 0 \\ v_{\min} &= \frac{1}{2} (a_{\min} - b_{\max} - c_{\max} + d_{\min}) = \frac{1}{2} (2a_{\min} - 2b_{\max}) = -d_{\max} \\ v_{\max} &= \frac{1}{2} (a_{\max} - b_{\min} - c_{\min} + d_{\max}) = \frac{1}{2} (a_{\max} - a_{\max}) = 0 \\ r_{\min} &= \frac{1}{2} (a_{\min} - b_{\max} + c_{\min} - d_{\max}) = \frac{1}{2} (2a_{\min} - 2b_{\max}) = -d_{\max} \\ r_{\max} &= \frac{1}{2} (a_{\max} - b_{\min} + c_{\max} - d_{\min}) = \frac{1}{2} (a_{\max} - a_{\max}) = 0. \end{aligned}$$

Therefore the new variables for a quadrilateral having the shorter edge are bounded by zero from above and $-d$ below. For the Regge conjugate one, the quantities are positive definite .

4.3.2 Conjugate quaternions

The diagonal action of Regge transformation Q in (4.3.3) suggests a straightforward interpretation in terms of 'conjugation' of quaternions. Recall that the algebra of quaternions \mathbb{H} is built by endowing \mathbb{R}^4 with the orthonormal Hamilton basis $(\mathbf{e}, \mathbf{i}, \mathbf{j}, \mathbf{k})$ defined by the properties $\mathbf{i}^2 = \mathbf{j}^2 = \mathbf{k}^2 = -\mathbf{i}\mathbf{j}\mathbf{k} = -\mathbf{e}$, where \mathbf{e} is a unit element. If Q is a quaternion with $Q = q_0\mathbf{e} + q_1\mathbf{i} + q_2\mathbf{j} + q_3\mathbf{k}$, then the conjugate of Q is

$$\bar{Q} = q_0\mathbf{e} - q_1\mathbf{i} - q_2\mathbf{j} - q_3\mathbf{k} \quad (4.3.4)$$

4.4. Regge symmetry for the volume operator

and

$$\bar{\mathcal{Q}} \mathcal{Q} = \mathcal{Q} \bar{\mathcal{Q}} = (q_0^2 + q_1^2 + q_2^2 + q_3^2) \mathbf{e} \equiv |\mathcal{Q}|^2 \mathbf{e}, \quad (4.3.5)$$

where $|\mathcal{Q}| = +(q_0^2 + q_1^2 + q_2^2 + q_3^2)^{1/2}$ is the modulus of \mathcal{Q} . Thus every non-zero quaternion has an inverse given by $\mathcal{Q}^{-1} = \bar{\mathcal{Q}} \cdot |\mathcal{Q}|^{-2}$.

It is possible to establish an isomorphism between the space of the parameters of quadrilaterals and a suitable subspace of the quaternion space. In fact, we should remember that the parameters have to satisfy quadrilateral inequalities, restricting thus the space of possible quaternions. In terms of the new variables (4.3.1) a quadrilateral quaternion is defined as

$$\mathcal{Q} = s \mathbf{e} + u \mathbf{i} + v \mathbf{j} + r \mathbf{k}$$

and the Regge transformed quadrilateral will be nothing but the conjugated quaternion $\bar{\mathcal{Q}}$.

Note that both the semi-perimeters and the modulus

$$|\mathcal{Q}|^2 = s^2 + u^2 + v^2 + r^2 = a^2 + b^2 + c^2 + d^2$$

are Regge invariant because in the parameter space the norm is preserved according to (4.2.8).

The adjective ‘‘conjugate’’ used for the geometric entities and quantities (quadrilaterals areas,...) associated with primed parameters, is now fully justified.

4.4 Regge symmetry for the volume operator

In the previous chapter, we have defined the volume operator and we have seen its asymptotic relation with the volume of a tetrahedron embedded in Euclidean 3-space. In Theorem 23 we have proven the invariance the volume of a tetrahedron under Regge transformation, so the semiclassical limit of the volume operator will be invariant under Regge transformation too. Here we will see that this asymptotic symmetry extend also at the quantum level.

To complete the proof of the existence of a full Regge invariance on the original eigenvalue problem (3.1.5) for the volume operator K , the following theorem holds true.

Theorem 24. *Regge symmetry is a symmetry of the volume operator, namely*

$$K \left| \begin{array}{cc} j_1 & j_2 \\ j_3 & j_4 \end{array} ; k \right\rangle = K \left| \begin{array}{cc} s - j_1 & s - j_2 \\ s - j_3 & s - j_4 \end{array} ; k \right\rangle = \lambda(k) \left| \begin{array}{cc} j_1 & j_2 \\ j_3 & j_4 \end{array} ; k \right\rangle$$

where $s = \frac{1}{2} \sum_{i=1}^4 \left(j_i + \frac{1}{2} \right)$. (4.4.1)

Proof. Se need to prove that the matrix representation (3.1.3) of the volume operator $\mathcal{M}_{J_{12}J_{12}}(K) \equiv \langle j'_{12} | K | j_{12} \rangle$ is invariant. The basic request is that the matrix dimensions coincides, and this is true because the dimension $D \times D$ of the matrix $\mathcal{M}_{J_{12}J_{12}}(K)$ is fixed by the inequalities (3.1.13). More precisely, we have already mentioned in Sec. 4.2.1.1 the strict analogy between the volume operator and the quadrilateral geometry. Thus inequalities (3.1.13) can be understood as constraints on the length ℓ of a diagonal of the quadrilateral with edge lengths $\{j_i + \frac{1}{2}\}_{i=1}^4$, so that the problem is equivalent to the discussion in subsection 4.2.1.3 and we get

$$D = 2 \min \left(\left\{ j_i + \frac{1}{2} \right\}_{i=1}^4, \left\{ j'_i + \frac{1}{2} \right\}_{i=1}^4 \right),$$

obviously invariant under Regge transformation.

The second step is to prove that the coefficients of the matrix (3.1.4) are the Regge symmetric, namely

$$\alpha(j_1 \dots j_4; \ell) = \alpha(j'_1 \dots j'_4; \ell).$$

This is straightforward on the basis of Theorem 18 because $\alpha(j_1 \dots j_4)$ is proportional to the product of the areas of two triangles sharing the given edge. \square

As a corollary of the previous theorem we have that the three-term recurrence relation (3.1.14) namely

$$\lambda_k \Psi_\ell^k + i \alpha_{\ell+1} \Psi_{\ell+1}^k - i \alpha_\ell \Psi_{\ell-1}^k = 0 \quad (4.4.2)$$

and its boundary conditions are both invariant under Regge transformation.

So we have finally proved that Regge symmetry is also a symmetry of the volume operator and consequently also of its eigenvalues. This generates an equivalence between two physically different systems which are indistinguishable from them spectrum. This analysis led us to find also a new relation between quadrilaterals and quaternions where Regge symmetry plays the central role of quaternionic conjugation.

In the next two figures [65] pictorial representations of the quadrilateral configurations are given, together with a concise review of the content of the current chapter.

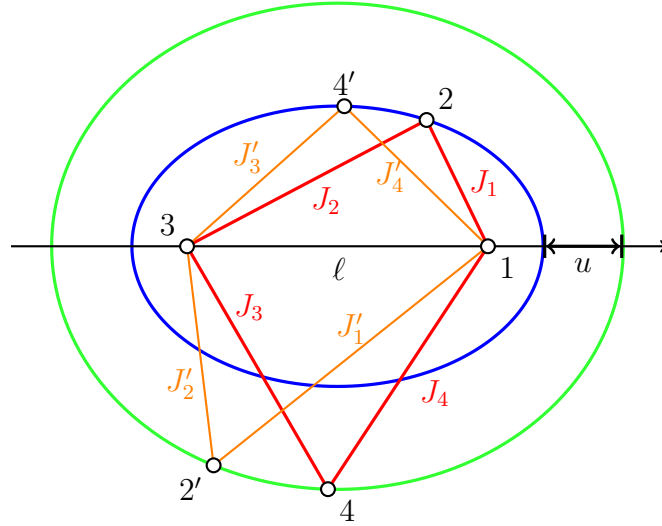


Figure 4.3: A quadrilateral and its Regge-conjugate illustrating the elementary spin network representation of the symmetric coupling scheme: each quadrilateral is dissected into two triangles sharing, as a common side, the diagonal ℓ . The other sides are of length $J_i = j_i + 1/2$ (and $J'_i = j'_i + 1/2$); ℓ , which is the discrete variable in Eq. (4.4.2), is shown as the distance between foci 1 and 3 of the confocal ellipses where the vertices of the quadrilaterals lie. The two sets of four side lengths of the Regge conjugate quadrilaterals are obtained by reflection with respect to the common semiperimeter s (Eq. (4.4.1)). This relationship can be interpreted either as concerted stretchings and shortenings by the parameter $r = (j_1 - j_2 + j_3 - j_4)/2$ introduced in [66], or by $v = (j_1 - j_2 - j_3 + j_4)/2$ occurring in the projective interpretation of Robinson [67]. Shown is also the difference between the semimajor axes of the two ellipses, $u = (j_1 + j_2 - j_3 - j_4)/2$. Signs are decided according to the choice of primed and unprimed quadrilaterals. Also, u and v would exchange their roles had we chosen the other diagonal $\tilde{\ell}$ as the variable ℓ . In Eq. (4.3.3) the orthogonal nature of this set of transformations is exhibited explicitly by the matrix W . The passage to the Regge conjugate configuration $(s, -u, -r, -v)$ is revealed as a quaternionic conjugation, motivating our nomenclature.

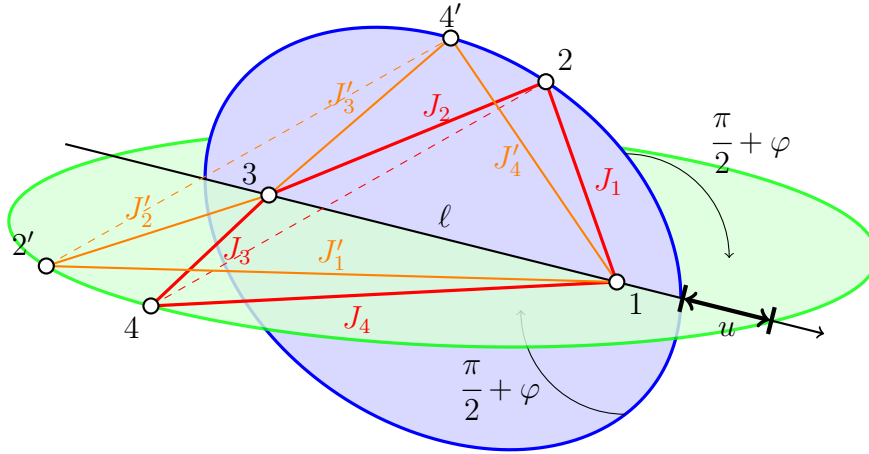


Figure 4.4: The two quadrilaterals of Fig. 4.3, looked at as a mechanical system, evolve creasing the pairs of triangles in which are dissected along ℓ , according to a torsion mode corresponding to the same dihedral angle $\frac{\pi}{2} + \varphi$ in both cases. Adding the edges $\overline{24}$ and $\overline{2'4'}$ two tetrahedra having the same volume can be visualized. In fact, their volume is proportional to H of Eq. (3.2.7) which is the product of the areas of two triangles divided by the length of the hinging edge times the sine of the dihedral angle. Thus classically the volume is an energy function which is a constant of motion along the classical trajectories which are solutions of the Hamilton equations $\frac{d\ell}{dt} = \frac{\partial H}{\partial \varphi}$, $\frac{d\varphi}{dt} = -\frac{\partial H}{\partial \ell}$. Indeed, edges $\overline{24}$ and $\overline{2'4'}$ would have the same length $\tilde{\ell} = j_{23}$ had we chosen to expand the volume operator in the basis of $\mathbf{J}_{23} = \mathbf{J}_2 + \mathbf{J}_3$: two different confocal ellipses would describe the system and the vertices 2, 4 would coincide with 2', 4' as the foci of the new ellipses. On the other hand, vertices 1 and 3 would split to give 1' and 3', say, lying on the new ellipses and belonging either to a quadrilateral or to its conjugate.

Chapter 5

Discrete polynomials families from generalized coupling

In Chapter 3 we have seen that eigenstates of the volume operator, conveniently expanded in the j_{12} basis, satisfy a three terms recurrence relation of the form

$$\lambda_k \psi_\ell^k + \alpha_{\ell+1} \psi_{\ell+1}^k + \alpha_\ell \psi_{\ell-1}^k = 0. \quad (5.0.1)$$

In this chapter we will see that we can associate with the volume operator a set of orthogonal polynomials. These polynomials have a behaviour which mimics that of classical polynomials of hypergeometric type. The Askey scheme organizes [42] the classical polynomials of hypergeometric type into a hierarchical, graph-like structure where each node is a particular polynomial while links are limiting process. In other words, one can reach each node of the scheme starting from the Racah polynomial and descending the hierarchy by suitable limits of their variables.

We have seen in Chapter 3, Equation (3.1.10), that eigenfunctions of volume operator can be seen as suitable factorizations of $6j$ symbols. Since Racah polynomials are $6j$ symbols (up to a phase), we expect that also polynomials associated with the volume operator belongs to some (possible enlarged) hypergeometric type.

5.1 Definition of the polynomials

According to Favard's theorem [57], any three-terms recurrence relation of the form (5.0.1) defines polynomials which are necessarily orthogonal on (suitable subsets of) the real axis.

Instead of using Eq. (5.0.1), we find it much more insightful to eliminate the square roots in order to get an unsymmetrical three-term recursion with polynomial coefficients. In other words we are looking for a three-term recurrence relation of the form

$$X_{\ell-1}c_{\ell-1} + Y_\ell c_\ell + Z_{\ell+1}c_{\ell+1} = 0 \quad (5.1.1)$$

Discrete and Continuous Wavefunctions and Spin Networks

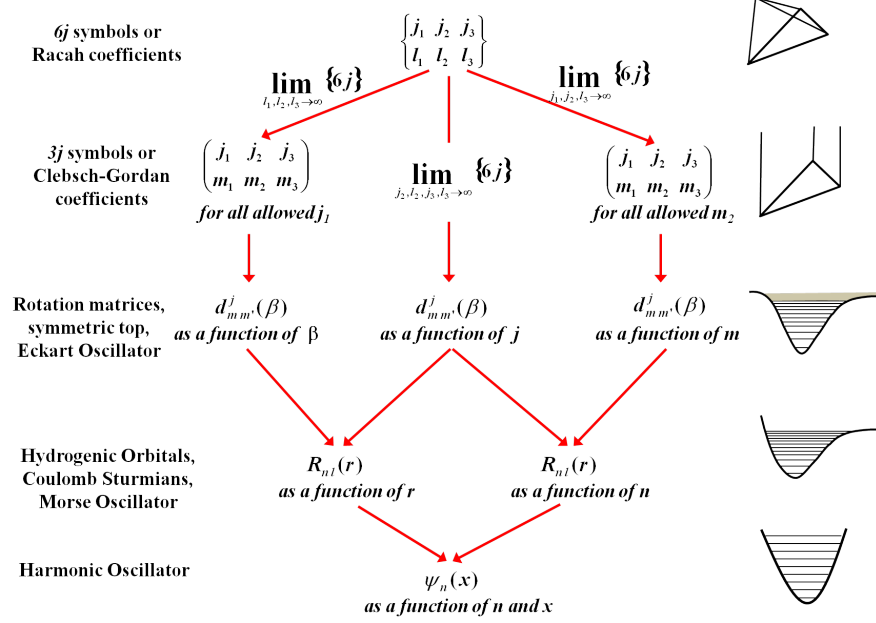


Figure 5.1: The Askey-scheme represented as the graph. Each arrow is a limit in the space of parameters. Here only the part of the scheme involving the recoupling theory of angular momenta is reported.[68]

where X , Y and Z are polynomials and do not contain square roots anymore. We rewrite c_ℓ as $Q_\ell g_\ell := c_\ell$ which gives

$$\left(X_{\ell-1} \frac{Q_{\ell-1}}{Q_\ell}\right) g_{\ell-1} + Y_\ell g_\ell + \left(Z_{\ell+1} \frac{Q_{\ell+1}}{Q_\ell}\right) g_{\ell+1} = 0.$$

If we require a symmetric structure like the one in (5.0.1) we would have¹

$$G_\ell g_{\ell-1} + Y_\ell g_\ell + G_{\ell+1} g_{\ell+1} = 0 \quad \Rightarrow \quad X_{\ell-1} \frac{Q_{\ell-1}}{Q_\ell} = Z_\ell \frac{Q_\ell}{Q_{\ell-1}},$$

where the last equality represent a two-terms recurrence relation that can be solved analytically and reads

$$\sqrt{\frac{X_{\ell-1}}{Z_\ell}} = \frac{Q_\ell}{Q_{\ell-1}} \quad (5.1.2)$$

$$\sqrt{Z_\ell X_{\ell-1}} g_{\ell-1} + Y_\ell g_\ell + \sqrt{Z_{\ell+1} X_\ell} g_{\ell+1} = 0. \quad (5.1.3)$$

We see that the symmetrization process generates coefficients with square

¹this is the same philosophy behind the symmetrization algorithm proposed in [69, 68] and [70].

5.1. Definition of the polynomials

roots and we can recognize that in (5.1.3) the coefficients are

$$G_\ell = \alpha_\ell = \sqrt{Z_\ell X_{\ell-1}} = \sqrt{\frac{F^2\left(\ell, a + \frac{1}{2}, b + \frac{1}{2}\right) F^2\left(\ell, c + \frac{1}{2}, d + \frac{1}{2}\right)}{(2\ell + 1)(2\ell - 1)}} \quad (5.1.4)$$

$$G_{\ell+1} = \alpha_{\ell+1} = \sqrt{Z_{\ell+1} X_\ell} = \sqrt{\frac{F^2\left(\ell + 1, a + \frac{1}{2}, b + \frac{1}{2}\right) F^2\left(\ell + 1, c + \frac{1}{2}, d + \frac{1}{2}\right)}{(2\ell + 3)(2\ell + 1)}}$$

and

$$g_\ell = \psi_\ell^k; \quad Y_\ell = k,$$

so that (5.0.1) can be rewritten according to the updated convention.

On the other hand, if we are interested in writing a polynomial recurrence relation, we can undo the symmetrization and arbitrarily choose Z_ℓ and X_ℓ (a factorization of the original coefficients α_ℓ). However, the final asymmetric three terms recurrence relation will not be unique.

5.1.1 Regge invariance

Among all the possible factorizations $\sqrt{Z_\ell X_{\ell-1}}$ in (5.1.4) of the coefficient α_ℓ defined in (3.1.4), we choose one which preserves the Regge-invariance of the three-terms recurrence relation. Namely, we ask that the new coefficients X_ℓ and Z_ℓ are invariant under the action of the Regge transformation. In this way the new three-term recurrence relation will be automatically Regge invariant and so will be its solutions. The numerator of α_ℓ

$$F^2\left(\ell, a + \frac{1}{2}, b + \frac{1}{2}\right) F^2\left(\ell, c + \frac{1}{2}, d + \frac{1}{2}\right)$$

admits a Regge invariant factorization:

$$[(A + B)^2 - \ell^2] [(C + D)^2 - \ell^2] \quad [(B - A)^2 - \ell^2] [(D - C)^2 - \ell^2]$$

where $A, \dots, D = a + \frac{1}{2}, \dots, d + \frac{1}{2}$.

This factorization can be interpreted geometrically once recognized that a combination of the parameters can be seen as the squared Heron formula

$$\begin{aligned} [(A + B)^2 - \ell^2] [(C + D)^2 - \ell^2] &= F^2(\alpha, \beta, \ell) = [(\alpha + \beta)^2 - \ell^2] [(\alpha - \beta)^2 - \ell^2] \\ [(B - A)^2 - \ell^2] [(D - C)^2 - \ell^2] &= F^2(\gamma, \delta, \ell) = [(\gamma + \delta)^2 - \ell^2] [(\gamma - \delta)^2 - \ell^2] \\ \begin{cases} (A + B) = (\alpha + \beta) \Rightarrow \alpha = \frac{1}{2}(A + B + C + D) =: s \\ (C + D) = (\alpha - \beta) \Rightarrow \beta = \frac{1}{2}(A + B - C - D) =: u \end{cases} \end{aligned}$$

The parameters s, u , together with r, v below, are those found in connection with quaternionic representation given in section 4.3.

$$\begin{cases} (B - A) = (\gamma + \delta) \Rightarrow \gamma = \frac{1}{2}(-A + B - C + D) =: -r \\ (D - C) = (\delta - \gamma) \Rightarrow \delta = \frac{1}{2}(-A + B + C - D) =: -v \end{cases}$$

Finally we can choose

$$\tilde{X}_\ell = \frac{F^2(s, u, \ell)}{(2\ell - 1)} \quad \tilde{Z}_\ell = \frac{F^2(r, v, \ell)}{(2\ell + 1)} \quad Y_\ell = -k \quad (5.1.5)$$

$$\sqrt{\frac{\tilde{X}_{\ell-1}}{\tilde{Z}_\ell}} = \frac{\tilde{N}_\ell}{\tilde{N}_{\ell-1}} = \sqrt{\frac{F^2(s, u, \ell - 1)(2\ell + 1)}{F^2(r, v, \ell)(2\ell - 3)}}$$

$$\frac{F^2(s, u, \ell - 1)}{(2\ell + 1)} p_{\ell-1}^k + \frac{F^2(r, v, \ell + 1)}{(2\ell - 1)} p_{\ell+1}^k = k p_\ell^k,$$

obtaining thus a new non-symmetric three-terms recurrence relation for the volume operator:

$$F^2(s, u, \ell - 1)(2\ell - 1) p_{\ell-1}^k + F^2(r, v, \ell + 1) p_{\ell+1}^k (2\ell + 1) = k (4\ell^2 - 1) p_\ell^k. \quad (5.1.6)$$

The latter is a three-terms recurrence relation built to be polynomial in ℓ and in the quaternionic parameters, and its solutions are related with the solutions of the eigenvalue equation by

$$p_\ell^k = N_\ell \psi_\ell^k$$

where N_ℓ is the solution two-terms recurrence relation

$$N_\ell = \sqrt{\frac{F^2(s, u, \ell - 1)(2\ell + 1)}{F^2(r, v, \ell)(2\ell - 3)}} N_{\ell-1}.$$

5.2 Algebraic approach to the Askey-scheme

5.2.1 Quadratic symmetry algebras

Following [71, 72], the quantum version of a classical dynamical algebra associated with a pair of ‘mutually integrable’ dynamical variables calls into play a triple K_1, K_2, K_3 of linear operators acting on a (suitably defined) Hilbert space with $K_{1,2}$ Hermitian and algebraically independent and $K_3 := [K_1, K_2]$ anti-Hermitian. The request that these generators do fulfill the Jacobi identity constrains the fundamental commutation relations to be of the form $(\{, \})$ is the anticommutator)

$$\begin{aligned} [K_1, K_2] &= K_3 \\ &= 2R K_2 K_1 K_2 + A_1 \{K_1, K_2\} + A_2 K_2^2 + C_1 K_1 + D K_2 + G_1 \\ &= 2R K_1 K_2 K_1 + A_1 K_1^2 + A_2 \{K_1, K_2\} + C_2 K_2 + D K_1 + G_2, \end{aligned} \quad (5.2.1)$$

where $R, A_{1,2}, C_{1,2}, D, G_{1,2}$ are real parameters (the structure constants) and the right-hand sides of the last two relations contain only Hermitian terms.

Such a kind of algebraic structures was actually introduced by Sklyanin [73] and they are called ‘quadratic’ algebras for the obvious reason that the commutators (Poisson brackets in the classical cases) are combinations of quadratic (and linear) terms in each of the generators. Mutual integrability is a sharper requirement with respect to the original formulation, and amounts to look at the symmetry algebra as a dynamical one –where K_1 is a constant of the motion for K_2 taken as the Hamiltonian operator, as well as the other way around. Further improvements in the the study of classical, quantum and q -deformed symmetries along these lines have been provided over the past few decades by a number of authors. Often the admissible structures associated with (5.2.1) and listed in the table below [71] are referred to as ‘Zhedanov’s algebras’ in the literature. Note that for completeness the last line includes the two ‘standard’ Lie algebras on three generators (whose commutation relations are by definition linear).

Classification of quadratic algebras

	R	A_1	A_2	$C \& D$
AW(3) (<i>Askey–Wilson</i>)	*	*	*	*
R(3) (<i>Racah</i>)	0	*	*	*
H(3) (<i>Hahn</i>)	0	0	*	*
J(3) (<i>Jacobi</i>)	0	0	*	0
Lie algebras: <i>su(2), su(1,1)</i>	0	0	0	*

The denominations of the algebras, Askey–Wilson, Racah, ..., are strongly reminiscent of the Askey–Wilson scheme of hypergeometric orthogonal polynomials of one (continuous or discrete) variable [42]. This is not accidental: rather, this remark turns out to be crucial in order to recognize the deep connection between algebraic symmetries of (quantum) systems and special function theory in a quite straightforward way. Indeed the ‘overlap functions’ stemming from the analysis of the eigenvalue problems for the operators K_1, K_2, K_3 which generate the quadratic algebras are, under mild conditions, orthogonal families of Wilson, Racah, Hanh, Jacobi, ..., Hermite polynomials. In what follows an account of a few technical details is given for the case of the Racah algebra **R(3)** which corresponds to set $R = 0$ in (5.2.1).

Suppose that the Hermitian operators K_1 and K_2 –defined on a separable Hilbert space and possibly depending on a same (finite) set of real parameters– are both ladder operators, namely possess discrete, evenly–spaced spectra, and start considering the eigenvalue problem for K_1

$$K_1 \psi_p = \chi_p \psi_p, \quad p = 0, 1, 2, \dots \quad \text{with} \quad \chi_{p+1} = \chi_p + 1. \quad (5.2.2)$$

5. Discrete polynomials families from generalized coupling

Then it can be easily shown that the operator K_2 is tridiagonal in this basis

$$K_2 \psi_p = \mathbf{a}_{p+1} \psi_{p+1} + \mathbf{a}_p \psi_{p-1} + \mathbf{b}_p \psi_p \quad (5.2.3)$$

and, similarly, by exchanging the role of K_1 and K_2 , one would get

$$K_2 \phi_s = \mu_s \phi_s, \quad s = 0, 1, 2, \dots \text{ with } \mu_{s+1} = \mu_s + 1 \quad (5.2.4)$$

and

$$K_1 \phi_s = \mathbf{c}_{s+1} \phi_{s+1} + \mathbf{c}_s \phi_{s-1} + \mathbf{d}_s \phi_s. \quad (5.2.5)$$

The (real) matrix coefficients $\mathbf{a}, \mathbf{b}, \mathbf{c}, \mathbf{d}$ can be evaluated explicitly in terms of the commutation relations (5.2.1) and contain also the parameters which the operators may depend on (such parameters are dropped in the present simplified treatment aimed to point out the overall structural properties). Once chosen suitable normalizations for the two sets of eigenbases (5.2.2) and (5.2.4), it is possible to introduce two families of overlap functions by resorting to the Dirac bracket convention (in which for instance $\langle x|\psi \rangle$ stands for the eigenfunction $|\psi \rangle$ of a system in the position representation)

$$\langle \phi_s | \psi_p \rangle \equiv \langle s | \psi_p \rangle \equiv \langle s | p \rangle \quad \text{and} \quad \langle \psi_p | \phi_s \rangle \equiv \langle p | \phi_s \rangle \equiv \langle p | s \rangle \quad (5.2.6)$$

which are both hypergeometric orthogonal polynomials of one discrete variable (the spectral parameter μ_s and χ_p respectively) to be identified, up to suitable rearrangements of the hidden parameters, with the Racah polynomial on the top of the Askey scheme [42].

In the K_1 -eigenbasis the operator K_3 satisfies

$$K_3 \psi_p = (\chi_{p+1} - \chi_p) \mathbf{a}_{p+1} \psi_{p+1} - (\chi_p - \chi_{p-1}) \mathbf{a}_p \psi_{p-1}, \quad (5.2.7)$$

where eigenvalues χ and matrix elements \mathbf{a} are iteratively evaluated from (5.2.2) and (5.2.3). K_3 has a discrete, in general not evenly-spaced spectrum found as a solution of

$$K_3 \varphi_n = \nu_n \varphi_n, \quad n = 0, 1, 2, \dots \quad (5.2.8)$$

It is worth noting that in general the diagonalization of K_3 cannot be carried out analytically, except in a few cases in which at least the lowest eigenvalues turn out to be representable in closed algebraic forms. The associated families of (normalized) overlap functions are denoted

$$\langle \varphi_n | \psi_p \rangle \equiv \langle n | p \rangle \quad \text{and} \quad \langle \psi_p | \varphi_n \rangle \equiv \langle p | n \rangle \quad (n = 0, 1, 2, \dots; p = 0, 1, 2, \dots) \quad (5.2.9)$$

and can be shown to be orthogonal (on different suitably defined lattices), each depending on one discrete variable, but in principle they might not be included into the Askey scheme.

5.2. Algebraic approach to the Askey-scheme

Similarly, other two families of (normalized) overlap functions associated with the pair K_2, K_3 can be defined by notation consistency as

$$\langle \varphi_n | \phi_s \rangle \equiv \langle n | s \rangle \quad \text{and} \quad \langle \phi_s | \varphi_n \rangle \equiv \langle s | n \rangle \quad (n = 0, 1, 2, \dots; s = 0, 1, 2, \dots). \quad (5.2.10)$$

A crucial feature of the Racah algebra $\mathbf{R}(\mathbf{3})$ and associated overlap functions is the duality property. It relies on the following transformation of the generators

$$K_1 \Leftrightarrow K_2; \quad K_3 \rightarrow -K_3 \quad (5.2.11)$$

which can be easily shown to represent an automorphism of the Racah algebra $\mathbf{R}(\mathbf{3})$. The notion of duality is extended to (all of) the sets of overlap functions introduced above. More precisely

- **i)** Under the automorphism (5.2.11) the discrete, evenly-spaced variables of the two hypergeometric families of overlap functions associated with K_1, K_2 given in (5.2.6) and their degrees as polynomials are interchanged. Since in the present case the operator K_3 is not called into play, the stronger property of ‘self-duality’ of these families holds true: both of them are recognized as Racah polynomials, as already mentioned above.
- **ii)** Referring to the families in (5.2.9), under the automorphism (5.2.11) the discrete, not evenly-spaced spectral variable ν_n of the first family, which is orthogonal on the evenly-spaced lattice $p = 0, 1, 2, \dots$, is turned into the second family, where the variable is p and the polynomial degree is given in terms of the labels $n = 0, 1, 2, \dots$ of the eigenvalues of K_3 . A similar property is shared by the families associated with the pair K_2, K_3 given in (5.2.10).

More details on the nature of the automorphism group and on the statements about the overlap functions will be reported in the next section when dealing with a specific ‘realization’ of the Racah algebra.

5.2.2 Generalized recoupling theory, Regge symmetry and duality

The realization of the Racah algebra $\mathbf{R}(\mathbf{3})$ within the setting of generalized $SU(2)$ recoupling theory was actually the issue addressed originally in [72] which has inspired further work on quadratic algebras. Combining the definitions and notation of section 5.2.1 with those of Chapter 3 it is straightforward to recognize the following correspondence

$$\begin{aligned} K_1 &= \mathbf{J}_{12}^2; \quad K_2 = \mathbf{J}_{23}^2; \\ K_3 &= [\mathbf{J}_{12}^2, \mathbf{J}_{23}^2] = -4i \mathbf{J}_1 \cdot (\mathbf{J}_2 \times \mathbf{J}_3) \equiv -4i K \end{aligned} \quad (5.2.12)$$

between the abstract ordered set of operators K_1, K_2, K_3 and its realization as $\mathbf{J}_{12}^2, \mathbf{J}_{23}^2, K$.

The next step would consist in associating eigenvalue equations and three-term recursion relations of the abstract approach with their realizations in generalized quantum (re)coupling theory. Here we do not enter into much details about this matter since the translation of (5.2.3) based on the pair K_1, K_2 represents the three-term recursion relation for the $6j$ coefficient in disguise (see *e.g.* [40]). The analysis for the pair K_1, K_3 which gives the abstract three-term relation as written in (5.2.7) is examined in details in [12] (and references therein) while its symmetrized counterpart is nothing but the discretized Schrödinger-like equation displayed already in (3.2.2) [65].

Focusing on the specific issue regarding the families of solutions of such relationships, one would directly be lead to establish the correspondence

$$\text{overlap functions} \longrightarrow \text{binary and symmetric recoupling coefficients,} \quad (5.2.13)$$

where the arrow stands for the specific realization (5.2.12) of **R(3)**. To achieve this goal in a transparent and consistent way a few more steps are needed, the first one of which consists in establishing suitable notations for all of the recoupling coefficients. The $6j$ symbol in (2.1.5) and the functions $\Psi_\ell^{(k)}$ in (3.1.6) are thus denoted and defined respectively as

$$\langle j_{23} | j_{12} \rangle \equiv \langle \tilde{\ell} | \ell \rangle \quad \text{and} \quad \Psi_\ell^{(k)} := \langle \ell | k \rangle. \quad (5.2.14)$$

Actually this is not a mere question of notation, since in this way the objects $\langle \bullet | \circ \rangle$ may reveal their ‘double’ meaning as *i)* quantum mechanical transition amplitudes, namely the square modulus $|\langle \bullet | \circ \rangle|^2$ is the probability that a system, prepared in the state $|\circ \rangle$, be measured to be in the state $|\bullet \rangle$; *ii)* eigenfunctions of the operator whose quantum number is in $|\circ \rangle$ in the representation labeled by the eigenvalue of the other operator, namely through the projection onto $\langle \bullet |$. The latter interpretation will be under focus in what follows and more details about the correspondence (5.2.13) can be worked out by introducing explicitly the (so far ignored) parameters of the problem. Upon replacement of the original (ordered) set of labeling of the four angular momenta forming a quadrilateral according to

$$(j_1, j_2, j_3, j_4) \mapsto (a, b, c, d), \quad (5.2.15)$$

the functionals are rewritten as

$$\langle \tilde{\ell} | \ell \rangle (a, b, c, d) \propto \left\{ \begin{array}{ccc} a & b & \ell \\ c & d & \tilde{\ell} \end{array} \right\} \quad \text{and} \quad \Psi_\ell^{(k)}(a, b, c, d) = \langle \ell | k \rangle (a, b, c, d). \quad (5.2.16)$$

Recall that geometrically the first functional is associated with a tetrahedron (ℓ and $\tilde{\ell}$ being a pair of opposite edges) and the second one to a quadrilateral (actually two triangles hinged by one of its diagonal, ℓ or $\tilde{\ell}$) bounding, so to speak, a portion of volume of amount λ_k , the eigenvalue of the volume operator given in (3.1.11). In order to select in a convenient way the Hilbert

space on which the volume operator acts and all the functionals above can be defined consistently, the role of Regge symmetries, originally introduced for the $6j$ [32], is crucial. Such symmetries in their original formulation are recognized as functional relations on the arguments (namely they cannot be derived by interchanging the $6j$ arguments as happens for the so-called ‘classical’ or tetrahedral symmetries) and read

$$\left\{ \begin{array}{ccc} a & b & \ell \\ c & d & \tilde{\ell} \end{array} \right\} = \left\{ \begin{array}{ccc} s-a & s-b & \ell \\ s-c & s-d & \tilde{\ell} \end{array} \right\} := \left\{ \begin{array}{ccc} a' & b' & \ell \\ c' & d' & \tilde{\ell} \end{array} \right\}, \quad (5.2.17)$$

where $s = (a+b+c+d)/2$ is the semi-perimeter of the parameter quadrilateral and in the last equality the new set (a', b', c', d') is defined. It can be checked that the total number of classical and Regge symmetries is 144, which equals the order of the product permutation group $S_4 \times S_3$.

Denoting by a the smallest value among the eight parameters $(a, b, c, d, a', b', c', d')$, it can be shown that a consistent ordering of the other parameters compatible with all the due inequalities is given by $\{a \leq b \leq d ; d - (b - a) \leq c \leq d + (b - a)\}$. This sort of gauge fixing implies that the whole problem becomes finite-dimensional and workable out for each fixed set of the parameters $(a, b, c, d) \in \mathbb{R}^4$. Moreover: *i*) the tetrahedron $\langle \tilde{\ell} | \ell \rangle (a, b, c, d)$ can be chosen as the reference one, calling $\langle \tilde{\ell} | \ell \rangle (a', b', c', d')$ its Regge-conjugate; *ii*) the same thing holds for the quadrilateral denoted $\langle \ell | k \rangle (a, b, c, d)$ and its conjugate $\langle \ell | k \rangle (a', b', c', d')$. More technical details about this specific parametrization and the denomination Regge-‘conjugate’ (as well as the proof that the volume operators and all quantities in its three-term recursion relation (3.1.11) are Regge-invariant) can be found in [30] and [65] respectively.

Coming back to the statement regarding the correspondence (5.2.13), the remarks above should have made clear that Regge symmetry is strictly related to the duality property of the Racah algebra discussed at the end of section 5.2.1. Note that in [72] it had been already recognized that (classical + Regge) symmetries do have the group structure given by $S_4 \times S_3$, to be identified with the automorphism group of the Racah algebra.

5.2.3 Classification of discrete polynomial families

In this section the focus will be on interconnections among the families of discrete orthogonal polynomials in view of the formalization presented in section 5.2.1 and summarized there in items **i**) and **ii**). The various cases, together with the most significant properties of each family, are summarized in table 5.1.

Comparing the notations adopted here –the bar stands for complex conjugation or simply transposition in the real cases– with those of section 5.2.1, it is straightforward to recognized that the classes **I**, **II** and **III** are in correspondence with the overlap functions in (5.2.6), (5.2.9) and (5.2.10) (restricted to finite sets by suitable choices of the omitted parameters), respectively.

5. Discrete polynomials families from generalized coupling

Finite families of discrete orthogonal polynomials [(a, b, c, d) fixed]

#	family	orthogonality on lattice	eigenvalue (related to the variable)	degree related to
I.A	$\langle \tilde{\ell} \ell \rangle$	$\sum_{\tilde{\ell}} \overline{\langle \tilde{\ell} \ell' \rangle} \langle \tilde{\ell} \ell \rangle = \delta_{\ell' \ell}$	$\ell(\ell + 1)$	$\tilde{\ell}$
I.B	$\langle \ell \tilde{\ell} \rangle$	$\sum_{\ell} \overline{\langle \ell \tilde{\ell}' \rangle} \langle \ell \tilde{\ell} \rangle = \delta_{\tilde{\ell}' \tilde{\ell}}$	$\tilde{\ell}(\tilde{\ell} + 1)$	ℓ
II.A	$\langle \ell k \rangle$	$\sum_{\ell} \overline{\langle \ell k' \rangle} \langle \ell k \rangle = \delta_{k' k}$	λ_k	ℓ
II.B	$\langle k \ell \rangle$	$\sum_k \overline{\langle k \ell' \rangle} \langle k \ell \rangle = \delta_{\ell' \ell}$	$\ell(\ell + 1)$	k
III.A	$\langle \tilde{\ell} k \rangle$	$\sum_{\tilde{\ell}} \overline{\langle \tilde{\ell} k' \rangle} \langle \tilde{\ell} k \rangle = \delta_{k' k}$	λ_k	$\tilde{\ell}$
III.B	$\langle k \tilde{\ell} \rangle$	$\sum_k \overline{\langle k \tilde{\ell}' \rangle} \langle k \tilde{\ell} \rangle = \delta_{\tilde{\ell}' \tilde{\ell}}$	$\tilde{\ell}(\tilde{\ell} + 1)$	k

Table 5.1: Summary of the families

5.2. Algebraic approach to the Askey-scheme

Looking at the family **IA**, observe that $\overline{\langle \tilde{\ell} | \ell' \rangle} := \langle \ell' | \tilde{\ell} \rangle = \langle \tilde{\ell} | \ell' \rangle$ by the convention chosen for $6j$ symbols in (2.1.5) (and similarly for **IB**). Thus ‘self-duality’ relations for class **I** read either way

$$\sum_{\tilde{\ell}} \langle \ell' | \tilde{\ell} \rangle \langle \tilde{\ell} | \ell \rangle = \delta_{\ell' \ell} \quad \text{and} \quad \sum_{\ell} \langle \tilde{\ell}' | \ell \rangle \langle \ell | \tilde{\ell} \rangle = \delta_{\tilde{\ell}' \tilde{\ell}} \quad (5.2.18)$$

once fulfilled the completeness relations $\Sigma |\tilde{\ell}\rangle \langle \tilde{\ell}| = \mathbb{I}$ and $\Sigma |\ell\rangle \langle \ell| = \mathbb{I}$ for the binary coupled eigenbases. Note that the operators associated with class **I** (\mathbf{J}_{12}^2 and \mathbf{J}_{23}^2) represent a ‘Leonard pair’ so that the associated overlap functions (recoupling coefficients) are necessarily hypergeometric of Racah type [74]. More generally, in connection with the analysis of the other classes, a stringent result holds true: any *finite* system of orthogonal polynomials whose dual is a finite system of orthogonal polynomials must be (possibly q -deformed) Racah or one of its limiting cases which constitute finite systems (refer to [75] for a modern monograph on hypergeometric polynomials in the Askey–Wilson scheme). Indeed here all the families are consistently defined, for fixed parameters (a, b, c, d) , as finite sets (recall the choice on the ordering discussed in connection with Regge symmetry) but the recognition of classes **II** and **III** as belonging to the Askey scheme is certainly not straightforward. (More precisely, the reduction process to specific hypergeometric functions of type ${}_4F_3$ would require to find out a closed algebraic form for the sets of eigenvalues of the volume operator for given parameters, a task not yet accomplished.)

For what concerns duality within class **II**, a first remark is about the bar operation: $\overline{\langle \ell | k \rangle}$ is $\langle k | \ell \rangle$, but the latter, unlike what happens for the $6j$, is not necessarily equal to $\langle \ell | k \rangle$ because this property actually depends on the volume operator K being Hermitian (imaginary antisymmetric) [12] or real symmetric (see [65] also for plots of the family of eigenfunctions $\langle \ell | k \rangle$). Anyway, both options can be included through a suitable notation into the duality relations

$$\sum_{\ell} \langle k' | \ell \rangle \langle \ell | k \rangle = \delta_{k' k} \quad \text{and} \quad \sum_k \langle \ell' | k \rangle \langle k | \ell \rangle = \pm \delta_{\ell' \ell} \quad (5.2.19)$$

according to the choice of the representation of K . Duality relations in class **III** are similar to (5.2.19), with $\tilde{\ell}$ taking the role of ℓ .

To conclude this general overview on duality relationships, a further remarkable property –transversal with respect to the classes– has to be mentioned, namely

$$\sum_k \langle \tilde{\ell} | k \rangle \langle k | \ell \rangle = \pm \langle \tilde{\ell} | \ell \rangle . \quad (5.2.20)$$

Such a ‘triangular relation’ (and the other ones that can be derived by using the properties of the single classes given above) closely resembles the Racah identity satisfied by three $6j$ symbols and might be used also to explore a formalization of the whole subject within the general scheme of tensor categories.

5.2.4 Limiting cases

The issue of asymptotic (semiclassical) limits of angular momentum functions is of continuous interest in many fields, ranging from special function theory [75] to applied quantum mechanics [76]. Here just a few remarks concerning two limiting cases of families **I.A** and **I.B** are sketched.

The reference model of asymptotics is the well-known limit of the $6j$ symbol for three large entries (see [3, 40]), $6j \rightarrow 3j$, where the latter is the Wigner symbol, the symmetrized version of a Clebsch–Gordan coefficient. The counterpart of this operation in the Askey scheme is achieved by moving one step downwards from top, namely from ${}_4F_3$ (Racah) to ${}_3F_2$ (Hahn and dual Hahn) hypergeometric families.

A new change of notation is needed which consists in restoring the string (j_1, j_2, j_3, j_4) for the parameters (see (5.2.15)) and in writing down as an array the functions in (5.2.16) (equivalently, in family **II.A**) according to

$$\Psi_\ell^{(k)}(j_1, j_2, j_3, j_4) \rightarrow \left\{ \begin{array}{cc|c} j_1 & j_2 & \ell \\ j_3 & j_4 & \lambda_k \end{array} \right\}, \quad (5.2.21)$$

where the vertical bars in front of the last column of this symbol indicate that not all of the entries are constrained by standard triangular inequalities, as happens for the $6j$. To address any limit in which (some of) the arguments of the symbols become large –a fact that implies that all of the arguments can be ‘running’– a convenient notation is to substitute capital to small letters. Thus the formal limiting process for the symbol in (5.2.21) when the arguments of the lower row become large can be displayed as a generalized $3j$ coefficient, denoted $3j$, related in turn to a generalized dual Hahn polynomial; schematically

$$\left\{ \begin{array}{cc|c} j_1 & j_2 & \ell \\ J_3 & J_4 & \Lambda_k \end{array} \right\} \rightsquigarrow \left(\begin{array}{cc|c} j_1 & j_2 & \ell \\ J_4 - \Lambda_k & \Lambda_k - J_3 & J_3 - J_4 \end{array} \right) \leftrightarrow 3j \text{ (dual Hahn family)}. \quad (5.2.22)$$

On applying a similar procedure to family **II.B** and denoting \tilde{L} the previous generic argument ℓ (playing the role of j_{23}), the resulting correspondence would read

$$\left\{ \begin{array}{cc|c} j_1 & j_2 & \lambda_k \\ J_3 & J_4 & \tilde{L} \end{array} \right\} \rightsquigarrow \left(\begin{array}{cc|c} j_1 & j_2 & \lambda_k \\ J_4 - \tilde{L} & \tilde{L} - J_3 & J_3 - J_4 \end{array} \right) \leftrightarrow 3j \text{ (Hahn family)}. \quad (5.2.23)$$

A few comments on these results are in order. As already noticed, the symbols in round brackets on the right-hand sides of (5.2.22) and (5.2.23) are generalized counterparts of $3j$ coefficients, the arguments in the lower row being interpreted as magnetic quantum numbers. They actually share with standard $3j$ s a suitable formulation of Regge symmetry [44] and their properties as orthogonal families are inferred from three-term recursion relationships. The latter can in turn be derived as limits of the three-term recursions at the upper level (in particular, the relation for (5.2.22) can be quite easily worked out).

5.2. Algebraic approach to the Askey-scheme

The motivation for associating dual Hahn and Hahn families respectively is related with the specific lattices these three-term recursion relations are defined on. Thus it is found that the relation for (5.2.22) mimics the behavior of the relation of a $3j$ on a quadratic lattice ($\ell(\ell + 1)$), so that it is functionally similar to the standard dual Hahn polynomial family. Conversely, the relation for (5.2.23) mimics the behavior of the relation of a $3j$ on a linear lattice (given by scaling the quantum number $m \equiv J_3 - J_4$) and thus these functions represent counterparts of the Hahn polynomial family.

5. Discrete polynomials families from generalized coupling

Chapter 6

Lorentzian Regge Calculus

In this chapter we address “collective” dynamics of PL (piecewise-linear) four-dimensional space-times. We are going to study how a collection of discrete simplices can be glued to build a 4-dimensional Lorentzian manifold.

This is motivated by recent work on the spinfoam model for quantum gravity [77, 78], a sophisticated quantization of Regge Calculus, where most of the analysis is done on space-like tetrahedra.

Here the overall topology of the simplicial dissections is taken to be $S_3 \times I$. Actually, this is the topology of any Freedman-Robertson-Walker closed universe, solution of the Einstein equations. Interest in this topology reside in the fact that it can be described with a finite number of simplices making the study easily computable.

Two different triangulations are described: the first simplicial manifold is found following an algorithm, the tent-like triangulation, proposed in [34]. The second triangulation is found combinatorially.

Both the triangulations fill up the portion of space-time between two 3-dimensional compact foliations (topologically S^3) in a sort of “sandwich”. Once fixed the arrow of time, namely choosing a future direction, and normalizing the interval $I := [0, 1]$, we can call one hypersurface “future” the one with $t = 1$ and “past” with $t = 0$.

This topology allows to compose “wider” space-times (longer evolutions) piling several copies of these triangulations, identifying the past 3-dimensional foliation of one with the future of another one and constructing thus a triangulation for a potentially infinitely long cylinder.

6.1 Peculiarities of the Lorentzian 4-simplex

In Chapter 2 we have introduced an “Euclidean” PL-manifold. This concept can be easily generalized to the Lorentzian case assuming that the vector space where the simplices are defined is a Minkowski space (here with mostly positive signature).

A tetrahedron with vertices $(abcd)$ in Euclidean 3-space, with coordinates for ex. $a^\alpha = (0, 0, 0)$, $b^\alpha = (1, 0, 0)$, $c^\alpha = (0, 1, 0)$, $d^\alpha = (0, 0, 1)$, is bordered by the triangles (abd) , (bac) , (cad) , (dbc) , which have outward pointing normal vectors $(\alpha, \beta, \gamma = 1, 2, 3)$

$$n_{abd\alpha} = \epsilon_{\alpha\beta\gamma}(b^\beta - a^\beta)(d^\gamma - a^\gamma) = \epsilon_{\alpha\beta\gamma}(a^\beta b^\gamma + b^\beta d^\gamma + d^\beta a^\gamma), \dots \quad (6.1.1)$$

where $\epsilon_{\alpha\beta\gamma}$ is the Levi-Civita symbol in three dimensions. These four 3-vectors satisfy a closure relation

$$\mathbf{n}_{abd} + \mathbf{n}_{bac} + \mathbf{n}_{cad} + \mathbf{n}_{dbc} = 0. \quad (6.1.2)$$

From Heron's formula, the squared areas of the triangles are $A_{abd}^2 = \frac{1}{4}\mathbf{n}_{abd}^2, \dots$; from Tartaglia's formula the volume of the tetrahedron is $\mathcal{V}_{abcd} = \frac{1}{6}\epsilon_{\alpha\beta\gamma}(b^\alpha - a^\alpha)(c^\beta - a^\beta)(d^\gamma - a^\gamma)$.

We shall extend this elementary geometry to Minkowskian 4-space. To the triangles bordering $(abcd)$ we associate antisymmetric tensors, defined as

$$S_{abd}^{\mu\nu} := (b - a)^{[\mu}(d - a)^{\nu]} = a^{[\mu}b^{\nu]} + b^{[\mu}d^{\nu]} + d^{[\mu}a^{\nu]}, \dots \quad (6.1.3)$$

where $[\dots]$ represents the antisymmetrization of the correspondig indexes. These tensors are 'simple', i.e. each can be written as the antisymmetrized product of two 4-vectors. One can show that if $S^{\mu\nu}$ is simple, so is its Hodge dual $*S^{\mu\nu} := \frac{1}{2}\epsilon^{\mu\nu\rho\sigma}S_{\rho\sigma}$. Simplicity implies that each tetrahedron has a normal 4-vector:

$$\begin{aligned} V_{abcd,\mu} &:= \epsilon_{\mu\nu\rho\sigma}(b - a)^\nu(c - a)^\rho(d - a)^\sigma = \\ &= \epsilon_{\mu\nu\rho\sigma}(b^\nu c^\rho d^\sigma + c^\nu a^\rho d^\sigma + a^\nu b^\rho d^\sigma + b^\nu a^\rho c^\sigma) : \\ V_{abcd,\mu}S_{bcd}^{\mu\nu} &= V_{abcd,\mu}S_{cad}^{\mu\nu} = V_{abcd,\mu}S_{abd}^{\mu\nu} = V_{abcd,\mu}S_{bac}^{\mu\nu} = 0. \end{aligned} \quad (6.1.4)$$

Given V_{abcd}^μ from the identity:

$$*S_{abd}^{\mu\nu}V_{abcd}^\lambda + *S_{abd}^{\nu\lambda}V_{abcd}^\mu + *S_{abd}^{\lambda\mu}V_{abcd}^\nu = -\epsilon^{\mu\nu\lambda\tau}S_{abd\tau\rho}V_{abcd}^\rho \quad (6.1.5)$$

since $S_{abd\tau\rho}V_{abcd}^\rho = 0$, assuming $V_{abcd}^\lambda V_{abcd\lambda} \neq 0$, we find (omitting the $abcd$ subscript):

$$*S_{abd}^{\mu\nu} = V^\mu \left[\frac{V_\lambda^*S_{abd}^{\lambda\nu}}{V^\rho V_\rho} \right] - \left[\frac{V_\lambda^*S_{abd}^{\lambda\mu}}{V^\rho V_\rho} \right] V^\nu = V^\mu N_{abd}^\nu - N_{abd}^\mu V^\nu := (V \wedge N_{abd})^{\mu\nu} \quad (6.1.6)$$

In this way we have defined the 4-vector N_{abd}^μ for the triangle (abd) of the tetrahedron $(abcd)$; this 4-vector is orthogonal to the triangle (abd) because

$$S^{\mu\nu} = -\frac{1}{2}\epsilon^{\mu\nu\rho\sigma}*S_{\rho\sigma} = -\epsilon^{\mu\nu\rho\sigma}V_\rho N_\sigma \quad (6.1.7)$$

6.1. Peculiarities of the Lorentzian 4-simplex

. and to V_μ :

$$N_{abd}^\mu V_\mu = N_{abd}^\mu S_{abd\mu\lambda} = 0.$$

With the 4-vectors defined for the other triangles N_{abd}^μ satisfies a closure relation like (6.1.2):

$$N_{abd}^\mu + N_{bac}^\mu + N_{cad}^\mu + N_{dbc}^\mu = 0. \quad (6.1.8)$$

In the two typical cases,

- $V^\mu = (1, \mathbf{0})$: we would have $N^\mu = (0, \frac{1}{2}\mathbf{n})$, \mathbf{n} defined in (6.1.1), and $*S^{0\alpha} = N^\alpha$;
- if $V^\mu = (0, 0, 0, 1)$, $*S^{3\mu} = N^\mu = (N^0, N^1, N^2, 0)$.

This construction does not work in the case $V^2 := V_\mu^\mu = 0$, which needs a separate treatment; excluding this case, it proves that the existence of a normal V^μ implies simplicity of all the $*S^{\mu\nu}$, and therefore of all the $S^{\mu\nu}$ of a tetrahedron.

Let us next consider a 4-simplex $(abcde)$. From the definition (6.1.4) follows that the normals to its five tetrahedra satisfy the closure relation:

$$V_{abcd}^\mu + V_{abec}^\mu + V_{abde}^\mu + V_{aced}^\mu + V_{bcde}^\mu = 0. \quad (6.1.9)$$

Any triangle will be shared by two tetrahedra with opposite orientation, e.g. (abd) by $(abcd)$ and $(abde)$; dropping suffixes, $V^\mu = V_{abcd}^\mu$ and $N^\mu = N_{abd}^\mu$, or $V'^\mu = V_{abde}^\mu$ and $N'^\mu = \frac{V_{abde\nu} *S_{abd}^{\nu\mu}}{V_{abde}^2}$. One also finds, from the definitions (6.1.4)(6.1.6) and (6.1.3), the following scalar identities:

$$*S_{abd}^{\mu\nu} *S_{abd\mu\nu} = -S_{abd}^{\mu\nu} S_{abd\mu\nu} = 2V^2 N^2 = 2V'^2 N'^2, \quad (6.1.10)$$

$$V_\lambda *S^{\lambda\sigma} V'_\sigma = V^2 (N \cdot V') = -V'^2 (N' \cdot V) \quad (6.1.11)$$

From (6.1.10) follows in particular that if V^2 has a different sign from V'^2 , the same must happen to N^2, N'^2 .

V^μ and N^μ , and V'^μ and N'^μ , are orthogonal, and each pair forms a complete set of 4-vectors in the space orthogonal to $S_{abd}^{\mu\nu}$. Their relationship can be expressed as:

$$V'^\mu = \frac{V \cdot V'}{V^2} V^\mu + \frac{V' \cdot N}{N^2} N^\mu, \quad N'^\mu = \frac{V \cdot N'}{V^2} V^\mu + \frac{N' \cdot N}{N^2} N^\mu \quad (6.1.12)$$

As a consequence, there are several equivalent ways of writing $*S_{\mu\nu}$:

$$\begin{aligned} *S^{\mu\nu} &= (V \wedge N)^{\mu\nu} = (V' \wedge N')^{\mu\nu} = \\ &= \frac{V_\rho *S^{\rho\sigma} V'_\sigma}{V^2 V'^2 - (V \cdot V')^2} (V \wedge V')^{\mu\nu} = \frac{V'^2 V^2}{V_\rho *S^{\rho\sigma} V'_\sigma} (N' \wedge N)^{\mu\nu}. \end{aligned}$$

To prove these relations, one derives from (6.1.12),(6.1.11) and from $V'^2 = \frac{(V \cdot V')^2}{V^2} + \frac{(V' \cdot N)^2}{N^2}$ the following expressions:

$$\begin{aligned} (N' \wedge N)^{\mu\nu} &= \frac{V \cdot N'}{V^2} (V \wedge N)^{\mu\nu} = \frac{V_\lambda^* S^{\lambda\sigma} V'_\sigma}{V^2 V'^2} (V \wedge N)^{\mu\nu} \\ (V \wedge V')^{\mu\nu} &= \frac{V' \cdot N}{N^2} (V \wedge N)^{\mu\nu} = \frac{V^2 V'^2 - (V \cdot V')^2}{V_\lambda^* S^{\lambda\sigma} V'_\sigma} (V \wedge N)^{\mu\nu}. \end{aligned}$$

Representing with an hat $(\hat{\quad})$ the vectors $V^\mu, N^\mu, V'^\mu, N'^\mu$ normalized to $+1$ those space-like and to -1 those time-like, the expressions in (6.1.12) become

$$\begin{aligned} \hat{V}'^\mu &= \epsilon(V^2)(\hat{V} \cdot \hat{V}')\hat{V}^\mu + \epsilon(N^2)(\hat{V}' \cdot \hat{N})\hat{N}^\mu \\ \hat{N}'^\mu &= \epsilon(V^2)(\hat{V} \cdot \hat{N}')\hat{V}^\mu + \epsilon(N^2)(\hat{N}' \cdot \hat{N})\hat{N}^\mu. \end{aligned}$$

where the function ϵ gives the sign of the scalar in its argument. Multiplying these relations on the left by \hat{V}'_μ, \dots , and using (6.1.10),(6.1.11), we derive the relationships between the scalar products. The latter are needed to calculate the hyper-dihedral angle associated with to the triangular face (the ‘‘bone’’):

$$\begin{aligned} \hat{V}'^2 &= \epsilon(V^2)(\hat{V} \cdot \hat{V}')^2 + \epsilon(N^2)(\hat{V}' \cdot \hat{N})^2; \\ \hat{N}'^2 &= \epsilon(V^2)(\hat{V} \cdot \hat{N}')^2 + \epsilon(N^2)(\hat{N} \cdot \hat{N}')^2; \\ 0 &= \epsilon(V^2)(\hat{V} \cdot \hat{V}')(\hat{V} \cdot \hat{N}') + \epsilon(N^2)(\hat{V}' \cdot \hat{N})(\hat{N} \cdot \hat{N}'); \\ 0 &= \epsilon(V^2)\hat{V} \cdot \hat{N}' + \epsilon(V'^2)\hat{V}' \cdot \hat{N} \end{aligned} \quad (6.1.13)$$

Up to this point, no assumption was made on the signs of $V^2, V'^2, V \cdot V'$ etc.. But now we can see that the cases that can actually arise, excluding light-like cases (namely those involving $V^2 = 0$ or $N^2 = 0$), are:

- $\hat{V}^2 = \hat{V}'^2 = 1, \hat{N}^2 = \hat{N}'^2 = 1$.
This is the case of a time-like bone between two time-like tetrahedra:
 $(\hat{V} \cdot \hat{N}') = -(\hat{V}' \cdot \hat{N}); \quad (\hat{N} \cdot \hat{N}') = (\hat{V} \cdot \hat{V}'); \quad (\hat{V} \cdot \hat{V}')^2 + (\hat{V}' \cdot \hat{N})^2 = 1$,
and
we can set: $(\hat{V} \cdot \hat{V}') = (\hat{N} \cdot \hat{N}') = \cos \phi, \quad (\hat{V} \cdot \hat{N}') = -(\hat{V}' \cdot \hat{N}) = \sin \phi$.
- $\hat{V}^2 = \hat{V}'^2 = 1, \hat{N}^2 = \hat{N}'^2 = -1$
This will have to be a space-like bone¹ between two time-like tetrahedra:
 $(\hat{V} \cdot \hat{N}') = -(\hat{V}' \cdot \hat{N}); \quad (\hat{N} \cdot \hat{N}') = -(\hat{V} \cdot \hat{V}'); \quad (\hat{V} \cdot \hat{V}')^2 = 1 + (\hat{V} \cdot \hat{N}')^2$
 $(\hat{V} \cdot \hat{V}') = \pm \cosh \eta, \quad (\hat{V} \cdot \hat{N}') = \sinh \eta$
- $\hat{V}^2 = \hat{V}'^2 = -1, \hat{N}^2 = \hat{N}'^2 = 1$.
This is the case of a space-like bone between two space-like tetrahedra:
 $(\hat{V} \cdot \hat{N}') = -(\hat{V}' \cdot \hat{N}); \quad (\hat{N} \cdot \hat{N}') = -(\hat{V} \cdot \hat{V}'); \quad (\hat{V} \cdot \hat{V}')^2 = 1 + (\hat{V}' \cdot \hat{N})^2$,
and
we can set: $(\hat{V} \cdot \hat{V}') = -(\hat{N} \cdot \hat{N}') = \pm \cosh \eta, \quad (\hat{V} \cdot \hat{N}') = -(\hat{V}' \cdot \hat{N}) =$

¹time-like bones can only have space-like normal 4-vectors.

6.2. Construction of foliated simplicial manifolds

$\mp \sinh \eta$. The upper signs apply when \hat{V} and \hat{V}' point both to the future or to the past, the lower signs when they point in opposite directions ².

- $\hat{V}^2 = -1, \hat{V}'^2 = 1, \hat{N}^2 = 1, \hat{N}'^2 = -1$
Again a space-like bone, but between a space-like and a time-like tetrahedron:
 $(\hat{V} \cdot \hat{N}') = (\hat{V}' \cdot \hat{N}); \quad (\hat{N} \cdot \hat{N}') = (\hat{V} \cdot \hat{V}'); \quad (\hat{V} \cdot \hat{N}')^2 = 1 + (\hat{V} \cdot \hat{V}')^2$, and we can set: $(\hat{V} \cdot \hat{N}') = (\hat{V}' \cdot \hat{N}) = \pm \cosh \eta, \quad (\hat{V} \cdot \hat{V}') = (\hat{N} \cdot \hat{N}') = \mp \sinh \eta$.

6.2 Construction of foliated simplicial manifolds

In the previous section we have defined the “hyper-diedral angles”, and now we can proceed to generalize the notion of defects angles, introduced in Chapter 2 for the Euclidean case, to the Lorentzian case following the prescription of [79]:

- time-like bone:

$$\theta_f = 2\pi - \sum_{\sigma_4(f)} (\phi_f)_{\sigma_4}, \quad \cos \phi_f = \hat{N} \cdot \hat{N}' \quad (6.2.1)$$

- space-like bone:

$$\theta_f = - \sum_{\sigma_4(f)} (\phi_f)_{\sigma_4}, \quad \sinh \phi_f = \epsilon(\hat{N}^2)\epsilon(\hat{V} \cdot \hat{N}')\hat{N} \cdot \hat{N}' \quad \text{if } |\hat{N} \cdot \hat{N}'| < |\hat{V} \cdot \hat{N}'|$$

$$\sinh \phi_f = \epsilon(\hat{N}^2)\epsilon(\hat{N} \cdot \hat{N}')\hat{V} \cdot \hat{N}' \quad \text{otherwise} \quad (6.2.2)$$

the first case will occur if $\hat{V}^2 = -\hat{V}'^2$, the second if $\hat{V}^2 = \hat{V}'^2 = -1$.

Notice that the sign ambiguity in the first case disappears.

The simplicial complex associated to the simplicial space-time is composed by the set of simplices:

$$\Delta_{\mathcal{M}} = \{v_j\}_{j=1}^{N_v} \cup \{e_j\}_{j=1}^{N_e} \cup \{t_j\}_{j=1}^{N_t} \cup \{\tau_j\}_{j=1}^{N_\tau} \cup \{\sigma_j\}_{j=1}^{N_\sigma}.$$

where

$d-$	simplex	
0	vertex	v
1	edge	e
2	triangle	t
3	tetrahedron	τ
4	4-simplex	σ

²in [barrettfoxon],[barrettetal] these two cases are referred to as ‘thick wedge’ and ‘thin wedge’ respectively. Notice that because of the closure relations, the V^μ cannot be all future or all past pointing in a given 4-simplex.

The combinatorial structure of the four dimensional simplicial manifold $\Delta_{\mathcal{M}}$ is encoded into the so called by the Dehn-Sommerville relations, which in the present case read

$$\begin{aligned}
 N_v(\Delta_{\mathcal{M}}) - N_v(\partial\Delta_{\mathcal{M}}) &= \sum_{i=0}^4 (-1)^{i+4} \binom{i+1}{1} N_i(\Delta_{\mathcal{M}}) = N_v - 2N_e + 3N_t - 4N_\tau + 5N_\sigma \\
 N_e(\Delta_{\mathcal{M}}) - N_e(\partial\Delta_{\mathcal{M}}) &= \sum_{i=1}^4 (-1)^{i+4} \binom{i+1}{2} N_i(\Delta_{\mathcal{M}}) = -N_e + 3N_t - 6N_\tau + 10N_\sigma \\
 N_t(\Delta_{\mathcal{M}}) - N_t(\partial\Delta_{\mathcal{M}}) &= \sum_{i=2}^4 (-1)^{i+4} \binom{i+1}{3} N_i(\Delta_{\mathcal{M}}) = N_t - 4N_\tau + 10N_\sigma \\
 N_\tau(\Delta_{\mathcal{M}}) - N_\tau(\partial\Delta_{\mathcal{M}}) &= \sum_{i=3}^4 (-1)^{i+4} \binom{i+1}{4} N_i(\Delta_{\mathcal{M}}) = -N_\tau + 5N_\sigma \\
 N_\sigma(\Delta_{\mathcal{M}}) - N_\sigma(\partial\Delta_{\mathcal{M}}) &= \sum_{i=4}^4 (-1)^{i+4} \binom{i+1}{5} N_i(\Delta_{\mathcal{M}}) = N_\sigma.
 \end{aligned} \tag{6.2.3}$$

Here $N_i(\Delta_{\mathcal{M}})$ denote the number of i -simplices in the simplicial manifold and $\partial\Delta_{\mathcal{M}}$ denotes its boundary. The Euler characteristic of the simplicial complex reads

$$\chi := N_v - N_e + N_t - N_\tau + N_\sigma. \tag{6.2.4}$$

Such relations must be satisfied by any self-consistent gluing process of 4-simplices and the Euler characteristic of the simplicial manifold is defined in (6.2.4).

In this case we focus on the topology $S_3 \times I$. We want to construct a 4-dimensional simplicial complex starting from a 3-dimensional one (the combinatorial counterpart of the space-like foliation). The boundary of a four dimensional polyhedron with tetrahedral faces is homeomorphic actually, PL-homeomorphic to the 3-sphere and will be our “triangulation” at time 0. In particular we are going to choose the simplest one: the boundary of a 4-simplex, namely a set of 5 tetrahedra glued together avoiding the formation of 2 dimensional boundaries.

6.2.1 Tent-like evolution for $S_3 \times I$

This algorithm was proposed by Sorokin several years ago [52] and consists in building a tent-like structure of 4-simplices around a vertex lying on a 3-dimensional boundary region.

6.2.1.1 A warm-up example $S_1 \times I$

In this triangulation we choose S_1 to be replaced by the boundary of a triangle, the simplest 1-dimensional closed simplicial complex. Notice however that this case can be more subtle than using other 1-simplicial complexes (such as the boundary of a square or of a pentagon etc.), in fact in the combinatorial

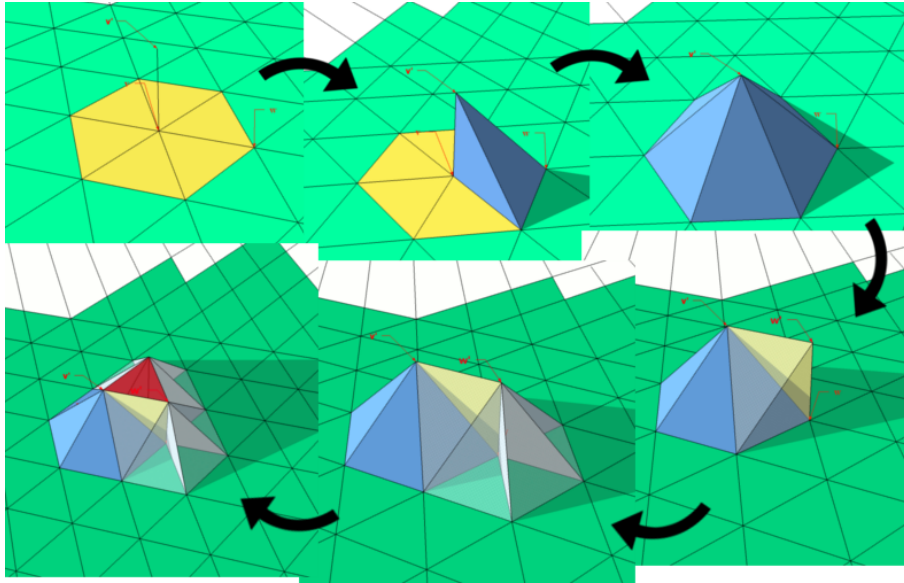


Figure 6.1: An illustration of the tent-like evolution algorithm for the $(2 + 1)$ dimensional case

analysis of the simplicial complex, it is possible to incur in a closed set of 1-simplices which can be confused with a 2-simplicial complex (a triangle) but it actually represent a different foliation of the simplicial complex. Even though this problem is trivial in 2 dimensions, when it occurs in 4-dimensional triangulations it is not, and this issue motivated this 2-dimensional example.

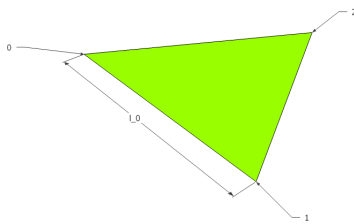


Figure 6.2: Base 1-simplex $\{0, 1, 2\}$ (Note: only the boundary of the triangle is considered).

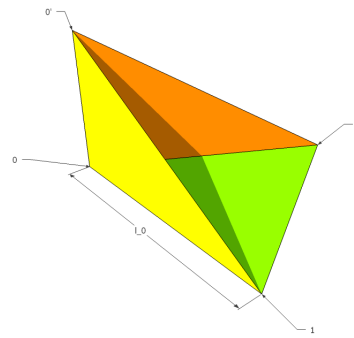


Figure 6.3: Vertex 0 "raised" to $0'$ and two triangles are glued to form the "tent"

- Start with the boundary of a triangle with vertices $\{0, 1, 2\}$ as represented in Fig. 6.2, glue two triangles sharing the edge $\{0, 0'\}$ (central "pole"); the two triangles are $\{0'01, 0'02\}$ as in Fig. 6.3. Notice here we have the case described above: a triangle $\{1, 2, 1'\}$ appears but it has not to be considered a 2-simplex because it is just a different foliation of the

2-dimensional simplicial complex and its topology is S_1 rather than D_2 (the two dimensional disk).

- Now “raise” $1 \rightarrow 1'$ gluing two triangles (Fig. 6.4). One $\{121'\}$ insists upon the base edge $\{12\}$. The other has to lie upon the diagonal edge $\{10'\}$.
- Finally raise $2 \rightarrow 2'$ gluing the last two triangles, a reversed “tent” is formed and it insists upon two diagonal edges.

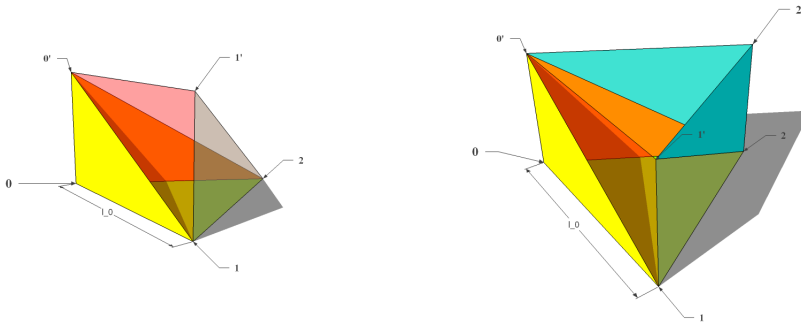


Figure 6.4: Vertex 1 “raised” to $1'$ Figure 6.5: Final step: 2 “raised” $2'$

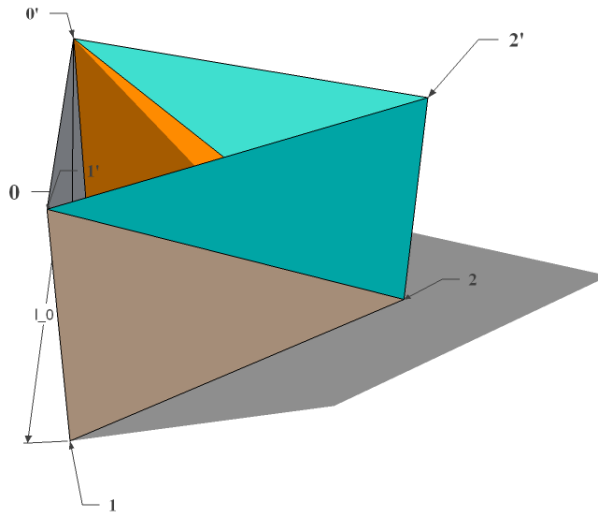


Figure 6.6: The 2-dimensional simplicial complex homeomorphic to the cylinder with finite height topologically $S_1 \times I$

It is thus possible to build a 2-simplex starting from a 1-complex. If we fix the orientation of the simplicial complex, we can choose the primed vertices to be inside the future light-cone of the respective unprimed vertices. The edges $\{e, e'\}$ will be time-like edges (with negative squared length). The edges with both primed and unprimed vertices are called *diagonal* and they can be either time-like or space-like.

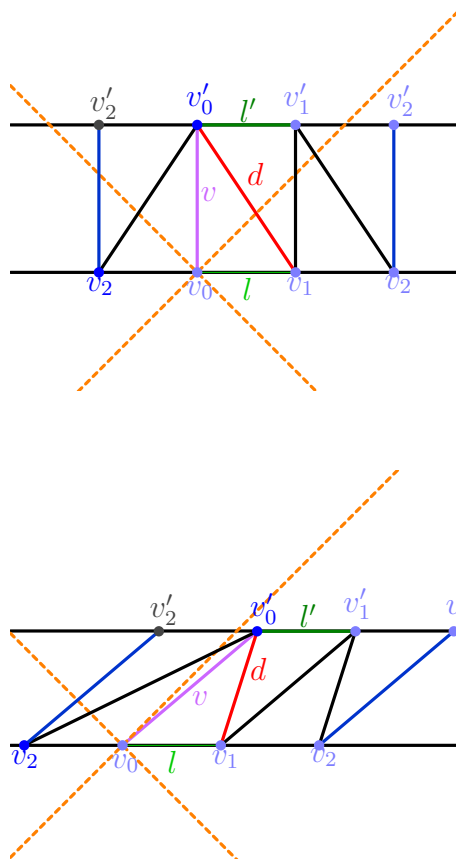


Figure 6.7: 2-d triangulation $S_1 \times I$. Above, $\{00'\}$ time-like; below, $\{00'\}$ space-like

One can choose to “squash” and “twist” the future triangle enough to get the situation where $1'$ is not in the future of 1 . Although this is an admissible triangulation, we will never consider it in this thesis.

6.2.1.2 The 4-dimensional case

The four dimensional case will have as base $t = 0$ boundary a 3-dimensional simplicial complex. In this case we choose the boundary of the 4-simplex (also known as 5-cell) with vertices $\{01234\}$. We are going to “evolve” it into another 5-cell in the “future” with vertices $\{0'1'2'3'4'\}$.

The five tetrahedra belonging to the base 5-cell are

$$T_b = \{0123, 0124, 0134, 0234, 1234\} \tag{6.2.5}$$

and the gluing algorithm is listed below:

- Raise the first vertex $0 \rightarrow 0'$ and around this “pole” build a “tent” adding the edges $0' \rightarrow \{1, 2, 3, 4\}$, namely gluing four 4-simplices with common

edge $e_{00'}$ or, equivalently, placing the four 4-simplices upon the base tetrahedra which share the vertex 0. These new four 4-simplices, namely

$$\Sigma_{00'} = \{0'0123, 0'0124, 0'0134, 0'0234\} \quad (0'1234) \quad (6.2.6)$$

generate the new tetrahedra

$$T_0 = 0' \begin{cases} 012 \\ 013 \\ 023 \\ 014 \\ 024 \\ 034 \end{cases} \quad T'_0 = 0' \begin{cases} 123 \\ 124 \\ 134 \end{cases} \quad T''_0 = 0' 234. \quad (6.2.7)$$

Each tetrahedron in T_0 is shared by two 4-simplices in $\Sigma_{00'}$ and we can say that they are “internal” to the tent-like structure. Tetrahedra in T'_0 and T''_0 at the moment belong to just one 4-simplex, thus we can expect that they will be part of new 4-simplices not yet introduced. From a combinatorial analysis ³ a “false” 4-simplex (in parenthesis in (6.2.6)) appears. We have already encountered a similar case for the 1 + 1-dimensional simplicial complex: $0'1234$ corresponds to the triangle $\{1, 2, 1'\}$ in the previous subsection, namely they corresponds to an alternative foliation of the simplicial complex, in this case with topology S^3 and only its boundary elements belong to our simplicial complex. Hence all tetrahedra are correct and we can combinatorially count them on the basis of the possible combinations of the vertices $\{0'01234\}$

$$\binom{6}{4} = \frac{6!}{4!(6-4)!} = \frac{5 \cdot 6}{2} = 15;$$

thus we get the 10 tetrahedra in 6.2.7 and 5 base tetrahedra T_b .

- Raise $1 \rightarrow 1'$, add edges $1' \rightarrow \{2, 3, 4; 0'\}$ which means gluing four 4-simplices sharing the edge $11'$. Only $11'234$ rests upon one of the base tetrahedra T_b in (6.2.5). In fact, in the previous step all the base tetrahedra but 1234 have been covered by 4-simplices. We left four tetrahedra uncovered but only three share the vertex 1 (those in T'_0). Three 4-simplices can lay on tetrahedra in T'_0 getting thus

$$\Sigma_{11'} = \{1'1234, 0'1'1 23, 0'1'1 34, 0'1'1 24\}.$$

³*e.g.* take the graph with links associated to the edges of the simplicial complex and nodes to the vertices; a 4-simplex corresponds combinatorially to a complete sub-graphs with 5 nodes

6.2. Construction of foliated simplicial manifolds

These 4-simplices carry 10 new tetrahedra:

$$T_1 = 1'1 \left\{ \begin{array}{l} 23 \\ 24 \\ 34 \\ 0'2 \\ 0'3 \\ 0'4 \end{array} \right. \quad T'_1 = 1'2 \left\{ \begin{array}{l} 0'3 \\ 0'4 \\ 34 \end{array} \right. \quad T''_1 = 0'1'34.$$

Tetrahedra in T_1 are internal and each one is shared by two 4-simplices of Σ_{11} while T'_1 and T''_1 are still uncovered tetrahedra (namely, they still belong to just one 4-simplex). In this step the first “future” 1-simplex $0'1'$ is introduced.

- Raise $2 \rightarrow 2'$, add edges $2' \rightarrow \{3, 4, 0', 1'\}$ and glue four 4-simplices sharing the edge $e_{22'}$. All base tetrahedra are already covered by 4-simplices in the previous steps. The 4-simplices lie on the remaining uncovered tetrahedra of the first step T''_0 and on the tetrahedra T'_1 and are

$$\Sigma_2 = 2'2 \left\{ \begin{array}{l} 340' \\ 341' \\ 31'0' \\ 41'0' \end{array} \right. \quad (340'1'2').$$

The ten new tetrahedra are

$$T_2 = 2'2 \left\{ \begin{array}{l} 34 \\ 30' \\ 31' \\ 40' \\ 41' \\ 1'0' \end{array} \right. \quad T'_2 = 2'3 \left\{ \begin{array}{l} 40' \\ 41' \\ 0'1' \end{array} \right. \quad T''_2 = 2'1'0'4$$

and a first “future” triangle is formed, $0'1'2'$.

- Raise $3 \rightarrow 3'$, add edges $3' \rightarrow \{4, 0', 1', 2'\}$ and glue four 4-simplices sharing the edge $e_{33'}$. As before, they lie on T'_2 and T''_1 and are

$$\Sigma_3 = 3'3 \left\{ \begin{array}{l} 40'1' \\ 40'2' \\ 41'2' \\ 0'1'2' \end{array} \right.$$

and the ten new tetrahedra are

$$T_3 = 3'3 \left\{ \begin{array}{l} 0'1' \\ 0'2' \\ 1'2' \\ 1'4 \\ 2'4 \\ 0'4 \end{array} \right. \quad T'_3 = 3'4 \left\{ \begin{array}{l} 0'2' \\ 1'2' \\ 0'1' \end{array} \right. \quad \mathbf{T}_f = \mathbf{0'1'2'3'}.$$

The first future tetrahedron appears $T_f'' = 3'0'1'2'$.

- Raise $4 \rightarrow 4'$, add edges $4' \rightarrow \{0', 1', 2', 3'\}$ and glue four 4-simplices sharing the edge $e_{44'}$. Again, they lie on T_3' and T_2'' and are

$$\Sigma_4 = 4'4 \begin{cases} 0'1'2' \\ 0'1'3' \\ 0'2'3' \\ 1'2'3' \end{cases} .$$

The ten new tetrahedra added in this last step are

$$T_4 = 4'4 \begin{cases} 1'2' \\ 1'3' \\ 2'3' \\ 0'2' \\ 0'3' \\ 0'1' \end{cases} \quad \mathbf{T}_f' = 4' \begin{cases} 0'1'2' \\ 0'1'3' \\ 0'2'3' \\ 1'2'3' \end{cases} .$$

All the tetrahedra in T_f' above are part of the future slice. It is possible to recognize the reversed “tent”-like structure: in fact, the four 4-simplices share the pole $e_{44'}$, and, moreover, each 4-simplex owns a tetrahedron in the future slice (future 5-cell). This step would exactly coincide with the first one had we switched the future 5-cell with the past one.

With the algorithm described so far, we have built the simplicial dissection Δ_{tent} made of 20 4-simplices (in Table 6.1) having as boundary two 5-cell polytopes.

Σ_0	0'0123	0'0124	0'0134	0'0234
Σ_1	0'1'1 23	0'1'1 34	0'1'1 24	1'1234
Σ_2	22'340'	22'341'	22'31'0'	22'41'0'
Σ_3	33'40'1'	33'40'2'	33'41'2'	33'0'1'2'
Σ_4	44'0'1'2'	44'0'1'3'	44'0'2'3'	44'1'2'3'

Table 6.1: 4-simplices introduced at each step

Each step introduces 5 new edges and 6 internal and 4 external tetrahedra. The number of triangles can be evaluated combinatorially or counting the number of shortest cycles in the graph in Fig. 6.8. Recall that a 5-cell has 5 vertices, 10 edges, 10 triangles and 5 tetrahedra, we can count all the simplices in the triangulation:

$$\begin{aligned} N_v(\Delta_{\text{tent}}) &= 10, & N_e(\Delta_{\text{tent}}) &= 35, & N_t(\Delta_{\text{tent}}) &= 60, \\ N_r(\Delta_{\text{tent}}) &= 55, & N_\sigma(\Delta_{\text{tent}}) &= 20. \end{aligned}$$

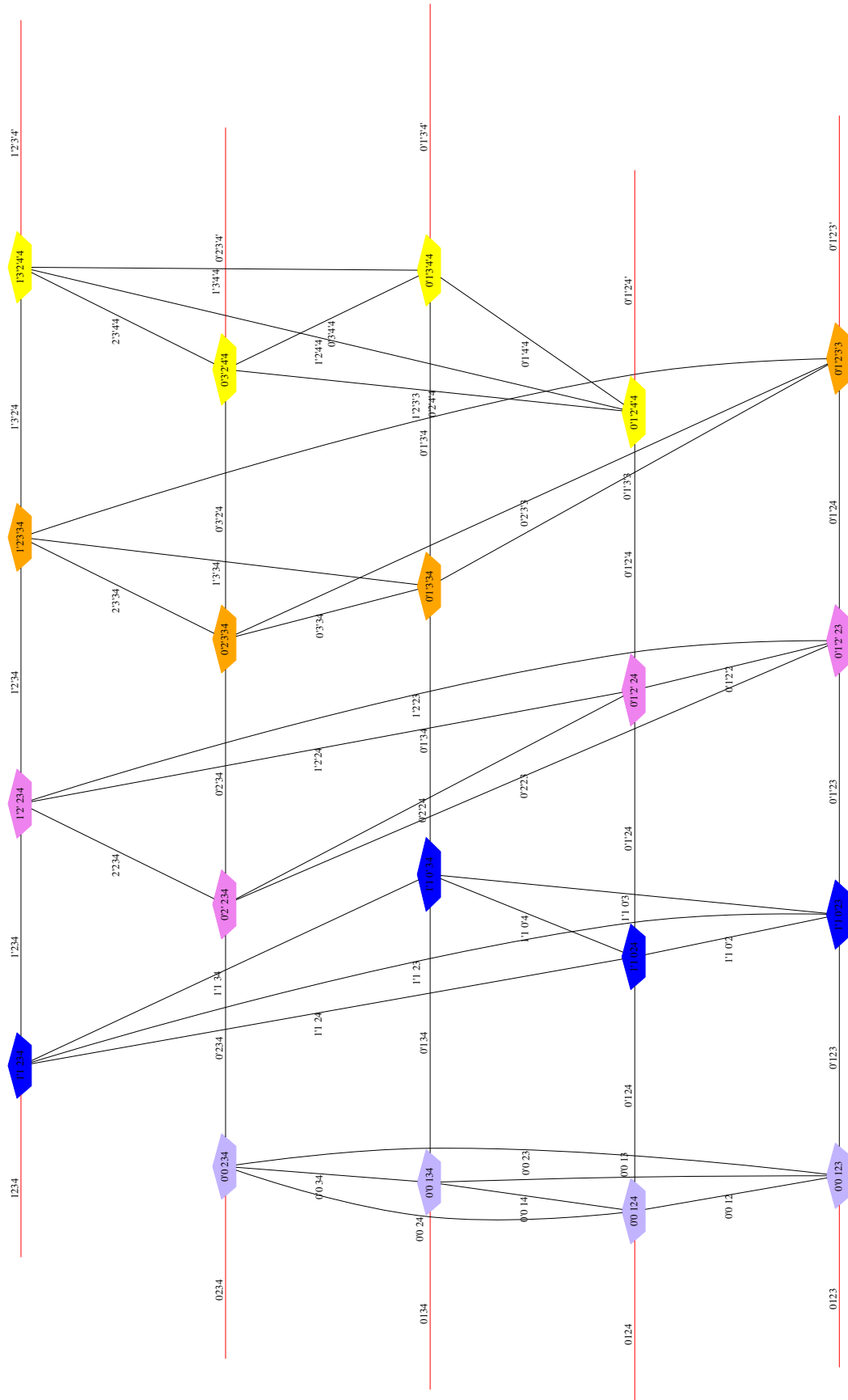


Figure 6.8: Dual graph of the “Tent-like” evolution: each vertex is a 4-simplex, each edge a tetrahedron. Red edges represents tetrahedra belonging to the foliations at time 0 and at time 1.

Among these, the following ones belong to the boundaries:

$$N_v(\partial\Delta_{\text{tent}}) = 10, \quad N_e(\partial\Delta_{\text{tent}}) = 20, \quad N_t(\partial\Delta_{\text{tent}}) = 20, \quad N_\tau(\partial\Delta_{\text{tent}}) = 10.$$

One can easily verify that the Euler characteristic (6.2.4) is

$$\chi(\Delta_{\text{tent}}) = 10 - 35 + 60 - 55 + 20 = 0$$

and all the Dehn-Sommerville relations in (6.2.3) are satisfied.

This algorithm can be easily generalized to other base triangulations and it is useful to build 4-dimensional manifolds with difficult topologies. However, this algorithm does not treat all the base tetrahedra on the same footing. For the case in consideration (the 5-cell base) another triangulation can be built which is homogeneous respect to all the base tetrahedra. This combinatorial triangulation applies only to the 5-cell case.

6.2.2 Symmetric triangulation of $S_3 \times I$

The algorithm to build this triangulation is easier if we focus on the edges. We label again the vertices 0, 1, 2, 3, 4 at time 0, $0', 1', 2', 3', 4'$ at time 1; having a 5-cell as base triangulation, vertices at equal times are all connected to each other by 10 space-like ‘horizontal’ links 01, 02, ..., 34, and then $0'1', 0'2', \dots, 3'4'$; vertices at time 0 are all connected by links to all the vertices at time 1 except that corresponding vertices 0, $0', \dots, 4, 4'$ are not connected.

In the slice between time 0 and time 1 there will be 5 4-simplices with four vertices at time 0 and one at time 1, we shall call them ‘type [4,1]’, 5 of type [1,4], 10 of type [3,2], 10 of type [2,3]; overall:

v	e	t	τ	σ
5	10	10	5	#
#	20	60	70	30
5	10	10	5	#

This is consistent with the the Dehn-Sommerville relations, that in 4-d, if \mathcal{M} is a 4-manifold bounded by $\partial\mathcal{M}$, are

$$N_k(\mathcal{M}) - N_k(\partial\mathcal{M}) = \sum_{i=0}^4 (-1)^{i+4} \binom{i+1}{k+1} N_i(\mathcal{M}), \quad k = 0, \dots, 4$$

$$\begin{array}{rcccccc} 10 - 10 = & 10 & -2 \cdot 40 & +3 \cdot 80 & -4 \cdot 80 & +5 \cdot 30 \\ 40 - 20 = & & -40 & +3 \cdot 80 & -6 \cdot 80 & +10 \cdot 30 \\ 80 - 20 = & & & +80 & -4 \cdot 80 & +10 \cdot 30 \\ 80 - 10 = & & & & -80 & +5 \cdot 30 \\ 30 = & & & & & +30 \end{array}$$

If we consider two slice, there are no σ , no τ and no t with vertices at time +1 and time -1, because there are no edges linking vertices at these

6.2. Construction of foliated simplicial manifolds

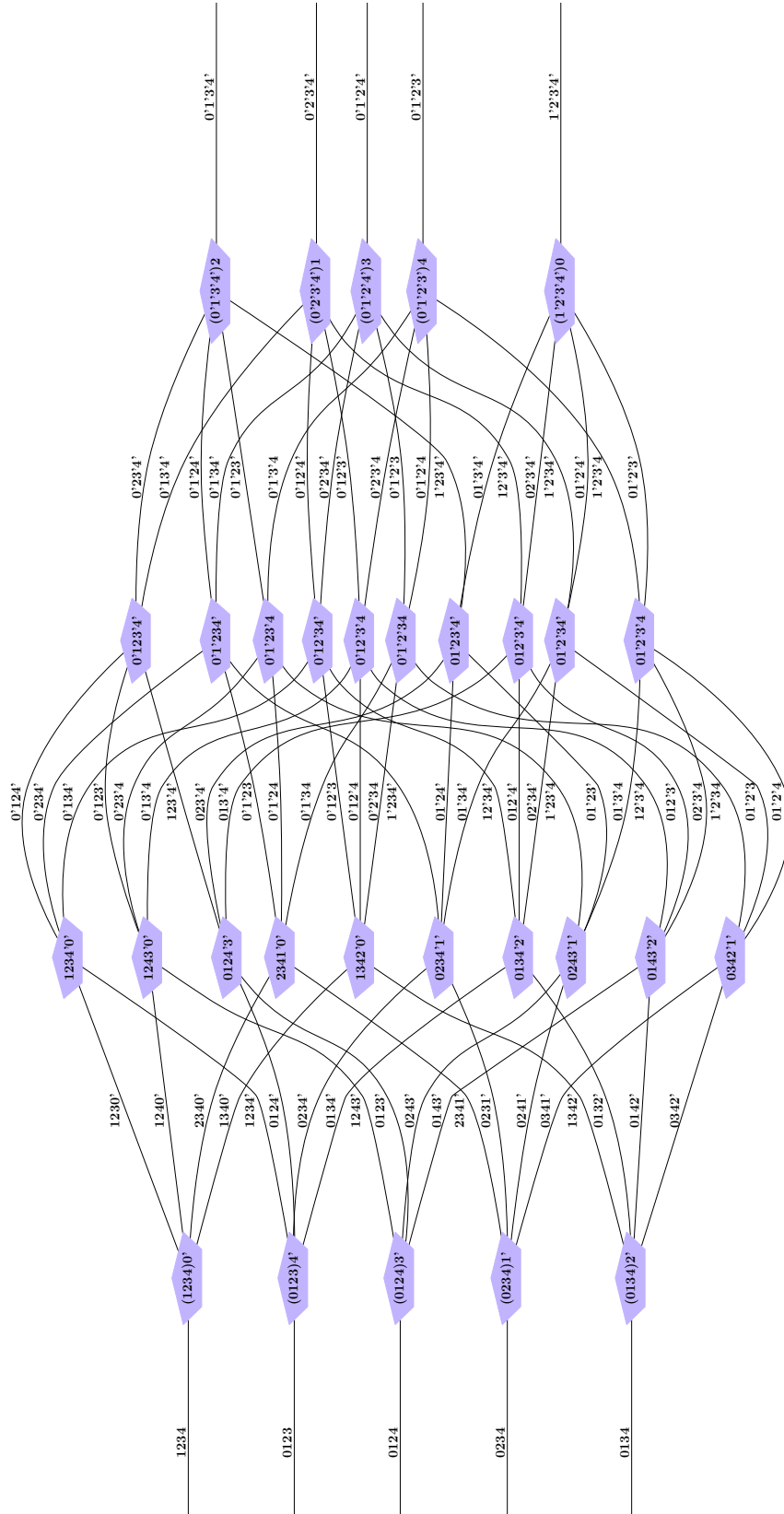


Figure 6.9: Dual graph of the homogeneous evolution: each vertex is a 4-simplex, each edge a tetrahedron.

two times. The same applies to the cylinder one obtains with two slices, which has $N_k(\partial \cdot \text{sym}) = N_k(\partial \cdot \text{sym})$, $N_k(\cdot \text{sym}) = 2N_k(\cdot \text{sym}) - \frac{1}{2}N_k(\partial \cdot \text{sym})$, i.e. $N_k(\cdot \text{sym}) = 15, 70, 150, 155, 60$.

A different way of looking at this triangulation is through its dual graph in Fig. 6.9, namely through a gluing process of 4-simplices similarly to what described in the previous subsection. In this case, we have to treat all the tetrahedra on the same footing:

1. we introduce five independent 4-simplices, each one upon a base tetrahedron; we don't want to introduce new vertices, so the 4-simplices have four unprimed base vertices and one primed future vertex.
2. Each tetrahedron have to be shared by two 4-simplices, apart for those belonging to the boundary (namely, those in the base 5-cell or in the future 5-cell); the 5-simplices introduced in 1 have 4 not shared tetrahedra each. If we glued 20 new independent 4-simplices we would have introduced a total of 25 future vertices, so the 4-simplices cannot be independent. Actually all the future vertices have been already introduced in the previous step. 4-simplices thus have to share edges and shared triangles. Differently to what happens in the tent-like algorithm, there cannot be tetrahedra shared between 4-simplices introduced in the same step. That's because we want to treat all the 5 base and 5 future tetrahedra on the same footing, each 4-simplex can have at most four tetrahedra available at each step, so it would not fulfill this homogeneity requirement. 4-simplices to be introduced in this step can have only two future vertices, thus $\binom{5}{2} = \frac{5!}{3!2!} = \frac{5 \cdot 4}{2} = 10$ 4-simplices are glued. Having two future vertices, they have also 2 tetrahedra with 3 base vertices and 1 future vertex that have to belong also to the 4-simplices of the first step.
3. Each 4-simplex in the previous step has $5 - 2 = 3$ available tetrahedra. They can have one more future vertex (we can only add one vertex at each step, otherwise it would mean that we are gluing a 4-simplex upon a triangle and not upon a tetrahedron), so the 4-simplices are $\binom{5}{3} = \frac{5!}{5!3!} = 10$. Each 4-simplex has 3 tetrahedra shared with simplices of the previous step.
4. Finally, $\binom{5}{4} = 5$ 4-simplices are glued. Each of them have to share four tetrahedra with 4-simplices of the previous step and one is left. Those remaining tetrahedra are the blocks forming the future 5-cell.

6.3 Some remarks on the dynamics

At this point, following Section 2.2, we could introduce the edge lengths to the triangulations, namely the dynamical variables of the classical system.

A very useful trick can be used to treat Lorentzian and Euclidean signature on the same footing and it permits to calculate the quantities described in section 6.1 in few passages. Edge lengths of the simplices are scalar quantities so they are invariant under coordinate changes

$$(l_{ij}^2) = \eta_{\mu\nu}(v_i - v_j)^\mu(v_i - v_j)^\nu = g_{\mu'\nu'}(v'_i - v'_j)^{\mu'}(v'_i - v'_j)^{\nu'} \quad (6.3.1)$$

where v_i^μ are the coordinates of the i th vertex of a simplex in the usual orthogonal coordinates where the metric is $\eta = \text{diag}(-1, +1, +1, +1)$ or $\text{diag}(+1, +1, +1, +1)$. It is possible [80] to associate with each 4-simplex a coordinate system such that a vertex v_0 lies in the origin of the Minkowski space while vectors pointing to the other vertices build an orthonormal base, namely $v_i^\mu = \delta_{i-1}^\mu$. Inverting (6.3.1) the metric reads

$$g_{\mu\nu} = -\frac{1}{2}(l_{ij}^2 - l_{i0}^2 - l_{j0}^2). \quad (6.3.2)$$

Using this coordinate system, 4-vectors N, V introduced in section 6.1 are simply linear combination of Kronecker deltas and the scalar products in (6.2.1) and (6.2.2) are just functions of the metric (6.3.2) and its inverse [79]. With this method, the signature of the system is only encoded the edge lengths 6.3.2.

If a matter part (*e.g.* pure dust) is considered, this dynamical system correspond to the 33th Problem listed by Wheeler in 1964 [4]. Varying the edge lengths we would be able to write down the Regge equations of the system and solve them numerically like in [34, 81, 82].

The two PL-manifolds presented in the previous section are not the best choice if one is interested in Numerical Relativity. They are both a coarse-grained approximation of a cylindrical space-time, which in Einstein General Relativity, for the homogeneous and isotropic case, can be solved even analytically. But, the interest in this particular triangulations resides on the fact that they are composed by a very small number of simplices (20 and 30 4-simplices). The “tent-like triangulation”, can be easily generalized to initial surfaces with different topologies and initial triangulations with different number of simplices, making the evolution local and even parallelizable [34] and providing thus an example of a practical framework for Numerical Regge Calculus.

The PL-manifold described by the graph in Fig.6.9, instead, is not easily generalizable to different initial simplicial surfaces (combinatorial constrains apply), on the other hand it provides a triangulation which is homogeneous, namely all the 4-simplices are treated on the same footing with respect to the initial foliation. Moreover, due to its homogeneity, it has only four different kind of simplices (only two if we considered the time reversal symmetry). This features make this triangulation an ideal candidate to be promoted as a base

triangulation for a Spinfoam model (the path integral approach to quantum gravity) as proposed in [83].

Dynamical evolution, in Einstein General Relativity, is driven by equations of motion of hyperbolic type, namely we are dealing with a causal evolution. In Regge Calculus, on the other hand, the role of causality is not well understood with consequences also in those quantum gravity models based on a discrete space-time. Looking at Regge Calculus as a finite element approximation of space-time, causality have to be connected to the Courant–Friedrichs–Lewy condition [84] and the models we presented can be a useful tool to study this issue.

Conclusions

In this thesis we have analyzed aspects of the theory of discretized geometries, ranging from the quantum dynamics of a single three dimensional simplex to the classical dynamics of a collection of 4-simplices. Such a journey have lead us to highlight the importance of the Regge symmetry since

- it constrains the shape dynamics of a single tetrahedron;
- it relates different tetrahedra equating their quantum representations;
- it gives insight into the geometry of quadrilaterals. Each quadrilateral has a conjugate twin which, in particular configurations, can coincide with itself and that unveils a deep relation with the quaternionic algebra;
- Regge symmetry is the key tool to understand the classical motion of a four-bar linkage mechanical systems and its link to the the quantum dynamics of tetrahedra;
- finally, it permits to introduce families of orthogonal polynomials. These polynomials have a very promising feature: they are symmetric with respect to the coupling of four angular momenta, so we think they can find applications as suitable basis for calculations in quantum chemistry and quantum molecular dynamics.

In the final part of the thesis, we have moved to study the collective behaviour of collection of simplices. We have limited the study to those collections which can represent a space-time manifold. We have found two triangulations which might play an important role in the analysis of the issue of causality in the spinfoam models of quantum gravity. In fact, they are built as 3+1 space-times and thus naturally encode the arrow of time; furthermore, they are “small”, namely they are made of a small number of simplices and offer the possibility of an analytic approach to the system rather than a numeric one.

We can summarize further developments in three different directions: the *Askey-like scheme*, the *q-analog* and the *quantum collective dynamics*.

Askey-like scheme

With the help of the formalization through quadratic algebras described in Section 5.2, it can be possible to develop a hierarchy for polynomial families of the volume operator based on suitable limits like those described in Figure 5.1. This achievement would support the use of these orthogonal polynomials in applications. This task would be simplified by the use of the new variables of quaternionic nature defined in Chapter 3.

The q -analog

The set of orthogonal polynomials of hypergeometric type allows an interesting generalization through the introduction of a continuous parameter q . This parameter distinguishes the family called “classical” ($q = 1$) to those called “quantum”, $q \neq 1$. The Askey-scheme is actually a subset of a wider scheme called Askey-Wilson scheme which include the first as the limit $q \rightarrow 1$.

This kind of generalization has no reasons not to hold for the orthogonal polynomials associated with the volume operator studied in Chapters 2 and 5. The approach to this generalization can be twofold: we can find a new three-terms recurrence relation defining this generalized polynomials following the use of the $6j$ -symbol in Levy-Leblond [7] but replacing it with the one defined by Kirillov and Reshetikhin in 1989 [85]. Another approach could exploit the power of the quadratic algebras described in Section 5.2 to write down a three-terms recurrence relation for the volume operator introducing the q -deformation keeping the coefficient $R \neq 0$ in (5.2.1).

There is also an important physical reason that justifies this possible research line: as already mentioned, the volume operator plays a fundamental role in Loop Quantum Gravity and spin foam models: in these discrete approaches to quantum gravity when a cosmological constant is present the gauge group is deformed to be a quantum-group (see *e.g.* [86, 87]) and the quantum orthogonal polynomials of hypergeometric type are bases for the harmonic analysis of the quantum-groups.

Finally, the q -analog can be interesting for a deeper understanding of the Regge symmetry. Roberts [26] proved that two tetrahedra related by a Regge symmetry are scissor-congruent, namely one tetrahedron can be cut into a finite number of pieces which glued together form the Regge-conjugate tetrahedron. A constructive proof, however, has not yet been found for the Euclidean tetrahedron. On the other hand, Moanthy [88] found a constructive proof for the scissor-congruence of two hyperbolic tetrahedra. Taylor and Woodward [89] conjectured that the q -analog of the $6j$ symbol is semiclassically related to non-Euclidean tetrahedra and in particular, when $q \in \mathbb{R}$, are related to hyperbolic tetrahedra. It would be very interesting to study at the quantum level the interplay between the Moanthy cuts and the parameter q . We think that a possible constructive proof for the Euclidean case can be reached.

Quantum collective dynamics

A quantum generalization of the collective dynamics in four dimensions can be developed continuing the spinfoam program for the quantization of spacetimes. In particular it would be interesting to build the partition functions for the triangulations introduced in Chapter 6. A promising development in this direction is the work by Immirzi [83] which clarifies many points in the Lorentzian spinfoam models using actually one of the triangulations developed in Chapter 6.

On the other hand, in three-dimensions we can directly exploit what we have studied for the volume operator, a schematic list of ongoing works follows:

- convolution rules for overlap functions (specifically, symmetric recoupling coefficients) of Racah algebra;
- composition rules of collections of quadrilaterals able to provide new classes of integrable quantum systems to be associated with extended quantum geometries.

Bibliography

- [1] T. Regge. “General relativity without coordinates”. In: *Il Nuovo Cimento* 19.3 (Feb. 1961), pp. 558–571.
- [2] Roger Penrose. “Angular momentum: an approach to combinatorial space-time”. In: *Quantum theory and beyond* (1971), pp. 151–180.
- [3] G. Ponzano and T. Regge. “Semiclassical limit of Racah coefficients”. In: *Spectroscopic and group theoretical methods in physics*. Ed. by F. Bloch et al. Amsterdam: North-Holland, 1968, pp. 1–98.
- [4] John Archibald Wheeler. “Geometrodynamics and the issue of the final state”. In: *Relativity, Groups and Topology*. Ed. by Bryce DeWitt Cecile & DeWitt. London: Gordon and Breach, 1964, pp. 317–522.
- [5] V.G. Turaev and O.Y. Viro. “State sum invariants of 3-manifolds and quantum 6j-symbols”. In: *Topology* 31.4 (1992), pp. 865–902.
- [6] A. Chakrabarti. “On the coupling of 3 angular momenta”. In: *Annales de l’institut Henri Poincaré Sect. A* 1 (1964), pp. 301–327.
- [7] Jean-Marc Lévy-Leblond and Monique Lévy-Nahas. “Symmetrical Coupling of Three Angular Momenta”. In: *Journal of Mathematical Physics* 6.9 (1965), pp. 1372–1380.
- [8] Carlo Rovelli and Lee Smolin. “Discreteness of area and volume in quantum gravity”. In: *Nuclear Physics B* 442.3 (Nov. 2, 1994), pp. 593–619. arXiv: [gr-qc/9411005](https://arxiv.org/abs/gr-qc/9411005).
- [9] Roberto De Pietri and Carlo Rovelli. “Geometry eigenvalues and the scalar product from recoupling theory in loop quantum gravity”. In: *Physical Review D* 54 (Aug. 1996), pp. 2664–2690. arXiv: [gr-qc/9602023](https://arxiv.org/abs/gr-qc/9602023).
- [10] Abhay Ashtekar and Jerzy Lewandowski. “Quantum Theory of Geometry II: Volume operators”. In: *Advances in Theoretical and Mathematical Physics* 11.2 (Nov. 10, 1997), pp. 388–429. arXiv: [gr-qc/9711031](https://arxiv.org/abs/gr-qc/9711031).
- [11] R. Loll. “Volume Operator in Discretized Quantum Gravity”. In: *Physical Review Letters* 75 (Oct. 1995), pp. 3048–3051. arXiv: [gr-qc/9506014v1](https://arxiv.org/abs/gr-qc/9506014v1).

-
- [12] Gaspare Carbone, Mauro Carfora, and Annalisa Marzuoli. “Quantum states of elementary three-geometry”. In: *Classical and Quantum Gravity* 19.14 (July 21, 2002), p. 3761. arXiv: [gr-qc/0112043](#).
- [13] Krzysztof A. Meissner. “Eigenvalues of the volume operator in loop quantum gravity”. In: *Classical and Quantum Gravity* 23 (2006), pp. 617–626. arXiv: [gr-qc/0509049](#) [[gr-qc](#)].
- [14] Donald E. Neville. “Volume operator for spin networks with planar or cylindrical symmetry”. In: *Physical Review D* 73.12 (June 2006), p. 124004. arXiv: [gr-qc/0511005](#).
- [15] Donald E. Neville. “Volume operator for singly polarized gravity waves with planar or cylindrical symmetry”. In: *Physical Review D* 73 (June 2006), p. 124005. arXiv: [gr-qc/0511006](#).
- [16] Johannes Brunnemann and Thomas Thiemann. “Simplification of the spectral analysis of the volume operator in loop quantum gravity”. In: *Classical and Quantum Gravity* 23 (2006), pp. 1289–1346. arXiv: [gr-qc/0405060](#) [[gr-qc](#)].
- [17] Johannes Brunnemann and David Rideout. “Properties of the volume operator in loop quantum gravity: I. Results”. In: *Classical and Quantum Gravity* 25.6 (Mar. 21, 2008), p. 065001. arXiv: [0706.0469](#).
- [18] Johannes Brunnemann and David Rideout. “Properties of the volume operator in loop quantum gravity: II. Detailed presentation”. In: *Classical and Quantum Gravity* 25.6 (Mar. 21, 2008), p. 065002. arXiv: [0706.0382](#).
- [19] Eugenio Bianchi and Hal M. Haggard. “Discreteness of the volume of space from Bohr-Sommerfeld quantization”. In: *Physical Review Letters* 107 (June 6, 2011), p. 011301. arXiv: [1102.5439](#).
- [20] Eugenio Bianchi and Hal M. Haggard. “Bohr-Sommerfeld Quantization of Space”. In: *Physical Review D* 86 (Aug. 10, 2012), p. 124010. arXiv: [1208.2228](#).
- [21] John Schliemann. “The Large-Volume Limit of a Quantum Tetrahedron is a Quantum Harmonic Oscillator”. In: (July 23, 2013). arXiv: [1307.5979](#).
- [22] Carlo Rovelli. “Zakopane lectures on loop gravity”. In: (Aug. 3, 2011). arXiv: [1102.3660](#).
- [23] E.P. Wigner. *Group Theory and Its Application to the Quantum Mechanics of Atomic Spectra*. Pure and applied Physics. Academic Press, 1959.
- [24] Donald E. Neville. “A Technique for Solving Recurrence Relations Approximately and Its Application to the 3-J and 6-J Symbols”. In: *Journal of Mathematical Physics* 12.12 (1971), pp. 2438–2453.

BIBLIOGRAPHY

- [25] Klaus Schulten and Roy G. Gordon. “Semiclassical approximations to 3j- and 6j-coefficients for quantum-mechanical coupling of angular momenta”. In: *Journal of Mathematical Physics* 16.10 (1975), pp. 1971–1988.
- [26] Justin Roberts. “Classical 6j-symbols and the tetrahedron”. In: *Geometry & Topology* 3 (Mar. 22, 1999), pp. 21–66. arXiv: [math-ph/9812013](https://arxiv.org/abs/math-ph/9812013).
- [27] Mauro Carfora, Annalisa Marzuoli, and Mario Rasetti. “Quantum Tetrahedra”. In: *The Journal of Physical Chemistry A* 113.52 (2009), pp. 15376–15383.
- [28] P.A. Braun. “WKB method for three-term recursion relations and quasienergies of an anharmonic oscillator”. English. In: *Theoretical and Mathematical Physics* 37.3 (1978), pp. 1070–1081.
- [29] P. A. Braun. “Discrete semiclassical methods in the theory of Rydberg atoms in external fields”. In: *Reviews of Modern Physics* 65 (Jan. 1993), pp. 115–161.
- [30] Vincenzo Aquilanti et al. “Semiclassical mechanics of the Wigner 6j-symbol”. In: *Journal of Physics A: Mathematical and Theoretical* 45.6 (Feb. 17, 2012), p. 065209. arXiv: [1009.2811](https://arxiv.org/abs/1009.2811).
- [31] Hal Mayi Haggard. “Asymptotic Analysis of Spin Networks with Applications to Quantum Gravity”. PhD thesis. University of California, Berkeley, Spring 2011.
- [32] T. Regge. “Symmetry properties of Racah’s coefficients”. In: *Il Nuovo Cimento* 11.1 (Jan. 1, 1959), pp. 116–117.
- [33] C. Dewitt and B. DeWitt, eds. *Relativity, Groups and Topology, 1963 (Les Houches Lectures) Relativite, Groupes et Topologie*. Gordon and Breach, 1964.
- [34] John W. Barrett et al. “A Parallelizable Implicit Evolution Scheme for Regge Calculus”. In: (Nov. 1994). eprint: [gr-qc/9411008](https://arxiv.org/abs/gr-qc/9411008).
- [35] P. A. Collins and Ruth M. Williams. “Dynamics of the Friedmann Universe Using Regge Calculus”. In: *Physical Review D* 7.4 (Feb. 1973), pp. 965+.
- [36] A. Messiah. *Quantum Mechanics*. Dover books on physics. Dover Publications, 1999.
- [37] LC Biedenharn and James D Louck. *Angular Momentum in Quantum Physics: Theory and Application, Encyclopedia of Mathematics and its Applications*. Addison-Wesley, Englewood Cliffs, 1981.
- [38] L. C. Biedenharn and J. D. Louck. *The Racah-Wigner Algebra in Quantum Theory (Encyclopedia of Mathematics and its Applications)*. 1st ed. Cambridge University Press, July 2009.

-
- [39] R. M. Williams and P. A. Tuckey. “Regge calculus: a brief review and bibliography”. In: *Classical and Quantum Gravity* 9.5 (May 1, 1992), p. 1409.
- [40] D.A. Varshalovich. *Quantum Theory Of Angular Momemtum*. World Scientific, Oct. 1988.
- [41] A.P. Yutsis, I. B. Levinson, and V. V. Vanagas. *Mathematical Apparatus of the Theory of Angular Momentum*. I.P.S.T., Dec. 1960.
- [42] Richard Askey et al. *Orthogonal polynomials and special functions*. SIAM, 1975.
- [43] Mirco Ragni et al. “Exact computation and asymptotic approximations of 6j symbols: Illustration of their semiclassical limits”. In: *International Journal of Quantum Chemistry* 110.3 (2010), pp. 731–742.
- [44] T. Regge. “Symmetry properties of Clebsch-Gordon’s coefficients”. English. In: *Il Nuovo Cimento* 10.3 (1958), pp. 544–545.
- [45] A.F. Nikiforov and S.K. Suslov. “Classical orthogonal polynomials of a discrete variable on nonuniform lattices”. English. In: *Letters in Mathematical Physics* 11.1 (1986), pp. 27–34.
- [46] L.C. Biedenharn and A. Lohe. *Quantum Group Symmetry and Q-Tensor Algebras*. World Scientific Publishing Company, Incorporated, 1995.
- [47] T.B. Rushing. *Topological embeddings*. Pure and Applied Mathematics. Elsevier Science, 1973.
- [48] Jan Ambjørn, M. Carfora, and A. Marzuoli. *The Geometry of Dynamical Triangulations*. Lecture Notes in Physics v. 50. Springer, 1997.
- [49] J. Cheeger, W. Müller, and R. Schrader. “Lattice gravity or Riemannian structure on piecewise linear spaces”. In: *Unified Theories of Elementary Particles*. Ed. by P. Breitenlohner and H.P. Dürr. Vol. 160. Lecture Notes in Physics. Springer Berlin Heidelberg, 1982, pp. 176–188.
- [50] Jeff Cheeger, Werner Müller W.ller, and Robert Schrader. “On the curvature of piecewise flat spaces”. English. In: *Communications in Mathematical Physics* 92.3 (1984), pp. 405–454.
- [51] J.M. Morvan. *Generalized Curvatures*. Geometry and Computing, 2. Springer Berlin Heidelberg, 2008.
- [52] Rafael Sorkin. “Time-evolution problem in regge calculus”. In: *Physical Review D* 12.2 (July 1975), pp. 385+.
- [53] Sabine Hossenfelder. *Einstein on the discreteness of space-time*. Blog. 2010.
- [54] Tullio Regge and Ruth M. Williams. “Discrete structures in gravity”. In: *Journal of Mathematical Physics* 41.6 (2000), pp. 3964+. arXiv: gr-qc/0012035.

BIBLIOGRAPHY

- [55] M. Carfora and A. Marzuoli. *Quantum Triangulations: Moduli Spaces, Strings, and Quantum Computing*. Lecture notes in physics. Springer, 2012.
- [56] Marko Vojinovic. “Cosine problem in EPRL/FK spinfoam model”. In: (Aug. 26, 2013). arXiv: 1307.5352.
- [57] F.V. Atkinson. *Discrete and Continuous Boundary Problems (Mathematics in Science and Engineering, Vol. 8)*. Academic Press, Feb. 1964.
- [58] Eric Jones, Travis Oliphant, Pearu Peterson, et al. *SciPy: Open source scientific tools for Python*. 2001–.
- [59] Daniel Zwillinger. *CRC Standard Mathematical Tables and Formulae, 32nd Edition (Discrete Mathematics and Its Applications)*. 32nd ed. CRC Press, June 2011.
- [60] Michael Kapovich and John Millson. “On The Moduli Space Of Polygons In The Euclidean Plane”. In: *Journal of Differential Geometry* 42 (1994), pp. 133–164.
- [61] Michael Kapovich and John J. Millson. “The Symplectic Geometry of Polygons in Euclidean Space”. In: *Journal of Differential Geometry* 44 (1998), pp. 479–513.
- [62] J.M. McCarthy and G.S. Soh. *Geometric Design of Linkages*. Interdisciplinary applied mathematics. Springer, 2010.
- [63] J. L. Coolidge. “A Historically Interesting Formula for the Area of a Quadrilateral”. English. In: *The American Mathematical Monthly* 46.6 (1939), pages.
- [64] R. G. Littlejohn. “private communication”.
- [65] Vincenzo Aquilanti, Dimitri Marinelli, and Annalisa Marzuoli. “Hamiltonian dynamics of a quantum of space: hidden symmetries and spectrum of the volume operator, and discrete orthogonal polynomials”. In: *Journal of Physics A: Mathematical and Theoretical* 46.17 (May 3, 2013), pp. 175303+. arXiv: 1301.1949.
- [66] Ana C. Bitencourt et al. “Exact and Asymptotic Computations of Elementary Spin Networks: Classification of the Quantum-Classical Boundaries”. In: *Lecture Notes in Computer Science*. Vol. 7333. Springer, 2012, pp. 723–737. arXiv: 1211.4993.
- [67] G. de B. Robinson. “Group Representations and Geometry”. In: *Journal of Mathematical Physics* 11.12 (1970), pp. 3428–3432.
- [68] Vincenzo Aquilanti et al. “Hydrogenic orbitals in momentum space and hyperspherical harmonics: Elliptic Sturmian basis sets”. In: *International Journal of Quantum Chemistry* 92.2 (2003), pp. 212–228.

-
- [69] Vincenzo Aquilanti, Andrea Caligiana, and Simonetta Cavalli. “Hydrogenic elliptic orbitals, Coulomb Sturmian sets, and recoupling coefficients among alternative bases”. In: *International Journal of Quantum Chemistry* 92.2 (2003), pp. 99–117.
- [70] Yu. F. Smirnov. “On factorization and Algebraization of difference equation of hypergeometric type”. In: *Proc. Int. Workshop on Orthogonal Polynomial in Math. Physics*. Ed. by M. Alfaro et al. Universidad Carlos III, Leganés (Madrid). 24-26 June 1996 1996, pp. 153–161.
- [71] Ya.I Granovskii, I.M Lutzenko, and A.S Zhedanov. “Mutual integrability, quadratic algebras, and dynamical symmetry”. In: *Annals of Physics* 217.1 (1992), pp. 1–20.
- [72] Ya A Granovskii and AS Zhedanov. “Nature of the symmetry group of the 6j-symbol”. In: *Zh.Eksper. Teoret. Fiz* 94 (1988), pp. 49–54.
- [73] Evgeny Konstantinovich Sklyanin. “Some algebraic structures connected with the Yang-Baxter equation”. In: *Functional Analysis and its Applications* 16.4 (1982), pp. 263–270.
- [74] Douglas A Leonard. “Orthogonal polynomials, duality and association schemes”. In: *SIAM Journal on Mathematical Analysis* 13.4 (1982), pp. 656–663.
- [75] R. Koekoek, P. Lesky, and R.F. Swarttouw. *Hypergeometric Orthogonal Polynomials and Their q -Analogues*. Springer monographs in mathematics. Springer, 2010.
- [76] Vincenzo Aquilanti et al. “Combinatorics of angular momentum recoupling theory: spin networks, their asymptotics and applications”. In: *Theoretical Chemistry Accounts* 123 (3 2009), pp. 237–247.
- [77] Jonathan Engle et al. “LQG vertex with finite Immirzi parameter”. In: *Nuclear Physics B* 799.1-2 (2008), pp. 136–149.
- [78] John W. Barrett et al. “Lorentzian spin foam amplitudes: graphical calculus and asymptotics”. In: *Classical and Quantum Gravity* 27.16 (Aug. 21, 2010), pp. 165009+. arXiv: 0907.2440.
- [79] Leo Brewin. “Fast algorithms for computing defects and their derivatives in the Regge calculus”. In: *Classical and Quantum Gravity* 28.18 (Nov. 8, 2010), pp. 185005+. arXiv: 1011.1885.
- [80] J. Fröhlich. “Regge calculus and discretized gravitational functional integrals”. In: *Non-Perturbative Quantum Field Theory: Mathematical Aspects and Applications. Selected Papers of Jürg Fröhlich*. Vol. 15. Advanced Series in Mathematical Physics. Singapore; River Edge, U.S.A.: World Scientific, 1992, pp. 523–545.
- [81] A. De Felice and E. Fabri. “The Friedmann universe of dust by Regge Calculus: study of its ending point”. In: (Sept. 2000). arXiv: gr-qc/0009093.

BIBLIOGRAPHY

- [82] Parandis Khavari and Charles C. Dyer. “Aspects of Causality in Regge Calculus”. In: (Sept. 2008). eprint: 0809.1815.
- [83] Giorgio Immirzi. “A Note on the Spinor Construction of Spin Foam Amplitudes”. In: (2013). arXiv: 1311.6942 [gr-qc].
- [84] Peter D. Lax. “Hyperbolic difference equations: a review of the courant-friedrichs-lewy paper in the light of recent developments”. In: *IBM Journal of Research and Development* 11.2 (Mar. 1967), pp. 235–238.
- [85] A. N. Kirillov and N. Yu. Reshetikhin. “Representations of the algebra $U_q(\mathfrak{sl}(2))$, q -orthogonal polynomials and invariants of links”. In: *Infinite-dimensional Lie algebras and groups (Luminy-Marseille, 1988)*. Vol. 7. Adv. Ser. Math. Phys. World Sci. Publ., Teaneck, NJ, 1989, pp. 285–339.
- [86] Karim Noui and Philippe Roche. “Cosmological Deformation of Lorentzian Spin Foam Models”. In: *Classical and Quantum Gravity* 20.14 (Nov. 29, 2002), pp. 3175–3213. arXiv: gr-qc/0211109.
- [87] Eugenio Bianchi and Carlo Rovelli. “A note on the geometrical interpretation of quantum groups and non-commutative spaces in gravity”. In: *Physical Review D* 84.2 (May 13, 2011). arXiv: 1105.1898.
- [88] Yana Mohanty. “The Regge symmetry is a scissors congruence in hyperbolic space”. In: *Algebraic & Geometric Topology* 3 (Jan. 24, 2003), pp. 1–31. arXiv: math/0301318.
- [89] Yuka U. Taylor and Christopher T. Woodward. “ $6j$ symbols for $U_q(\mathfrak{sl}_2)$ and non-Euclidean tetrahedra”. In: *Selecta Math. (N.S.)* 11.3-4 (2005), pp. 539–571.

Acknowledgments:

I would like to thank my supervisor Prof. Annalisa Marzuoli, who suggested and carefully followed this project. This thesis would not have been possible without her help, and patience. I'd like to thank Prof. Vincenzo Aquilanti, collaborator for most of the research reported in this thesis, from whom I have learned a lot; and Prof. Giorgio Immirzi who is my mentor since my Bachelor in Perugia and collaborator on the research reported in Chap. 6. I thank the referees, Prof. Robert Littlejohn and Prof. Patrizia Vitale for their valuable and constructive reviews which helped me to improve this thesis. Finally, I am grateful to Dr. Claudio Dappiaggi for all the discussions we had and for his precious suggestions and support in Pavia.

ISBN 978-88-95767-73-4



9 788895 767734 >

ISBN 978-88-95767-73-4